REPORT No. FAA-RD-78-57

DAYTON AIRCRAFT CABIN FIRE MODEL VALIDATION

PHASE 1

Charles D. MacArthur
John F. Myers

University of Dayton
Research Institute
Dayton, Ohio 45469

March 1978

Final Report

Prepared for

U.S. DEPARTMENT OF TRANSPORTATION
FEDERAL AVIATION ADMINISTRATION
Systems Research & Development Service
Washington, D.C. 20590

Technical Report Documentation Page

1. Report No.	2. Government Accession No.	3. Recipient's Catalog No.
FAA-RD-78-57		

4. Title and Subtitle	5. Report Date
Dayton Aircraft Cabin Fire Model Validation - Phase I	March 1978
	6. Performing Organization Code: UDRI-TR-78-44
7. Author(s): Charles D. MacArthur, John F. Myers	8. Performing Organization Report No.
9. Performing Organization Name and Address: University of Dayton Research Institute, 300 College Park Avenue, Dayton, Ohio 45469	10. Work Unit No. (TRAIS)
	11. Contract or Grant No.: FA74WA-3532
12. Sponsoring Agency Name and Address: Department of Transportation, Federal Aviation Administration, Systems Research and Development Service, Washington, D.C. 20590	13. Type of Report and Period Covered: Final Report, June 1976-November 1977
	14. Sponsoring Agency Code

15. Supplementary Notes

16. Abstract

Results are presented of an evaluation of the Dayton Aircraft Fire Model (DACFIR) by comparison to seven full-scale cabin mock-up fire tests. Refinements made to the mathematical model as a result of the comparison are given. Refinements include a generalization of the treatment of the cabin geometry to include cabins of various widths, improved thermal radiation modeling, computation of oxygen consumption, and a treatment of forced ventilation. A laboratory testing program to acquire flammability, smoke, and gas generation data on the furnishing materials of the full-scale test is described. Based on the results of the comparisons, sections of the mathematical model which require further refinement are identified and some appropriate refinements are suggested.

17. Key Words	18. Distribution Statement
aircraft fire safety, fire research, aircraft interior materials, smoke and toxic gases, aircraft cabin fires, enclosed fire, fire tests, mathematical fire model, computer simulation	Document is available to the public through the National Technical Information Service, Springfield, Virginia 22151

19. Security Classif. (of this report)	20. Security Classif. (of this page)	21. No. of Pages	22. Price
UNCLASSIFIED	UNCLASSIFIED	142	

Form DOT F 1700.7 (8-72) Reproduction of completed page authorized

PREFACE

This report was prepared by the University of Dayton Research Institute for the Federal Aviation Administration Systems Research and Development Service under Contract FA74WA-3532 during the period June 1976 to December 1977. The report describes a comparison of Dayton Aircraft Cabin Fire Model (DACFIR) to a series of aircraft cabin mock-up fire tests and the refinement and extension of the model based upon the comparison.

Technical administration of this work was provided by Mr. Charles C. Troha of the Systems Research and Development Service (ARD-520). Work was performed at the University of Dayton under the supervision of Mr. Nicholas A. Engler. Other personnel at the University who have contributed to this program include Mr. Peter M. Kahut, Mr. Steven G. Vondrell, and Mr. Richard E. Feldmann. The laboratory data collection program performed under subcontract by the Boeing Commercial Airplane Company was directed by Dr. James M. Peterson with contributions by Mr. Robert D. Lechner, Dr. Allen E. Senear, and Mr. Everett A. Tustin. Much of the original development of the DACFIR model was directed by Mr. Jerry B. Reeves who also guided the early work on this refinement program. The authors would like to thank Ms. Jacquelin Aldrich for her patient assistance in preparing the manuscript.

METRIC CONVERSION FACTORS

Approximate Conversions to Metric Measures

Symbol	When You Know	Multiply by	To Find	Symbol
	LENGTH			
in	inches	*2.5	centimeters	cm
ft	feet	30	centimeters	cm
yd	yards	0.9	meters	m
mi	miles	1.6	kilometers	km
	AREA			
in^2	square inches	6.5	square centimeters	cm^2
ft^2	square feet	0.09	square meters	m^2
yd^2	square yards	0.8	square meters	m^2
mi^2	square miles	2.6	square kilometers	km^2
	acres	0.4	hectares	ha
	MASS (weight)			
oz	ounces	28	grams	g
lb	pounds	0.45	kilograms	kg
	short tons (2000 lb)	0.9	tonnes	t
	VOLUME			
tsp	teaspoons	5	milliliters	ml
Tbsp	tablespoons	15	milliliters	ml
fl oz	fluid ounces	30	milliliters	ml
c	cups	0.24	liters	l
pt	pints	0.47	liters	l
qt	quarts	0.95	liters	l
gal	gallons	3.8	liters	l
ft^3	cubic feet	0.03	cubic meters	m^3
yd^3	cubic yards	0.76	cubic meters	m^3
	TEMPERATURE (exact)			
°F	Fahrenheit temperature	5/9 (after subtracting 32)	Celsius temperature	°C

*1 in = 2.54 (exactly). For other exact conversions and more detailed tables, see NBS Misc. Publ. 286, Units of Weights and Measures, Price $2.25, SD Catalog No. C13.10:286.

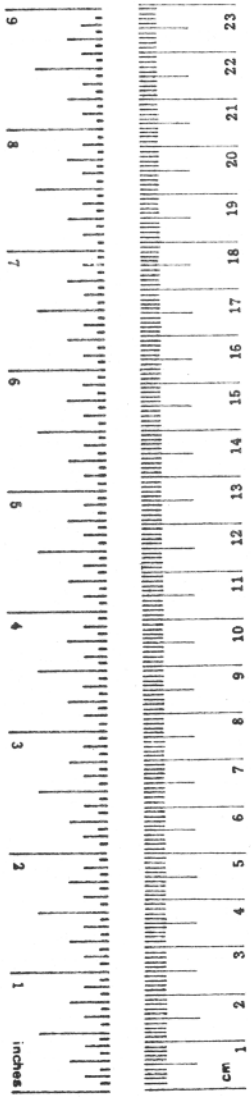

Approximate Conversions from Metric Measures

Symbol	When You Know	Multiply by	To Find	Symbol
	LENGTH			
mm	millimeters	0.04	inches	in
cm	centimeters	0.4	inches	in
m	meters	3.3	feet	ft
m	meters	1.1	yards	yd
km	kilometers	0.6	miles	mi
	AREA			
cm^2	square centimeters	0.16	square inches	in^2
m^2	square meters	1.2	square yards	yd^2
km^2	square kilometers	0.4	square miles	mi^2
ha	hectares (10,000 m^2)	2.5	acres	
	MASS (weight)			
g	grams	0.035	ounces	oz
kg	kilograms	2.2	pounds	lb
t	tonnes (1000 kg)	1.1	short tons	
	VOLUME			
ml	milliliters	0.03	fluid ounces	fl oz
l	liters	2.1	pints	pt
l	liters	1.06	quarts	qt
l	liters	0.26	gallons	gal
m^3	cubic meters	35	cubic feet	ft^3
m^3	cubic meters	1.3	cubic yards	yd^3
	TEMPERATURE (exact)			
°C	Celsius temperature	9/5 (then add 32)	Fahrenheit temperature	°F

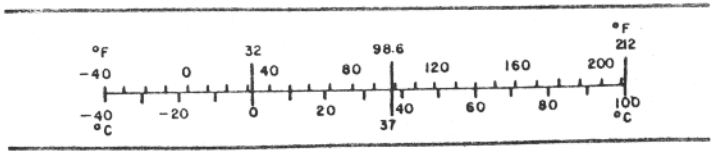

TABLE OF CONTENTS

SECTION 1
INTRODUCTION

This report describes the results of an evaluation and refinement of the Dayton Aircraft Cabin Fire (DACFIR) Model. The DACFIR model was used to make computer simulations of several full scale aircraft cabin and cabin mock-up fire tests. Comparisons of the test results to the model's predictions were used to verify the computer code, evaluate the model's performance, and refine the model.

The DACFIR model was developed by the University of Dayton Research Institute (UDRI) for the Federal Aviation Administration (FAA), to enable the smoke and toxic gas emissions from the burning of interior materials in a cabin fire to be predicted from laboratory test data on these materials. The development of the basic mathematical model is described in Volumes I, II, and III of Department of Transportation (DOT) Report FAA-RD-76-120 [1].

Originally the DACFIR model was developed specifically for simulating fires in wide-body aircraft. Certain parts of the original computer program concerned with the cabin geometry limited the model's application to this type of aircraft. No full scale fire tests have, however, been conducted for wide-body cabins while the results of several series of tests of standard body cabins are available. In order to evaluate the model's performance, a program was initiated to do the following.

(1) Modify the DACFIR program so that both wide-body and standard-width cabin geometry could be used.

(2) Collect information on past full scale burn tests and select a number of these tests to be simulated with the DACFIR model.

---

[1] Reeves, J.B. and C.D. MacArthur, "Dayton Aircraft Cabin Fire Model", Volumes I, II, and III, FAA-RD-76-120, June 1976.

(3) Collect laboratory test data on the interior materials used in the selected full scale tests.

(4) Simulate each full scale test with the DACFIR model and compare the model's results to those of the test.

(5) Identify areas in which the DACFIR model requires refinement and make the indicated refinements where possible.

Based upon the results of the comparison and refinement process, suggested guidelines were established for future full-scale tests to validate the model.

Modifications made to the program, both for the purpose of simulating fires in standard body cabins and as a result of comparisons to full scale tests, are described in Section 2 of this report. Section 3 presents the results of the comparison of the refined model to the full-scale tests and analyzes the model's performance in simulating these cases. Section 4, Conclusions, summarizes the results of this study. Four appendices are added to the report. Appendix A presents the development of a proposed major refinement to the DACFIR model concerning the simulation of the cabin atmosphere dynamics. Appendix B describes the laboratory data collection program conducted in support of the validation exercise. Appendix C is a User's Guide for the computer program which implements the refined version of the model. Appendix D contains derivations of several equations presented in the body of the report.

SECTION 2
REFINEMENT OF THE DACFIR MODEL

This section describes the modifications and refinements of the DACFIR model made as a result of this validation exercise. The modified and refined version of the model is designated as Version 2 of DACFIR or DACFIR2 for short. DACFIR2 retains the basic mechanism for the representation of the fire involvement of the cabin interior materials used in the original model. The paragraphs below give a brief review of the structure of the DACFIR model. For a more complete description, see Reference [1].

In the DACFIR model, the interior surfaces of an aircraft cabin - the floor, ceiling, sidewalls, etc. - are assumed to be flat and have either an exactly horizontal or vertical orientation. To chart the progress of a fire burning on or impinging on a surface, the surface is divided into square elements 0.5 feet on a side; the fire behavior of the material composing the surface being approximated by monitoring the state of each element. Four "fire behavior" states are assumed: (1) virgin; (2) smoldering; (3) flaming; and (4) charred. An element of material in the virgin or charred state does not emit smoke, heat, or gases while an element in the smoldering state may emit smoke and gases but not heat. Elements in the flaming state are the active participants in the fire emitting heat, smoke, and gases. Further, the rates of heat, smoke, and gas release for flaming elements are functions of the imposed heat flux, mainly radiant, fed back from the flames of the fire involving the element.

Transitions of elements from one state to another occur by several mechanisms: creeping flame spread over a surface from groups of flaming elements to adjacent elements not yet ignited, contact and envelopment by flames from a near-by fire striking a surface, and the transition to smoldering caused by the radiant level from a near-by fire. The rates and times that govern these transitions as well as the rates of emission of heat, smoke, and

gases are quantities supplied as input data for the program and are obtained from laboratory measurements made on small samples of the cabin materials.

Once the DACFIR model has determined at a given time in the simulation the states of all elements and the rates of emission of heat, smoke, and toxic gases from those elements actively or passively involved in the fire, the next task is to determine the condition of the cabin atmosphere. The emitted heat, smoke, and gases are used as input to a model of the cabin atmosphere to update its descriptive parameters: temperature, visibility, and gas concentrations which bear upon occupant survival and escape. The cabin gas dynamics model divides the cabin atmosphere into two zones, an upper zone consisting of combustion products and heated and vitiated air, and a lower zone consisting of cooler ambient air. The fire pumps lower zone air into the upper zone which grows in thickness at a rate determined by the fire size, the loss of gas through cabin exits, and the transfer of heat from this zone.

The following sections present the refinements made to the basic model. To simulate fires in cabins of standard width, added flexibility was provided in the model's description of cabin geometry. The gas dynamics calculations were upgraded so that oxygen depletion, forced ventilation, and the effect of a circular cabin cross-section could be included. The radiation heat transfer computations were refined by adding a gray gas approximation for upper zone radiation and by relating the flame radiation to the flame soot concentration.

An alternative approach to modeling the cabin atmosphere, in which calculation of fore-aft temperature and concentration gradients are made, was investigated as a candidate replacement for the present, spatially lumped gas dynamic model. While this new approach appears promising it has not as yet been sufficiently developed so that it may be integrated into the complete DACFIR2 model. For this reason, a description of this horizontal-gradient model has been placed in Appendix A of this report.

2.1 CABIN INTERIOR GEOMETRY

Version 1 of DACFIR was constructed specifically for the simulation of fires within wide-body aircraft cabins. The wide-body cabin arrangement of seats, overhead compartments, and other features does not vary significantly between different wide-body models. Sufficient flexibility was incorporated into Version 1 so that all of the current wide-body cabin configurations could be handled. However, no full scale burn tests of wide-body cabins were available while a relatively comprehensive and well documented amount of test data could be found for cabins of standard width, i.e., that of the B 707/727/737 or DC-8/9 width. Modifications were therefore required to allow the DACFIR model to represent cabin configurations for standard body widths including the older overhead structure of shelf-like hatracks and the more curved sidewall and ceiling surfaces of these smaller fuselages.

A technique was developed through which the user of the DACFIR2 program need only supply a few overall dimensions of the cabin lining surfaces (i.e., the floor, sidewalls, hatracks/stowbins, etc.) and the components of the unit vector normal to the surface. The program assembles the surfaces in the proper arrangement, divides the surfaces into the unit elements, and sets all indices and counters necessary for the fire simulation to proceed over the surfaces. All common transport category cabin interior linings can be represented by this method.

The increased geometric flexibility required a more rigorous definition of the cabin coordinate system. All dimensions, locations, and directions in DACFIR2 are now specified in a single coordinate system. A right-handed cartesian system is used with the origin located in the forward lower right-hand corner of the cabin as viewed facing forward. This coordinate system is shown in Figure 2-1. The figure also shows a typical location for the "detailed section", that part of the cabin

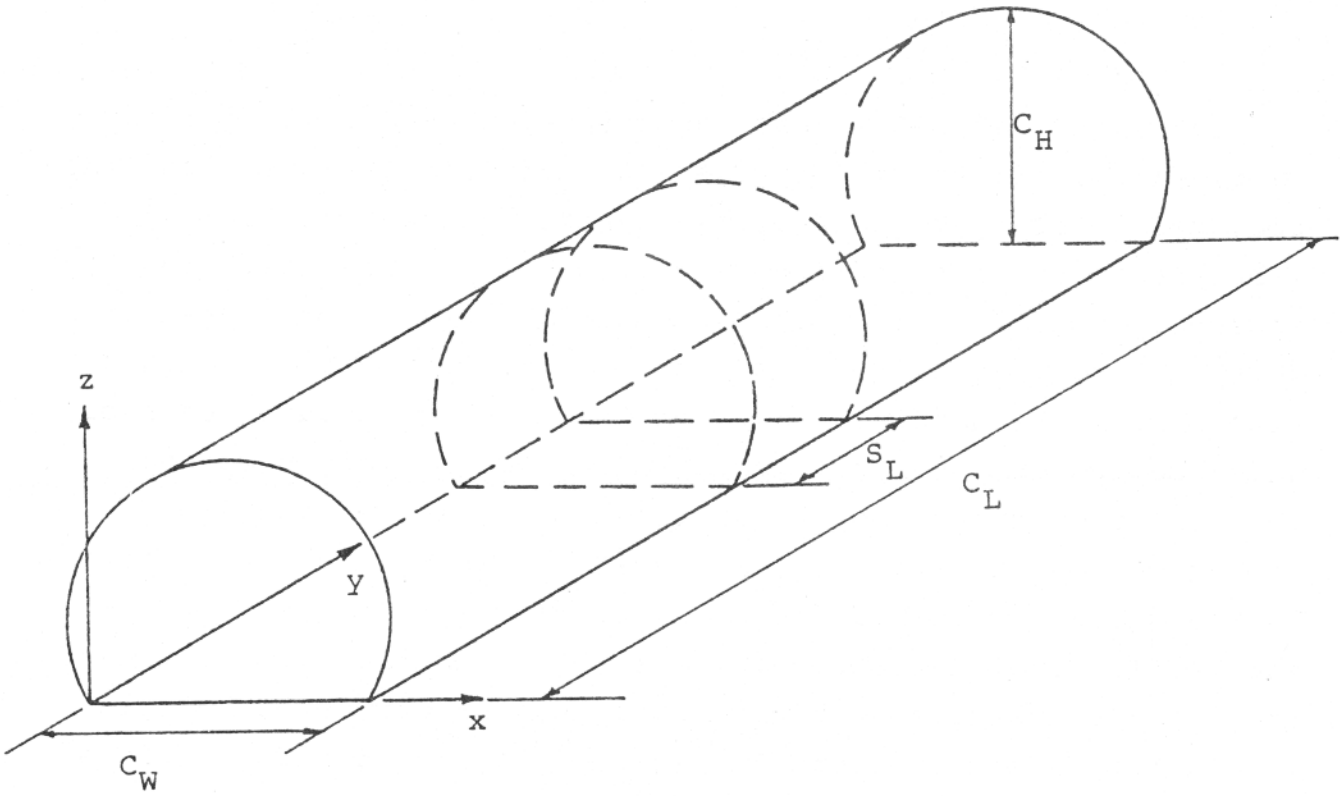

Figure 2-1. Cabin Coordinate System. C_L is the cabin length, C_W is the cabin width, C_H is the cabin height, S_L is the detailed section length. The detailed section contains the materials involved in the fire.

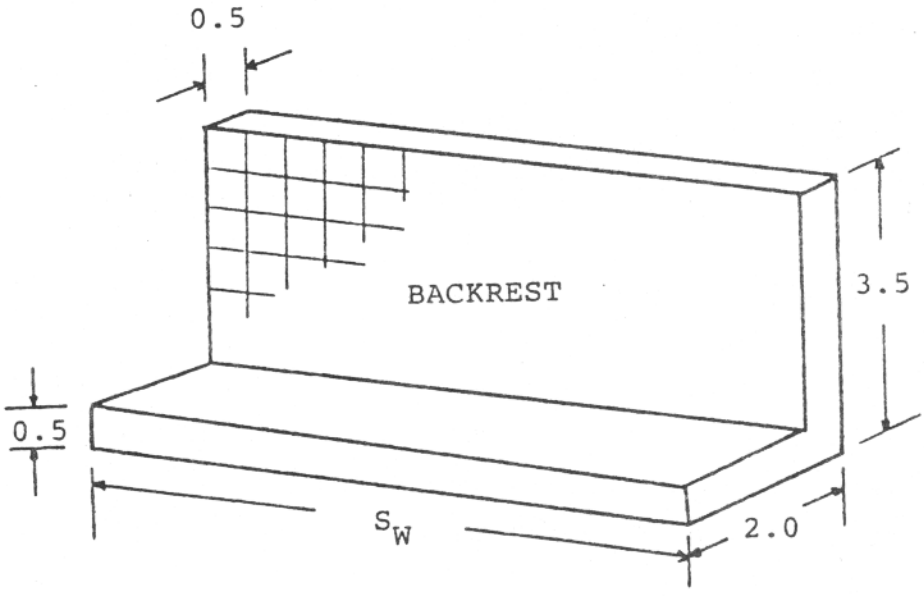

Figure 2-2. Seat Group Configuration. S_W is the seat group width given as a multiple of 0.5 feet. All other seat dimensions are fixed as shown in units of feet.

in which the fire is assumed to originate and thus where the materials are divided into elements for the tracking of the fire. It is in this area that all of the burning is assumed to occur during the simulation period and therefore a considerable savings in computer memory can be realized by keeping track of elements only within this region. The gas dynamics model, however, considers the entire cabin volume.

In DACFIR2, surfaces are assumed to be planar and oriented horizontally or vertically as in the original model. The vector normal to a surface is input to identify the surface orientation and a "z displacement" is also used to locate the bottom edge of the surface with respect to the cabin floor. For horizontal surfaces, the z displacement is the distance from the floor to any point on the surface (as all points are equidistance from the floor). A surface width is specified which is the surface a dimension for vertical surfaces and the x dimension for horizontal surfaces. The dimension of all surfaces in the y direction is taken to be the same as the detailed section length.

Seat positions and seat row widths are user definable in DACFIR2. Seats are modeled in DACFIR2 with the same bench-like approximation of the original model. Seats side by side in a row are regarded as a single bench seat, called a seat group, whose width may be specified provided that it is an integer multiple of 0.5 feet. The other dimensions of a seat are assumed constant. The seat cushion is 1.5 feet from back to front; the backrest 3.5 feet high, and both cushion and backrest are 0.5 feet thick. Figure 2-2 shows the seat configuration and dimensions. Up to nine seat groups may be represented in the model, each with a different width if required. All seats are assumed to face forward, the vertical backrest planes perpendicular to, and the horizontal cushion planes parallel to the floor. The location of each seat group is given by specifying the x and y coordinates of the forward right-hand corner of the seat cushion as viewed by a person sitting in the seat.

An improved method of specifying cabin doors, window exits, or other vents in the cabin walls has also been included in DACFIR2. In the first version of the program, only vents whose opening extended from floor level to a specified height were allowed, that is, only exit doors were recognized. The full-scale tests selected to validate the model used both natural and forced ventilation from air ducts at various heights and through doors of various widths and heights. To accommodate such features, DACFIR2 requires that the height and width of a vent be given and the distance from the top of the vent to the floor be specified.

2.2 THERMAL RADIATION

Two refinements to the methods of computing thermal radiation heat transfer have been made. The first concerns radiation from the hot gas layer to the surfaces in the upper and lower zones. The second is an improvement of the estimation of the local radiation from a fire to its fuel bed.

In the original DACFIR model the upper zone gas was assumed to be opaque and radiate as a black body at the upper zone gas temperature (see Section 5.4, pp. 53-56 of [1]). A step away from this simple estimate of the radiation has been taken by adopting the method of Quintiere[2] in estimating the upper zone gas emissivity as

$$\varepsilon_g = 1 - \exp[-(k_s S + k_g)L] \qquad (2\text{-}1)$$

where ε_g is the emissivity of the upper zone gas,

k_s is the total absorption cross section of the soot (smoke) in the gas (ft^2/particle),

k_g is the gas band absorption coefficient (ft^{-1}),

S is the upper zone smoke concentration (particles/ft^3), and

L is the upper zone thickness (ft) which is used as the radiation mean beam length in this case.

---

[2] Quintiere, J., "The Growth of Fire in Building Compartments", presented at the ASTM-NBS Symposium on Fire Standards and Safety, National Bureau of Standards, Gaithersburg, Maryland, 1976.

The value of k_s was chosen as 0.1054 ft^2/particle of smoke. It is assumed that the soot radiation is not a function of wavelength (gray gas) so that the absorption by the soot is the same for thermal radiation as it is in the visual. Quintiere's value for the gas band absorption coefficient, k_g, of 0.1 ft^{-1} has been adopted. With the upper zone total emissivity, ε_g, defined by Equation (2-1) the net radiation loss terms for the upper zone gas are

(2-2a) $$q_{ru} = \varepsilon_g \sigma A_u \bar{F}_u (T_u^4 - T_{su}^4)$$

and

(2-2b) $$q_{rl} = \varepsilon_g \sigma A_{xs} \bar{F}_l (T_u^4 - T_{sl}^4)$$

where

q_{ru} is the net radiation exchange between the upper zone gas and the upper walls and ceiling at temperature T_{su},

q_{rl} is the net radiation exchange between the upper zone gas and the lower walls and floor at temperature T_{sl},

A_u is the upper wall and ceiling area,

A_{xs} is the area of the interface between the upper zone gas and the lower zone gas,

$\bar{F}_u$ is the effective view factor for the exchange, and

$\bar{F}_l$ is the effective view factor for the gas and lower surfaces.

Equations (2-2a) and (2-2b) given here replace Equations (5-16c) and (5-17c) of [1]. The expressions used for $\bar{F}_u$ and $\bar{F}_l$ are given in Appendix D.

A second refinement of radiation heat transfer in the DACFIR model concerns the computation of flame radiation. The best estimate of the radiation feedback from a fire to its fuel is critical in the DACFIR model since this radiation level is used to select the proper values of flame spread and emission rates from the material's data. The original model used formulations of Dayan and Tien [3] for the radiation from a cylindrical flame to its base center and base edge. These formulations

---

[3] Dayan, A., and C.L. Tien, "Radiant Heating from a Cylindrical Fire Column", Combustion Science and Technology, Vol. 9, (1974), pp.41-47.

involved the assumption of a value for α_c, the total emittance of the flame at the center of its base. A simple estimate of this quantity was made as a linear function of the fire base radius in the original model. In DACFIR2 the development of Dayan and Tien has been followed further to relate α_c not only to the fire base radius but also to the flame absorption coefficient.

For sooty flames, the type expected in cabin fires, practically all of the radiation is due to the soot particles in the flame. Since measurements of the smoke generated by the cabin materials are available, and if it can be assumed that the flame is a gray gas, the emissivities of fires of the materials can be computed from the smoke generation data. Using these assumptions, a method was developed to express the absorption coefficient in terms of the smoke generation rate as

$$k_f = 0.21\dot{p}''(h_f g)^{-1/2} \tag{2-3}$$

where k_f is the flame absorption coefficient (ft^{-1}),

$\dot{p}''$ is the smoke generation rate of the fire fuel (particles/ft^2 · sec),

h_f is the flame height (ft), and

g is gravity (ft/sec^2).

The derivation of Equation (2-3) is given in Appendix D. Using this estimate of the flame absorption coefficient, the emittance at the fire base center is [3]

$$\begin{aligned}\alpha_c = {} & [1 - \exp(-1.8k_f h_f)] \\ & +[1 - \exp(-1.8k_f y_0)] \\ & -\{1 - \exp[-1.8k_f(h_f^2 + y_0^2)^{1/2}]\}\end{aligned} \tag{2-4}$$

where y_0 is the flame cylinder base radius (ft.). Equation (2-4) replaces Equation (4-2) of [1].

Reconsideration of the expression used in the original model for the radiation to the base edge led to a simplification by assuming the appropriate radiation intensity to be that at

the immedidate edge of the fire. The revised expression used in DACFIR2 which replaces Equation (4-1) of [1] is

$$q_1 = 0.5 e_b \alpha_c \tag{2-5}$$

where e_b is the assumed flame emissive power (16.3 Btu/ft^2 . sec).

2.3 OXYGEN DEPLETION

The depletion of oxygen from the upper zone gas by the burning of the cabin materials has been included in DACFIR2. The information to do this is available from the input data items for each material: Q_c, the heat of combustion (Btu/lbm), and γ, the stoichiometric oxygen to fuel mass ratio. Using these quantities, the heat released per unit mass of oxygen burned is given by

$$F_0 = Q_c/\gamma \tag{2-6}$$

where F_0 is the oxygen consumption factor (Btu released/ lbm O_2 consumed) for a given material.

Then, using the heat release rate for the material, the oxygen consumption rate is given by

$$\dot{w}_0 = q''/F_0 \tag{2-7}$$

where $\dot{w}_0$ has units of lbm of O_2/ft^2-sec and q" is the heat release rate of the material in units of Btu/ft^2-sec.

At each time step in the simulation, the individual oxygen consumption rates for each burning material are computed from Equation (2-7) using the appropriate heat release rates and areas in much the same fashion as the toxic gas generation is computed. The gas from which the oxygen is removed is that forming the upward flowing fire plume so that the upper zone is the oxygen depleted region. A conservation equation is used to compute the concentration of oxygen in the upper zone gas,

$$\frac{d}{dT}(Y_0 M_u) = (Y_{0a}\dot{m}_f - \Omega_0) - Y_0\dot{m}_0 + Y_0\dot{m}_i$$

where Y_0 is the mass fraction of oxygen in the upper zone,
M_u is the total mass of gas in the upper zone (lbm),

Y_{0a} is the ambient oxygen mass fraction (0.23),

$\dot{m}_f$ is the mass flow rate of fire plume gas into the upper zone (lbm/sec),

Ω_0 is the total oxygen consumption rate by all fires (lbm/sec), and

m_0 and m_i are the mass flow rates of gas out of ($\dot{m}_0$) and into ($\dot{m}_i$) the upper zone through vents (lbm/sec).

Following the development given in [1] for the upper zone temperature, the oxygen conservation equation can be simplified to eliminate $\dot{m}_0$. Written in the finite difference form used in the computer code, the expression is

$$\Delta Y_0 = [(Y_{0a} - Y_0)\ (\dot{m}_f + \dot{m}_i) - \Omega_0]\ t/M_u \tag{2-8}$$

where ΔY_0 is the change in upper zone oxygen concentration occurring in time Δt.

2.4 FORCED VENTILATION

Four of the seven full-scale burn tests to which the DACFIR model was compared involved forced ventilation of the cabin mock-up. The original model was designed to account for gas flow out of the upper zone and into the lower zone driven only by natural buoyancy, that is "natural" ventilation. Expressions were adopted, Equations (5-12a) and 5-12b) of [1], using the assumption that no mechanically imposed pressure difference exists between the inside and outside of the cabin. An attempt was made to develop expressions that would account for both types of flows simultaneously, for the most general application, but no satisfactory results were obtained. DACFIR2 was therefore revised using expressions for computing the flows through any vent (doors, escape hatches, or ventilation system) based totally on the pressure difference between the cabin interior and exterior developed by the ventilation system and by the expansion of the upper zone gas. A simple orifice flow relationship is employed for flow through a vent.

$$\dot{m}_0 = 0.68 A_v (2\Delta P \rho / g_c)^{1/2} \tag{2-9}$$

where $\dot{m}_0$ is the total mass outflow rate (lbm/sec),
A_v is the effective area of the vent (ft^2)
$\Delta P = P_{cabin} - P_{amb}$ is the interior-exterior pressure difference (lbf/ft^2),
g_c is the Newton constant (32.174 lbm-ft/lbf-sec^2),
and ρ is the density of the flowing gas (lbm/ft^3).

The factor 0.68 is an orifice coefficient. For a large vent, such as a door, the effective area of the vent is determined by computing the fraction of the vent within either the upper or lower zone, depending upon which flow is being calculated.

Cabin pressure is computed from the gas law as

$$P_{cabin} = \rho_u R T_u \tag{2-10}$$

where ρ_u and T_u are the upper zone density and temperature and the gas constant, R, has the value for air, 53.34 lbf-ft/lbm-°R.

Expressions of the form of Equation (2-9) are used for all pressure driven flows out of (or into) the upper and lower zones, the densities and vent areas being set to the appropriate values in each case. In the case of specified flow rates for certain vents, i.e., inflow of the forced ventilation, the mass flow rate produced by the system is fixed for that vent. The ventilation system is thus assumed to be able to overcome the pressure rise caused by the fire.

2.5 THERMAL DISCONTINUITY POSITION

The original DACFIR model was designed for the approximately rectangular interior of wide-bodied aircraft. In order to simulate fires in standard width cabin structures, the computer code was modified to account for a more cylindrical geometry. Assuming a truncated circular cabin cross section (see Figure 2-1) and known cabin width and height, expressions were derived for the cabin volume and surface area. These expressions replaced their rectangular-dependent counterparts in the equations describing the gas dynamics. In particular, a major change in coding

resulted from the thermal discontinuity position (upper layer depth) being implicitly related to cross sectional area rather than by the explicit relationship of the original model. Accordingly, an iterative scheme is employed to solve for the discontinuity position.

A switch is set at the start of DACFIR2 indicating selection of rectangular or cylindrical geometry. The equations for upper zone volume, V_u, and upper zone surface area, A_{su}, remain unchanged from the original model in the rectangular case. In the cylindrical case, the upper zone volume is

$$V_u = A_{xs}C_L = [r^2\cos^{-1}(1-L/S)-(r-1)(2rL-L^2)^{1/2}] \cdot C_L \qquad (2\text{-}11)$$

where L is upper zone depth, C_L is cabin length, and r is a radius defined by

$$r = (C_W^2/4 + C_H^2)/(2C_H)$$

where C_H is the cabin height and C_W the width. The upper surface area is given by

$$A_{su} = 2r\cos^{-1}(1-L/r) \cdot C_L \qquad (2\text{-}12)$$

The lower zone volume is calculated as the total volume less the upper volume, and an analogous relationship is used to obtain the lower surface area.

Another refinement to the original model was a correction for the seat volume contribution to the total cabin volume which is a factor in the upper zone depth calculation. The number of seat groups and standard seat group shape are used in the computation. A series of tests are made to determine the fraction of the total seat volume that is enveloped by the upper zone and a correction term is then obtained from this fraction for both the upper and lower zone volumes. With the corrected volumes known, the thermal discontinuity is obtained from Equation (2-11) or its equivalent for the rectangular cross section fuselage.

SECTION 3

COMPARISON OF THE MODEL TO SEVEN CABIN FIRE TESTS

This section presents the results of the comparison of DACFIR2 to seven full-scale cabin mock-up fire tests conducted during the Aerospace Industries Association Crashworthiness Development Program in 1968[4,5]. These fire tests were conducted to determine the effect of furnishing cabins with materials of improved fire resistance. Baseline cases were established by conducting tests with cabins furnished with materials in commercial use at the time. Several sets of improved materials were then tested under conditions identical to the baseline tests. A number of these tests involved candidate on-board suppression systems in addition to improved furnishing materials.

From the test series, six tests were initially selected as most appropriate for comparison to DACFIR2. The choice was dictated by considerations of materials used, ventilation conditions, and whether or not suppression was involved, since the present DACFIR model does not include fire suppression. A seventh test involving only an ignition source, a pan of jet fuel, was added later as a specific exercise for the gas dynamics calculation. After the validation tests (cases) were selected, the furnishing materials involved were identified and samples of the materials were obtained for laboratory testing. The results of laboratory tests were processed into a form compatible for input to the DACFIR2 program. Simulations of each case were made and the results put into tabular and graphical form for analysis.

---

[4] Nygren, L.O., and A.F. Deardorff, "AIA Crashworthiness Program - Fire Suppression Section - Results of Fire Suppressant System Survey and Tests", D6-19456-3TN, The Boeing Company, November 1968.

[5] Vaughn, G.F., Deardorff, A.F., and L.O. Nygren, "AIA Crashworthiness Program - Fire Suppression Section - Airplane Crash Fire Tests to Evaluate Fire Protection Improvement Devices and Materials", D6-19456-8TN, The Boeing Company, October 1968.

3.1 THE CABIN MOCK-UP FIRE TESTS

The seven fire tests selected for validation of the model may be divided into two groups.

3.1.1 15-Foot Cabin Mock-Up Tests

The first group consists of five tests conducted in a 15-foot long, constant cross-section stainless steel fuselage of 850 cubic foot volume. Four of the five tests involved furnishings. The fifth test - actually the averaged results of three tests - was a fuel pan calibration run involving only the ignition source in the bare metal fuselage. The cabin interior mock-up in the 15-foot mock-up tests consisted of side-wall panels, a hatrack, ceiling panels and three rows of simulated seats. These furnishings were installed on the port side of the fuselage only, the starboard side and floor remained bare metal. Figure 3-1 shows the cross section of the 15-foot cabin mock-up, and Figure 3-2 gives a plan view of the seat arrangement.

The interior furnishing used in each of the four 15-foot mock-up tests were as follows.

Case 15P - Present In-Serivce (1968) Materials

Sidewall:	Vinyl-coated aluminum sheet.
Hatrack:	Polyurethane foam covered with vinyl-coated fiberglass cloth.
Ceiling:	Paper-honeycomb-core, fire-retardant polyester-fiberglass-laminate-faced sandwich panel covered with vinyl-coated fiberglass.
Seats:	Muslin-covered polyurethane foam, upholstered in Nylon fabric.

Case 15A - Improved Materials Set "A"

Sidewall:	Enameled aluminum panels with PVF* surface film. (Samples of this material were not available for laboratory testing).

*Polyvinyl Fluoride

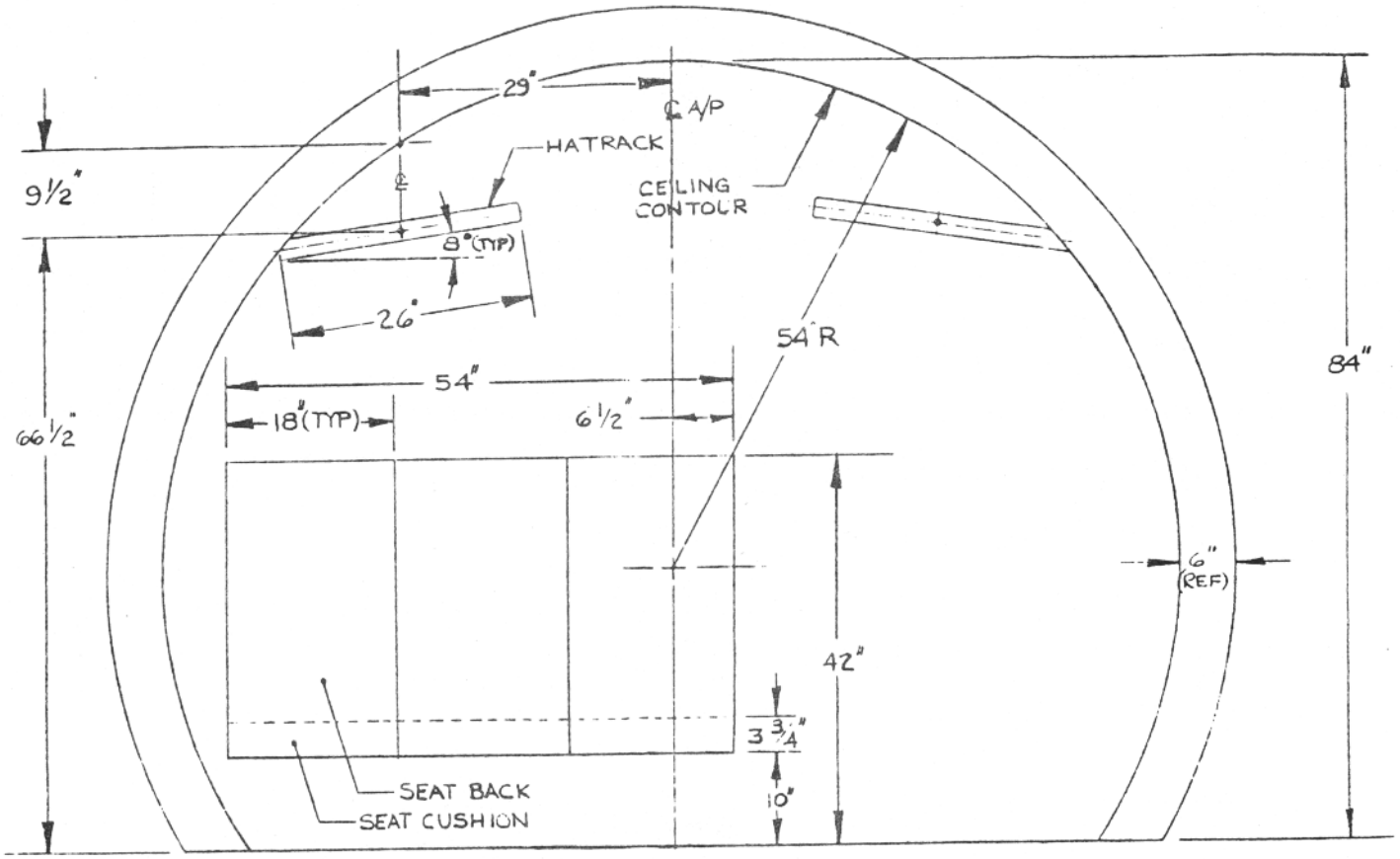

Figure 3-1. 15-Foot Cabin Mock-Up View Looking Forward

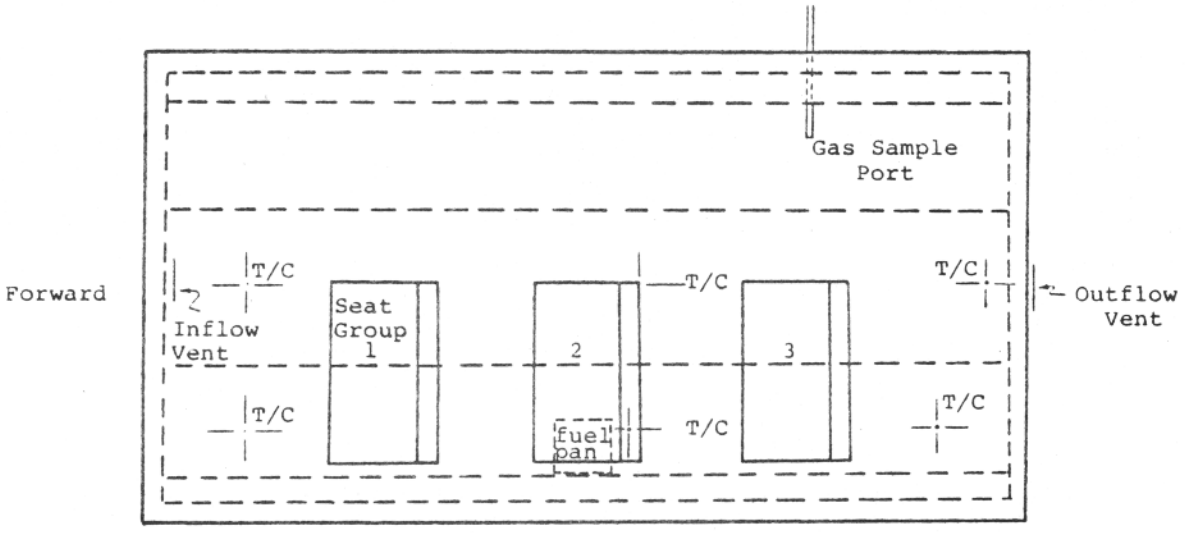

Figure 3-2. Plan View of the 15-Foot Cabin Mock-Up

Hatrack:	Nylon-honeycomb-core, fire-retardant epoxy fiberglass-laminate-faced sandwich panel covered with a fiberglass mat for padding and a final covering of vinyl-coated fiberglass.
Ceiling:	Nylon-honeycomb-core, fire-retardant epoxy fiberglass laminate-faced sandwich panel with printed PVF surface.
Seats:	Muslin-covered polyurethane foam upholstered with Nylon fabric.

Case 15B - Improved Materials Set "B"

Sidewall and Ceiling:	Nylon-honeycomb-core, fire-retardant epoxy fiberglass-laminate-faced sandwich panel with printed PVF surface.
Hatrack:	Nylon-honeycomb-core, fire-retardant epoxy fiberglass-laminate-faced sandwich panel with PVF.
Seats:	Flame-retardant polyurethane covered with a Nylon-fabric slip-cover, and upholstered with Nylon fabric.

Case 15C - Improved Materials Set "C"

Sidewall and Ceiling:	Nylon-honeycomb-core, fire-retardant epoxy fiberglass-laminate-faced sandwich panel with printed PVF surface.
Hatrack:	Nylon-honeycomb-core, fire-retardant epoxy fiberglass-laminate-faced sandwich panel with PVF surface.
Seats:	Fiberglass cushion in a Nylon slip-cover, upholstered with Nylon fabric.

Materials in the first case, 15P, were characteristic of the then in-service materials which involved extensive use of vinyl coated fabrics, paper honeycomb structural panels, and non-fire-retardant polyurethane (PU) foams. The improved materials of Case 15A included hatracks and ceilings of a nylon based honeycomb sandwich. The sidewall in this case was of an enameled

aluminum sheet construction, samples of which were not available for laboratory testing. Lack of this data may not completely invalidate comparison of the program to this case for reasons mentioned below. The materials of Cases 15B and 15C were identical except for the seat cushion material: a fire retardant polyurethane foam in 15B and an inert fiberglass padding in 15C. Comparison of the results of these two tests indicate the effect of the seat foam material which was suspected of being a major contributor to the fire.

Ventilation of the 15-foot cabin mock-up was provided by the forced flow from a regulated blower. Air entered the mock-up at a baffeled inlet duct forward and exited through a vent near ceiling level at the rear. A flow rate of 200 cubic feet per minute was maintained by the blower throughout the tests.

Ignition of the fire in each of the five 15-foot mock-up tests was accomplished in the same manner, a 12 inch by 12 inch (1 ft^2) metal pan filled with one quart of Jet A-1 fuel floating on water was placed beneath the center seat row next to the sidewall (see Figure 3-2). From 10 to 30 seconds were required for flames to spread over the entire fuel pool surface after ignition was initiated at one edge of the pan. When the fuel surface was completely involved in flame, that time was denoted as zero in the data collection process. The fire in each test was allowed to burn for 300 seconds (five minutes) after time zero.

Instrumentation in each of the 15-foot mock-up tests provided measurements of cabin atmosphere temperature and composition. Temperature was measured by six thermocouples: three located two inches below the ceiling on the cabin fore-aft centerline at one inch, 99 inches, and 144 inches from the aft bulkhead; and three located two inches below the left hatrack at 43 inches, 99 inches, and 133 inches from the aft bulkhead. Figure 3-2 shows the position of the six thermocouples.

The gas sampling port was located at 42 inches above the floor and the same distance forward of the aft bulkhead. The end of the tube forming the port extended approximately 24 inches into the cabin from the starboard sidewall (see Figures 3-1 and 3-2). Gas samples were withdrawn through the port and collected in plastic bags for chemical analysis. The cabin atmosphere was sampled for oxygen, carbon dioxide, carbon monoxide, hydrocarbons, acid gases, chlorides, fluorides, acrolein, Freon 1301, ammonia, nitrogen dioxide, carbonyls, and hydrogen cyanide. Concentrations of these gases were reported at 30 second intervals. The laboratory tests on the furnishing materials measured only the combustion products carbon dioxide, carbon monoxide, hydrogen chloride, hydrogen fluoride, hydrogen cyanide, and nitrogen dioxide and thus only the concentrations of these species, in addition to oxygen concentration, were used in comparisons to the computer simulations. Table 3-1 gives the measurement technique in the full scale testing for each substance and the estimate of measurement accuracy.

TABLE 3-1

ANALYSIS OF THE CABIN ATMOSPHERE - AIA CABIN FIRE TESTS

Substance	Method of Analysis	Accuracy
Oxygen	Potentiometric Oxygen Meter	$\pm$ 0.5% O_2
Carbon Dioxide	Volumetric Meter	$\pm$ 0.2% by volume
Carbon Monoxide	Detector tubes	$\pm$ 25% by volume
Hydrogen Chloride	Silver nitrate titration	*
Hydrogen Fluoride	Thorium nitrate-alzarin titration	*
Nitrogen Dioxide	Detector tubes	$\pm$ 25% by volume
Hydrogen Cyanide	Detector tubes	$\pm$ 25% by volume

*accuracy estimates for these substances not given in terms of a percentage of the measurement.

3.1.2 26-Foot Cabin Section Tests

The remaining two tests of the seven selected for comparison to the model were conducted in the aft 26 feet of a B727 fuselage cabin furnished to simulate a complete passenger cabin. Total cabin volume was about 2000 cubic feet. The first of these two tests, designated 26P, used furnishing characteristic of the then in-service materials. The other test, 26N, employed a set of improved materials. Materials used in the 26 foot fuselage cases were similar to those in Cases 15P and 15B with some additions such as carpet and passenger service units. The materials for each test were as follows.

Case 26P - Present In-Service (1968) Materials

Carpet:	Acrilan pile with muslin faced polyurethane foam pad.
Sidewall:	Vinyl-Aluminum laminate.
Window Reveals:	ABS
Window Dust Panes:	Acrylic
Hatrack:	Vinyl coated fiberglass, polyurethane foam, resin coated fiberglass, and resin impregnated paper honeycomb. Bull nose: ABS covering polyurethane foam.
Passenger Service Units:	ABS
Ceiling Panels:	Paper honeycomb core, resin coated fiberglass fabric, vinyl cover.
Seats:	Wool and muslin upholstered polyurethane foam.

Case 26N - Improved Materials

Carpet:	High temperature resistant nylon pile (material not available for laboratory testing).
Sidewall:	PVF faced nylon honeycomb core sandwich panels.
Window Reveals:	Polycarbonate

Window Dust Panes:	Polycarbonate and acrylic (alternating)
Hatrack:	PVF faced nylon honeycomb core sandwich panels.
Passenger Service Units:	Polycarbonate (units simulated by sheet stock).
Ceiling Panels:	PVF faced nylon honeycomb core sandwich panels.
Seats:	High temperature resistant nylon and muslin upholstered polyurethane foam.

Figure 3-3 shows a cross-section of the 727 cabin and Figure 3-4 gives a plan view of the seat locations for both tests.

Ventilation of the cabin was by natural flow out two openings, a 2 foot wide by 4 foot high exit at the aft and the second a 3 foot wide by 7 foot opening in the forward bulkhead. The ignition source was a 30 x 30 inch fuel pan containing seven quarts of Jet A-1 fuel on water. An 18 by 24 inch section of the cabin wall was cut out at floor level and a section 18 inches wide and 8 inches deep removed from the floor to simulate a fuselage rupture. The fuel pan was inserted in this region extending about half way into the cabin. Figure 3-5 shows this arrangement. Time zero for measurements in the 26-foot cabin tests was intended to be, as in the 15-foot mock-up cases, the time at which the entire fuel pan was involved in flames. This procedure was followed for 26P but problems were encountered with Case 26N. In this case flames would not enter the cabin but remained totally on the outside of the fuselage until an exterior wind screen was removed at 78 seconds after ignition. At that time flames did enter the cabin and came in contact with the interior materials. Time calibration of data in case 26N was therefore adjusted so that time zero was the point when flames entered the cabin. To prevent damage to the fuselage structure, case 26P was terminated with CO_2 extinguishment at 202 seconds and case 26N at 162 seconds (adjusted).

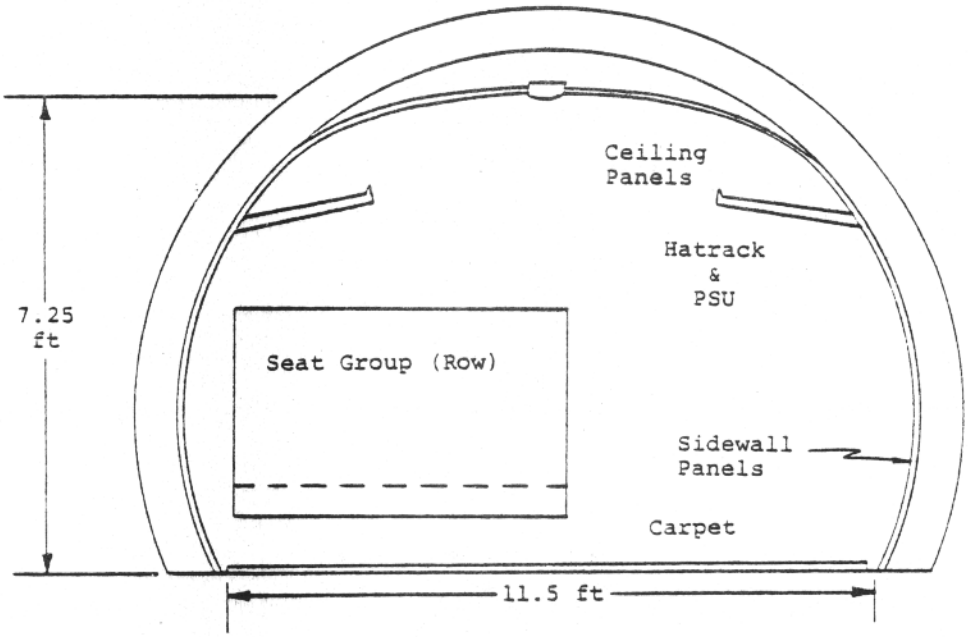

Figure 3-3. Cross Section of the 26 Foot Fuselage Test Section Only the position of the port seat row is shown.

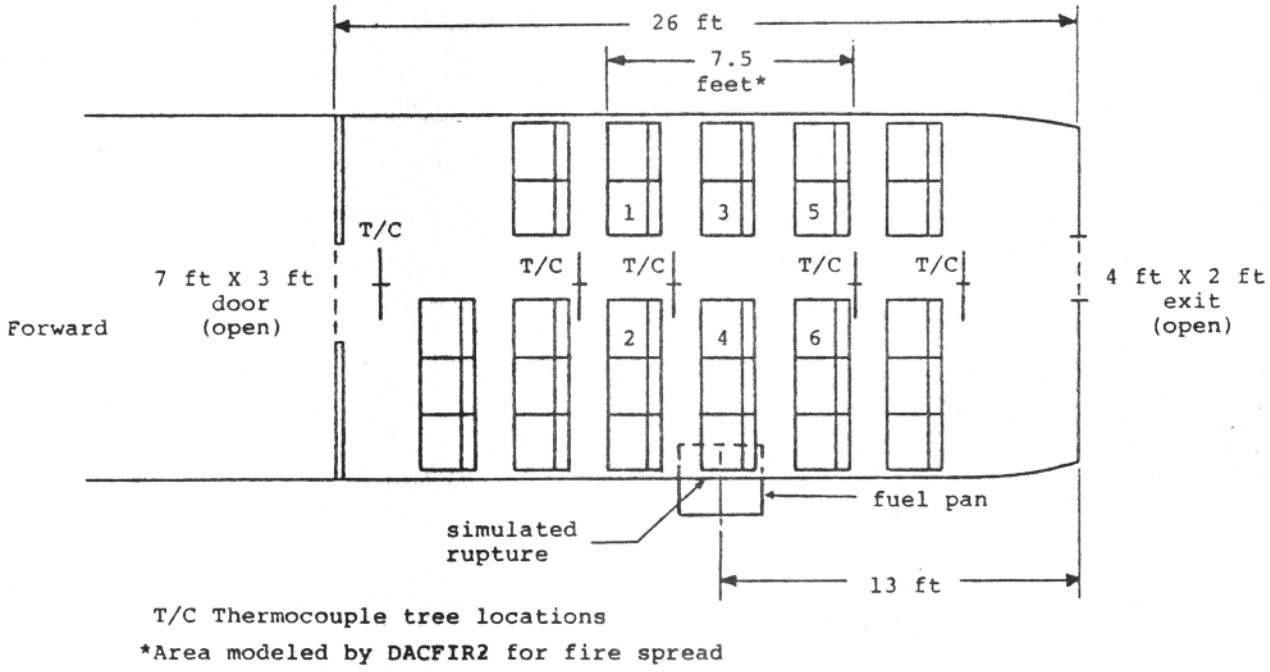

Figure 3-4. Plan View of the 26 Foot Fuselage Test Section

More instrumentation was used in the 26-foot fuselage tests than in the 15-foot mock-up tests. The temperature field of the cabin atmosphere was measured by 50 thermocouples located on five trees. Each tree provided measurements at the 10 points shown in Figure 3-6. The position of each tree in the cabin is shown in Figure 3-4. Gas sampling was made through two ports in the furnished section. Port A was 48 inches from the floor and directly opposite the ignition fire and port B was at the same vertical level and on the same side as A but near the forward bulkhead. These positions are shown in Figure 3-4. Samples of the cabin atmosphere were withdrawn at 30 second intervals and analyzed for the same compounds as the samples in the 15-foot mock-up cases (see Table 3-1). Additional temperature measurements were made in the 26-foot fuselage tests using shielded and aspirated thermocouples, calorimeters, and wet bulb thermocouples.

3.2 LABORATORY TESTS OF CABIN MATERIALS

Furnishing materials of the AIA-CDP cabin mock-up tests described above were subjected to a series of laboratory tests to provide input data for the DACFIR computer program. Tests were conducted under subcontract to UDRI by the Boeing Materials Services division of the Boeing Commerical Airplane Company. The final technical report submitted by Boeing is attached as Appendix B of this report and contains a full description of the testing program. Testing was conducted on samples of 25 separate materials. Three other materials used in the full scale burn tests could not be obtained for laboratory analysis.

Tests were made in the Ohio State University (OSU) combustion analyzer for the following:

- Rate of surface flame spread in horizontal, vertically upward, and vertically downward directions;
- Time to flame (ignite) when exposed to a small pilot flame;

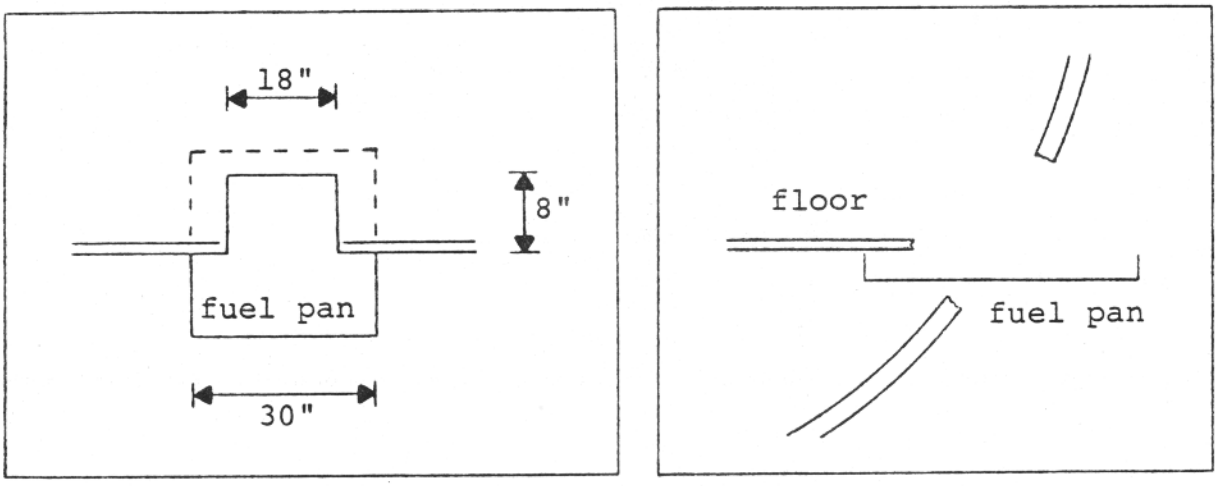

Figure 3-5. Fuel Pan Location Details - 26-Foot Cabin Cases

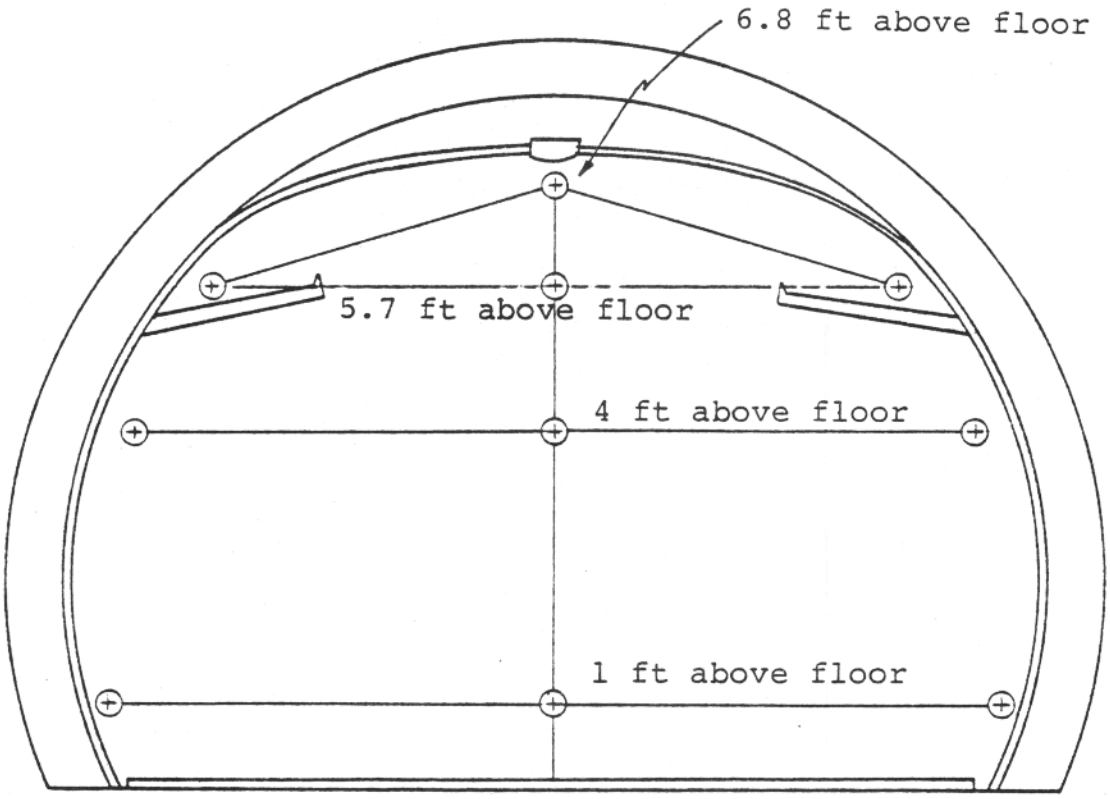

Figure 3-6. Thermocouple Locations in the 26-Foot Fuselage Test Section

- Time to burn (time from ignition to the burned out or charred state);
- Heat release rate and total heat released;
- Smoke release rate and total smoke released.

Each of these items was measured at four levels of externally applied heat flux, 1.32 Btu/ft^2-sec (1.5 W/cm^2), 2.20 Btu/ft^2-sec (2.5 W/cm^2). 3.08 Btu/ft^2-sec (3.5 W/cm^2), and 3.96 or 4.40 Btu/ft^2-sec (4.5 or 5.0 W/cm^2). Materials were tested in the OSU analyzer in the orientation(s) in which they were installed in the cabin.

Tests were also conducted on the materials in the smoldering state (radiant exposure only without pilot flame) in the OSU device for the data items.

- Time to smolder (time from start of exposure at given flux level to the start of pyrolysis)
- Time to char when smoldering (time from the start of smoldering to the finish)
- Rate of smoke release in the smoldering state.

Rate of heat release in the smoldering state was also measured but this quantity is not used by the present DACFIR model. (Examination of the measured rates of smoldering heat release show that they are almost always insignificant with respect to the flaming heat release rates, thus justifying their neglect.)

Flame spread rates and the various times of transition were recorded by Boeing and reported for individual runs and averages of several runs when more than one run was made. Rate of heat release and rate of smoke release data from the OSU analyzer were recorded on strip charts. The curves from these charts were automatically digitized and input to a data processing program that determined the total amount of heat and smoke release (by integration) and the maxima and time averages of these quantities. Results from multiple runs were also averaged and reported.

Testing of the interior materials for toxix gas generation was done using a National Bureau of Standards (NBS) Smoke Chamber specially modified for gas composition measurements. Concentrations of HCl, HF, HCN, NO_2, and SO_2 were measured with colorimetric indicator tubes while CO_2 and CO were measured by process instruments. Appendix B gives the details of these measurements.

Additional processing of the materials data supplied by Boeing was necessary in order to form input data for the DACFIR model. The type of treatment differed for each data item and is best described by considering each item in turn.

Flame spread rates Flame spread rates were converted to units of feet/sec from the reported units of inches/min.

Time to flame, Time to burn Two methods were used to determine the times of ignition and burnout. First a visual observation of these times was made for each test. Second, the heat release rate curve was examined to determine when, for example, a net positive rate of heat release indicated ignition or when the rate of heat release returned to zero indicating burn-out. While the second method appears at first to be more accurate, it was found that the thermal inertia of the OSU analyzer was so significant that times read from the raw heat release curves could lag behind the visual measurements as much as 30 seconds or more. The visual measurements were therefore used in all cases.

Heat Release Rate The Boeing computer program for processing the OSU analyzer data integrates the heat release rate curve to obtain total heat release. This value is reported in Joules/cm^2. After conversion to units to Btu/ft^2, the heat release rate for each material was computed by dividing the total heat released by the time to burn (average of all values if more than one run was made). The heat release rate used is therefore an average value, constant over the sample burn time.

Smoke Release Rate Cumulative smoke release was reported as optical density per unit sample area. This number was converted to "particles" of smoke released per unit area by dividing by the conversion factor 0.045757 ft^2/particle. An average release rate was then found by dividing the total smoke particles released per unit area by the time to burn or time to smolder out as appropriate.

Toxic Gas Release Rates The NBS Smoke Chamber is not a flow-through device; instead smoke and gases emitted by the sample accumulate within the 18-cubic feet of the chamber volume. Since a gas release rate is to be supplied as input to DACFIR, several operations were required to convert the reported concentration values to release rates. Concentrations of each gas specie of interest were measured at 1, 2, 4, and 10 minutes during the tests. The maximum concentration, usually that at 10 minutes, was converted to mass units using the chamber volume and assuming the chamber gas to be at atmospheric pressure and room temperature. The rate of emission per unit sample area was then computed from the reported value of time to burn out or time to smolder out and the sample area. Corrections to the release rates were made for two gases, CO_2 and CO. When samples were tested in the flaming mode, CO_2 was generated by the propane pilot flame. This rate, known independently from calibration runs using an inert sample, is about 340 ppm per minute. A small correction was also made for the atmospheric concentration of CO_2, 300 ppm. Generation of carbon monoxide by the pilot flame was also detected in calibration runs. The rate of generation varied with the radiant exposure level, decreasing at higher fluxes. (Indicating, perhaps, that CO is produced by quenching of the pilot on the cool sample surface). The maximum rate of 150 ppm/min was detected at a flux of 1.32 Btu/ft^2-sec (1.5 W/cm^2) and the smallest rate of 30 ppm at 4.4 Btu/ft^2-sec (5.0 W/cm^2). These rates were used to correct all CO emission data for flaming exposures.

3.3 COMPARISON OF THE DACFIR MODEL TO THE TEST RESULTS

The results of the DACFIR2 model's simulation of each of the seven cabin fire tests are discussed below. The comparison of the program output to the test data is given in two forms: (1) plots of the predicted and measured values of cabin gas temperature and composition; and (2) tables and figures giving the areas of burned material computed by the model and observed at the end of each test. Figures are also presented for smoke concentration, but since no quantitative smoke measurements were made in the tests only the model's results are shown. The results presented are those after all the refinements described in Section 2 were made and represent the current ability of DACFIR2 to reproduce these tests based upon the material input data used.

3.3.1 Case 15Z - Fuel Pan Calibration Tests

The first comparison of model and tests was for a series of "fuel pan calibration" tests conducted in the 15-foot mock-up fuselage without furnishing materials. The fire consisted of the one square-foot pan of Jet-A fuel. This fuel, fire size, and location were subsequently used as the ignition source in each test with materials. The ability of the DACFIR program to correctly simulate these "no-spread" burn tests was used as an intermediate step in validating the program.

Heat and smoke release rates for jet fuel were measured in the OSU analyzer and the values were used as input for the simulation of the fuel pan fire. Data on Jet A from Sarkos[7] was used to estimate the carbon monoxide production rate for the fuel. Since no direct measurements of CO_2 production could be found for jet fuel, this rate was estimated by assuming a simple combustion model (reaction equation) for the jet fuel. The rate of release of carbon as smoke was calculated

---

[7] Sarkos, C.P. "Measurement of Toxic Gases and Smoke from Aircraft Cabin Interior Materials Using the NBS Smoke Chamber and Colorimetric Tubes", FAA-RD-76-7, March 1976.

from the observed smoke release rate by a method of Seader and Ou[8]. With the rate of carbon release known for CO and smoke, the remaining carbon, about 94% of the total in the fuel, was assumed to occur as CO_2. Since the mass burning rate for the fuel is specified as input for the model a CO_2 rate could then be computed.

Figure 3-7 shows the computed upper zone temperature, solid curve, and the readings from two representative ceiling thermocouples, the broken curves. The pattern of temperature rise in the test is a general increase from the ambient, about 70°F, to between 250°F at the aft ceiling and 340°F at the center ceiling. The theoretical curve rises quickly to 218°F and then maintains a very slow rise to 245°F when the test was terminated. Figures 3-8, 3-9, and 3-10 show, respectively, the comparisons of measured and computed oxygen, carbon dioxide, and carbon monoxide concentrations. In each figure the observed and computed results seem to follow the same trends of slow increase, or decrease for O_2, throughout the run. The computed upper zone depth of this run (not shown) was quickly established at about 3.5 feet and grew slowly to 4.5 feet by 300 seconds.

The figures show generally good agreement between the model's predictions and the measured results for this fairly simple case in which there is no fire spread. In the comparison of temperatures, Figure 3-7, the rapid rise of the computed temperature is due to the assumptions of a steady-state fire and plume and a spatially uniform upper zone which does not mix with the lower zone. Most of the difference between the computed and observed results for the first two minutes is probably due to these assumptions since in the test the early gas motion in the upper cabin would be expected to include significant mixing. The approximately constant

---

[8] Seader, J.D., and S.S. Ou, "Correlation of the Smoking Tendency of Materials," Fire Research, Vol. 1, No. 1, March 1977.

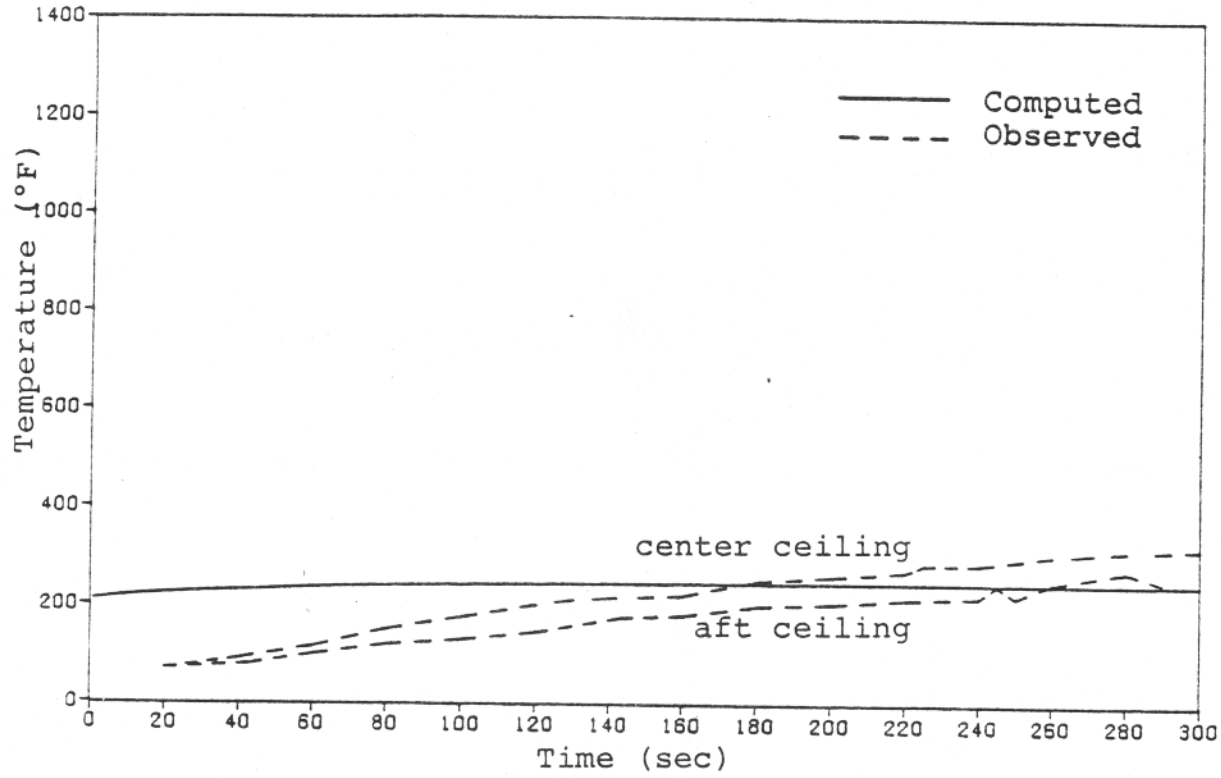

Figure 3-7. Upper Zone Temperature - Case 15Z

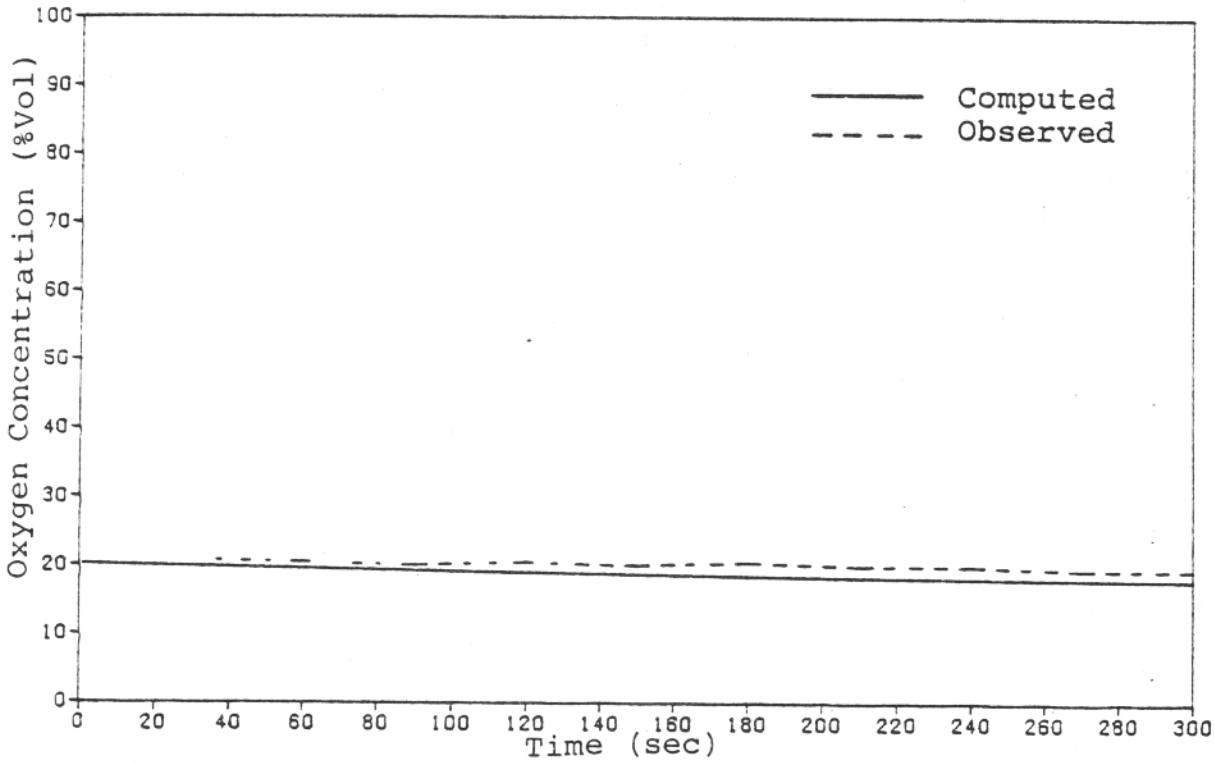

Figure 3-8. Oxygen Concentration - Case 15Z

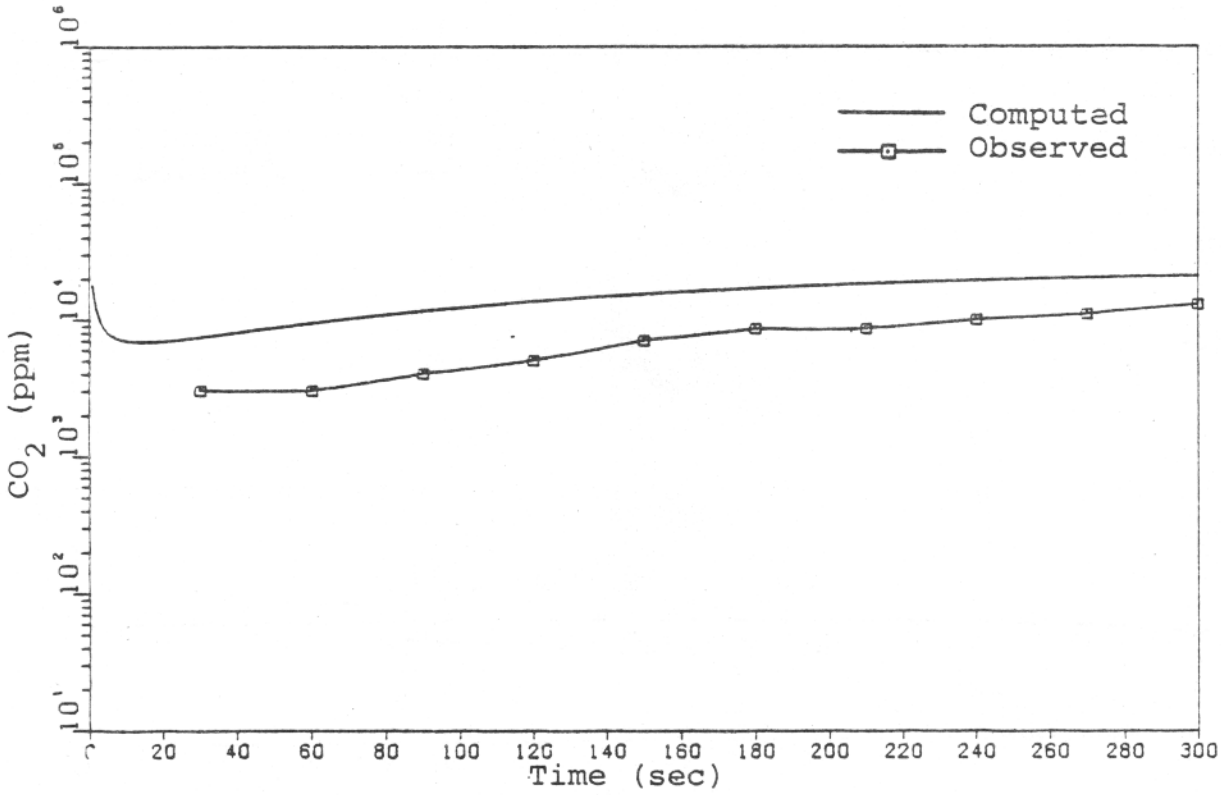

Figure 3-9. Carbon Dioxide Concentration - Case 15Z

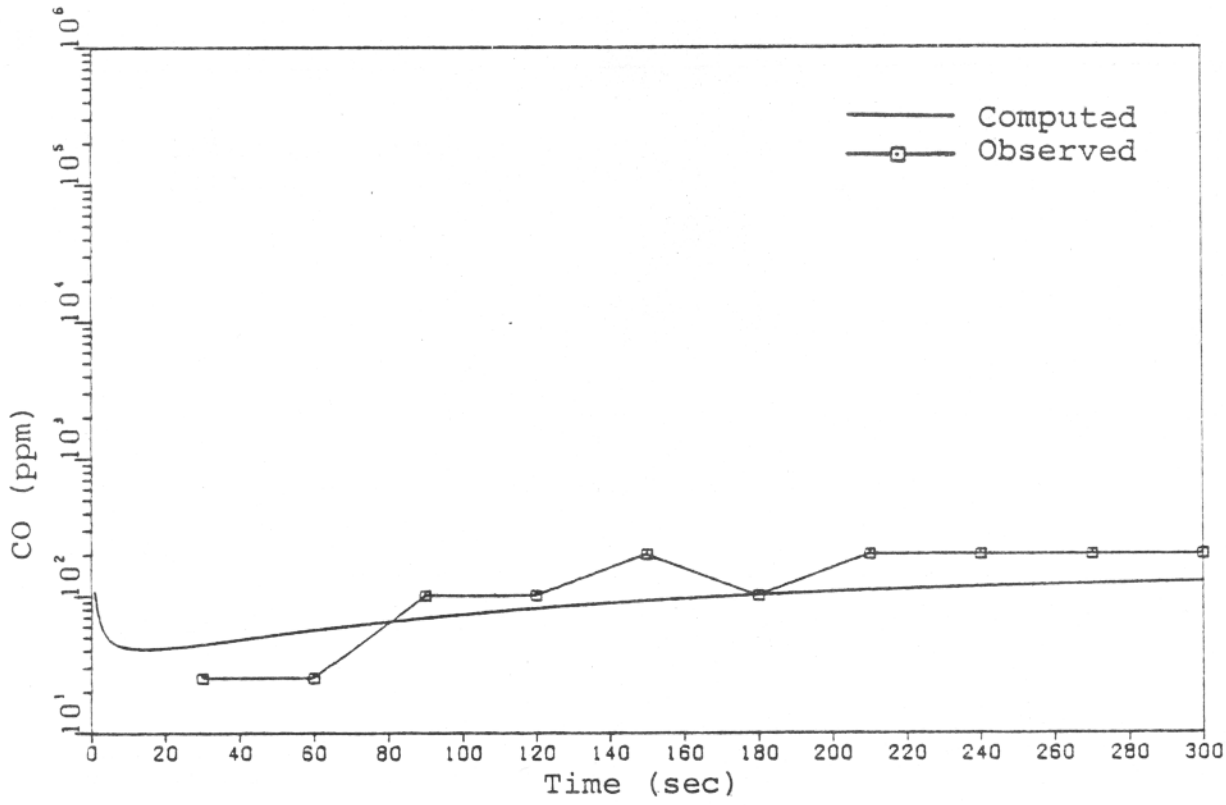

Figure 3-10. Carbon Monoxide Concentration - Case 15Z

difference, about 75°F, between the aft and center ceiling temperatures throughout the test indicates that some cooling of the horizontal ceiling flow occurs even in this short fuselage.

The model did well in predicting the accumulation of carbon monoxide and the consumption of oxygen and somewhat less well the CO_2 concentration. Since the method of establishing the input value of CO_2 production rate was rather approximate, the difference in the results is not surprising.

3.3.2 Case 15P - Present In-Service (1968) Materials

Figures 3-11 through 3-20 give the calculated and observed results from Case 15P, the pre-1968 furnishings in the 15 foot mock-up cabin. Figure 3-11 shows that the model predicts the upper cabin temperature reasonably well for the first three minutes of the test. After 180 seconds there seems to have been a flashover in the cabin mock-up as indicated by the sharp rise of the themocouple readings at 200 seconds. After the flashover the fire diminished substantially or self-extinguished as indicated by the falling temperature readings. The model does not consider flashover (the mechanism is as yet not well understood) and so the computed temperature rises slowly toward an equilibrium of about 1050°F during the last two minutes of the test. It is interesting to note, however, that if one simple criterion for flashover is used, that given by Quintiere[2] as an upper zone temperature of 600°C (1112°F), the gas temperature predicted by DACFIR2 reached the vicinity of 1050°F at about 215 seconds and thus the model indicates that flashover could have been expected at or near 200 seconds.

In Figure 3-12 the computed and observed oxygen concentrations are compared. It can be seen that the computed curve predicts a much lower oxygen concentration than that ovserved. The discrepancy is probably due to the assumption of complete (stoichiometric) burning by the model and so suggests

---

[2] Quintiere, op. cit.

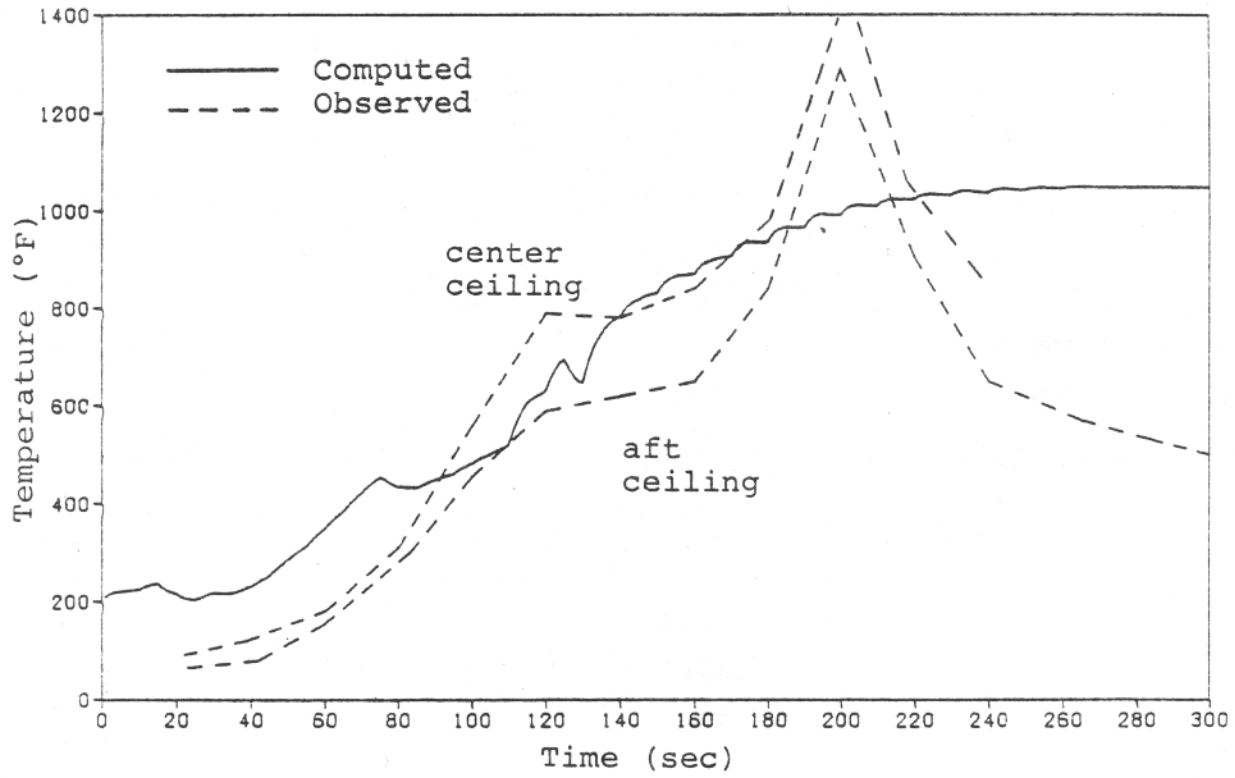

Figure 3-11. Upper Zone Temperature - Case 15P

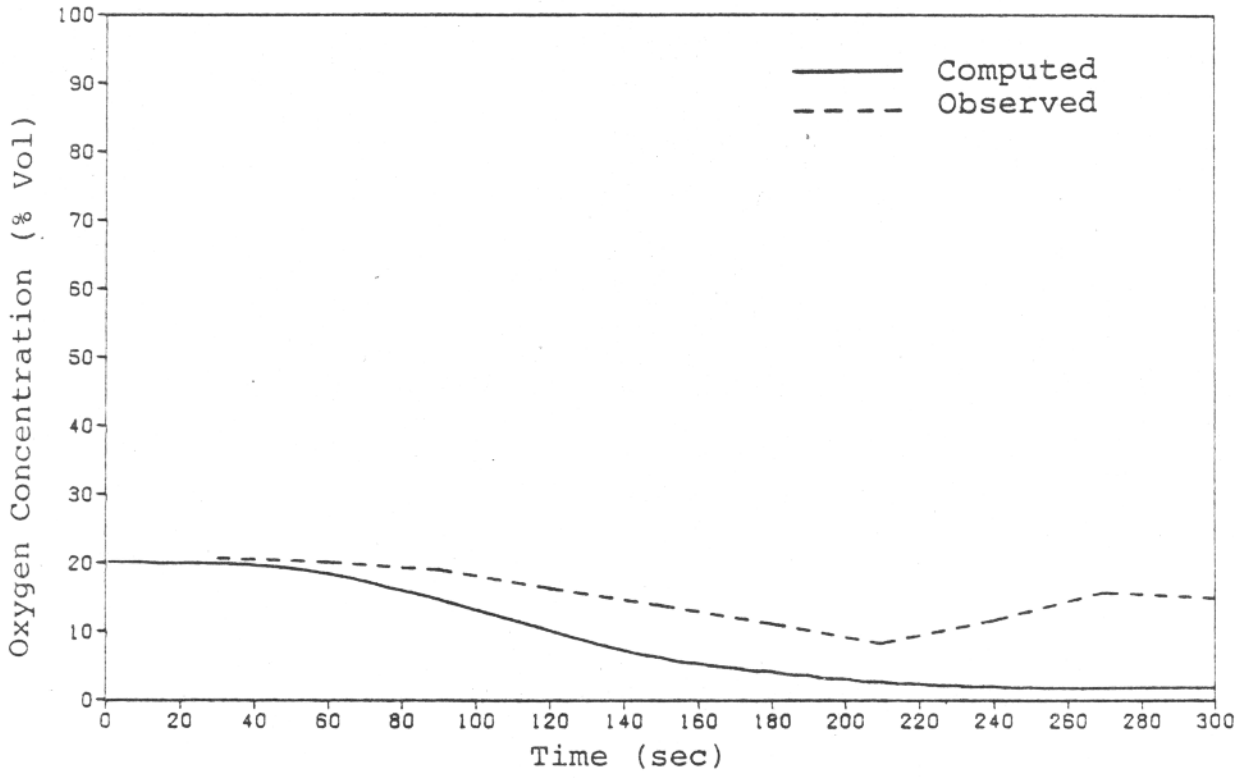

Figure 3-12. Oxygen Concentration - 15P

that the actual combustion efficiency is rather low. For the toxic gas accumulation Figures 3-13 through 3-17 show that, with the exception of HCl, the concentrations are reasonably well predicted throughout the test. Once again carbon dioxide is overestimated, and this could be primarily the effect of the ignition jet fuel fire. Figure 3-18 shows the predicted upper (hot gas) zone depth and Figure 3-19 the predicted smoke accumulation. As previously mentioned, no test results were available for comparison for these items. The figures show that the entire cabin volume fills with hot gas at about 110 seconds and that at about the same time the light transmission over one foot drops below one percent.

Figure 3-20 shows the predicted spread of the areas of burning material at several times in the simulation. The shaded region in the same figure shows the observed fire damage at the end of the test. Table 3-2 gives a quantitative comparison of the involvement of each surface as determined from the post-test damage assessment and by the progress of the fire in the simulation. Only the section used in the model is considered in the figure and table. This section normally contains all the floor, seat, and sidewall damage in the full scale test, while hatrack and ceiling damage can extend out of the section. The figure and table show that the model predicts well the total involvement of the hatrack and ceiling but generally overestimates the spread on the sidewall and seats. No spread could, of course, occur on the inert floor. The overestimate of flame spread on the chlorine containing vinyl sidewall is probably the reason (barring measurement error) for the disagreement in the HCl prediction. The figure also shows the flame spread from seat to seat in the row exposed to the ignition source. The model predicts an accelerating spread of flames over the seat row, while in the test the seat fire was more confined, involving mainly the seat over the fuel pan and the adjacent seat.

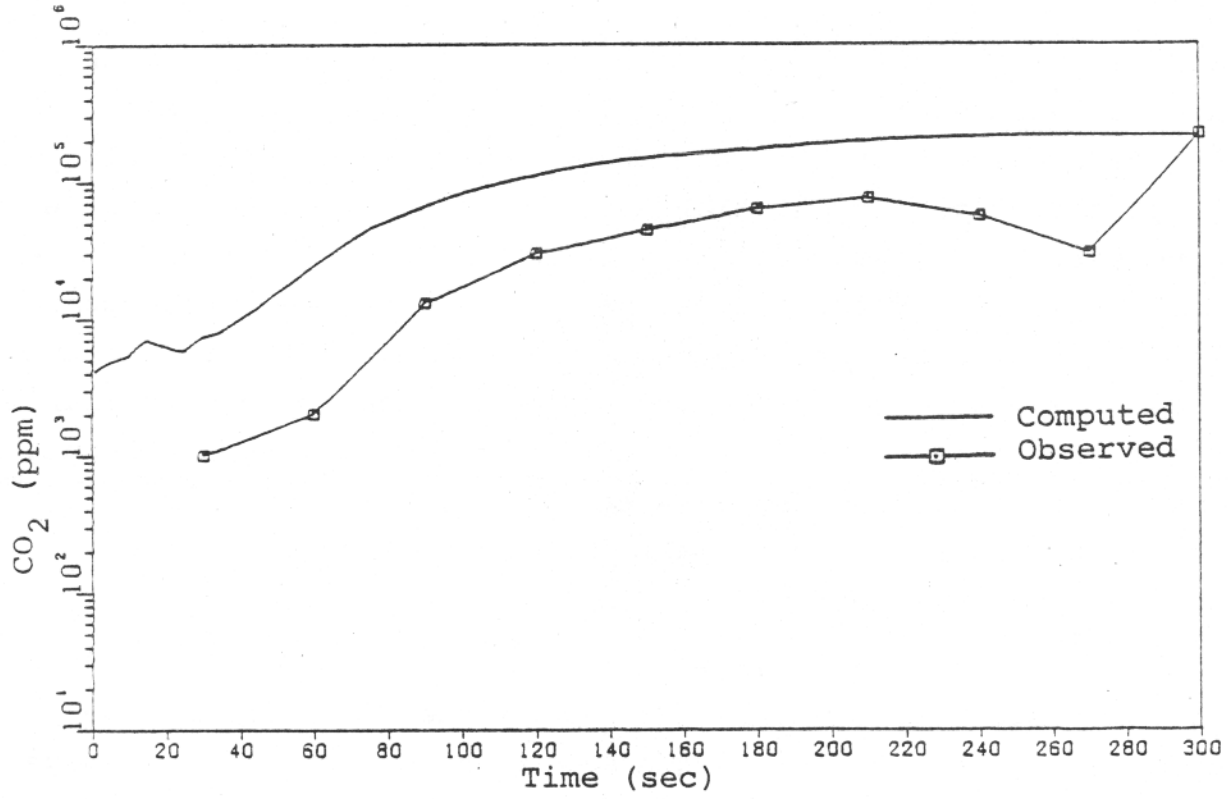

Figure 3-13. Carbon Dioxide Concentration - Case 15P

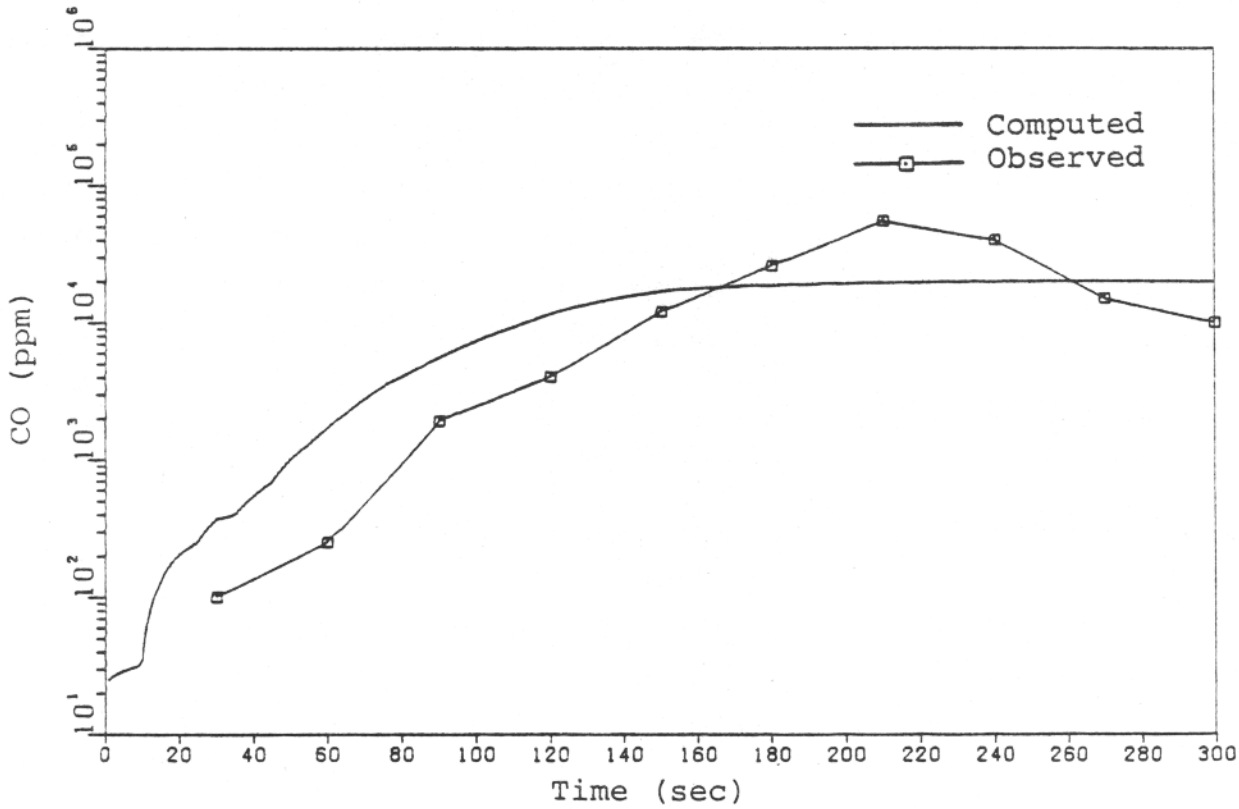

Figure 3-14. Carbon Monoxide Concentration - Case 15P

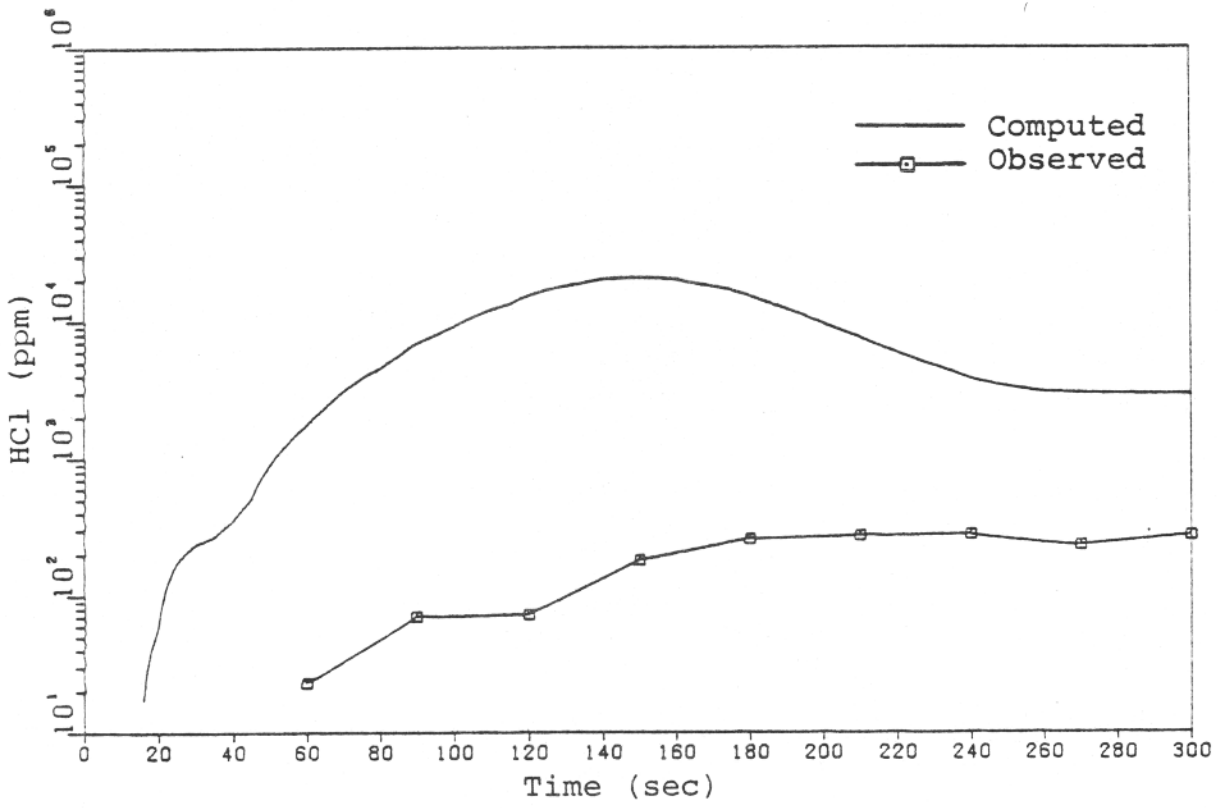

Figure 3-15. Hydrogen Chloride Concentration - Case 15P

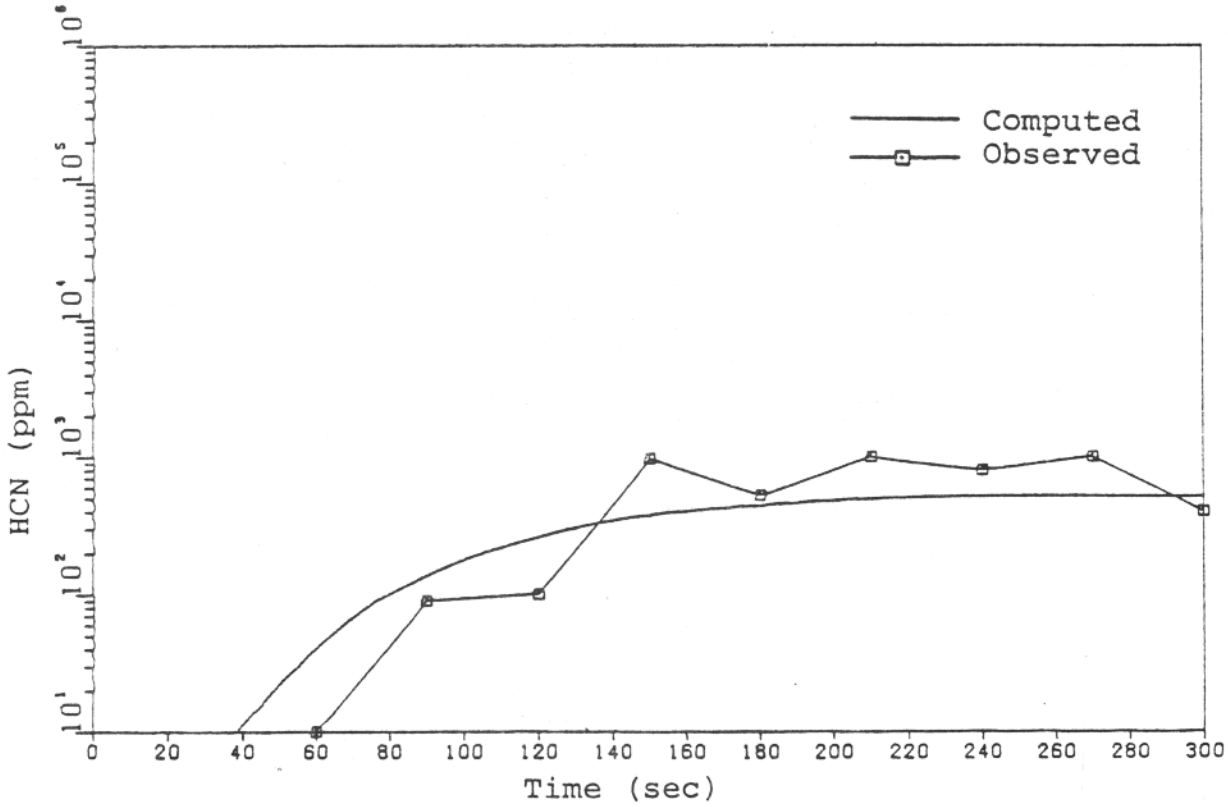

Figure 3-16. Hydrogen Cyanide Concentration - Case 15P

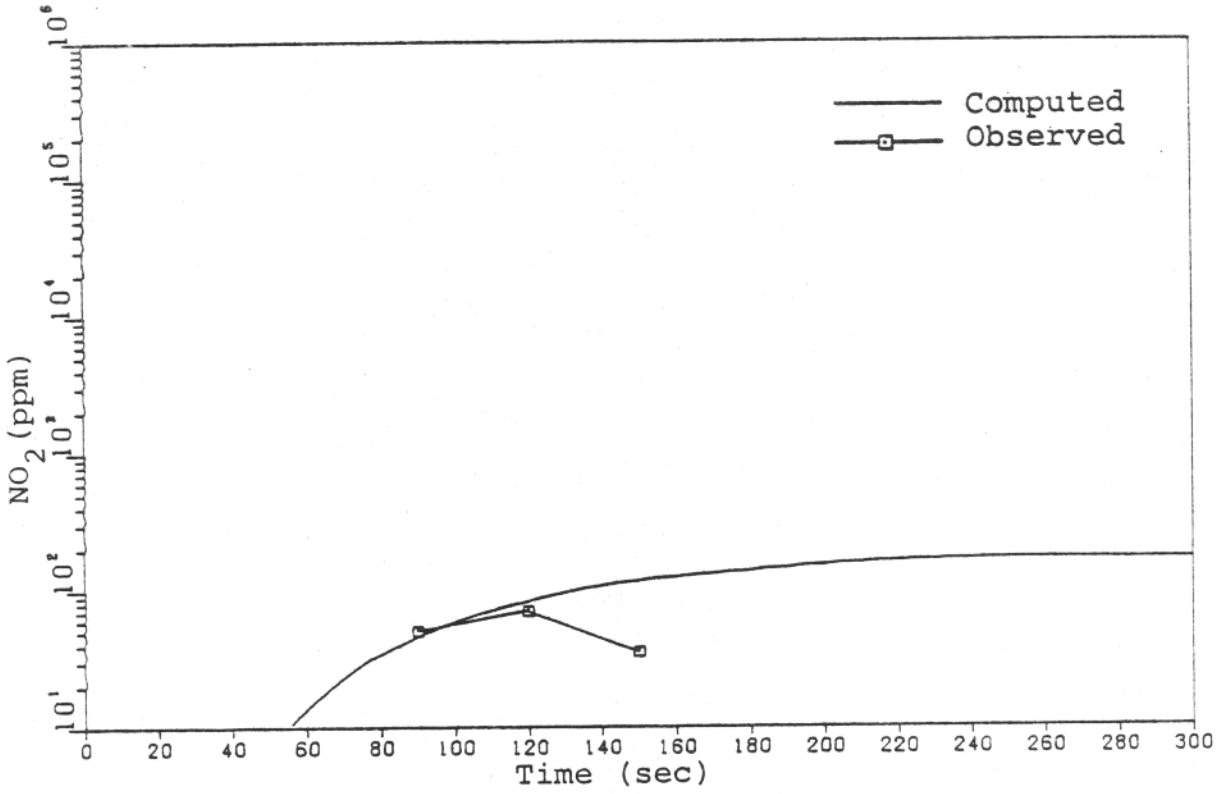

Figure 3-17. Nitrogen Dioxide Concentration - Case 15P

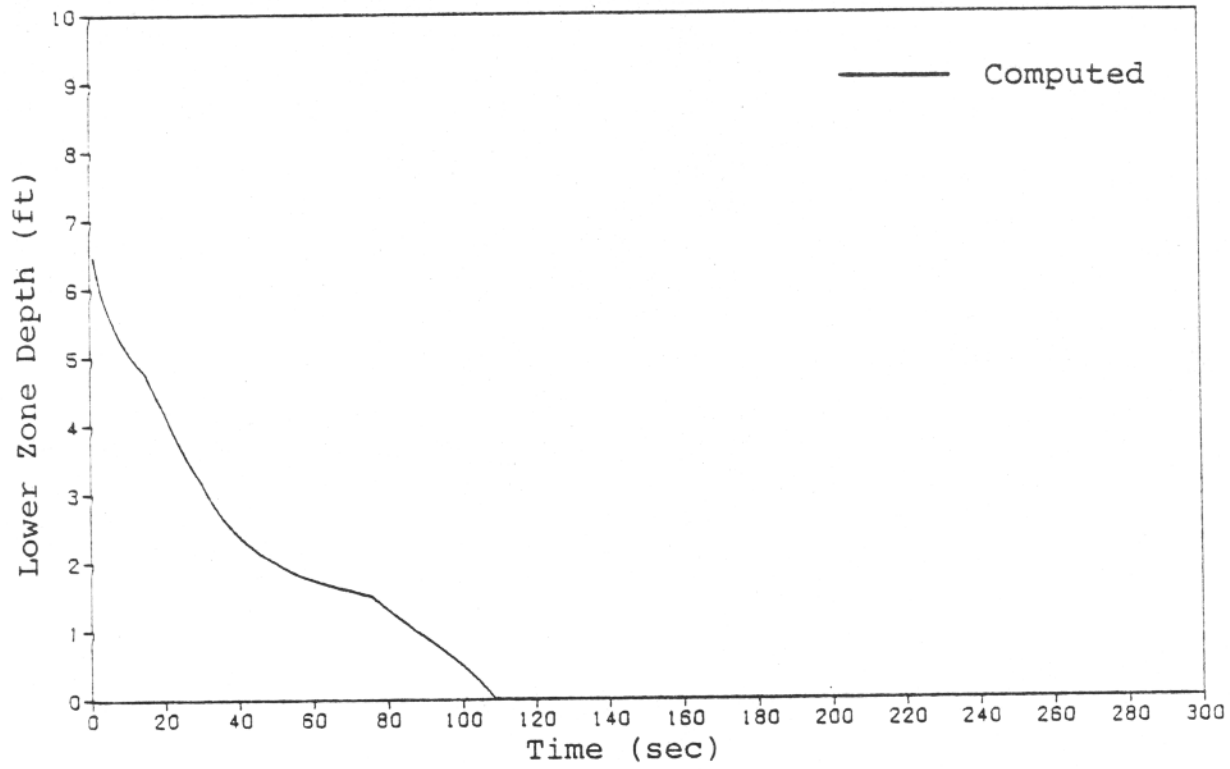

Figure 3-18. Lower Zone Depth - Case 15P

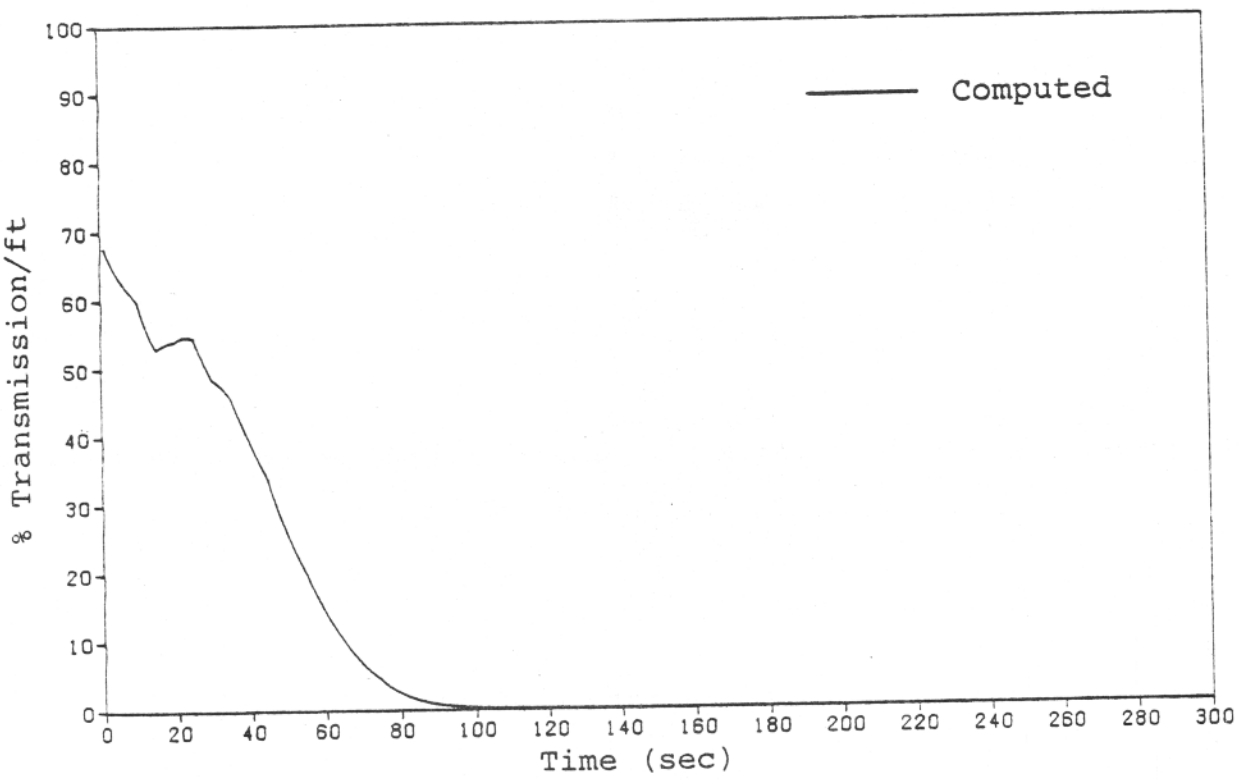

Figure 3-19. Smoke Accumulation - Case 15P

TABLE 3-2

COMPARISON OF SIMULATED AND OBSERVED AREAS OF DAMAGE - CASE 15P

	OBSERVED AREA[1]		COMPUTED AREA	
STRUCTURE	(ft^2)	% TOTAL EXPOSED	(ft^2)	% TOTAL EXPOSED
Sidewall	17 to 26	20 to 30	45.0	100
Hatrack	32.5	100	33.8	100
Ceiling	59.0	100	86.0[2]	100
Seats	25.0	55	49.5	100

[1] Damaged area within test section considered by model (center 7.5 ft of 15 ft length)

[2] Difference in percent figures due to differences in modeled and actual ceiling area

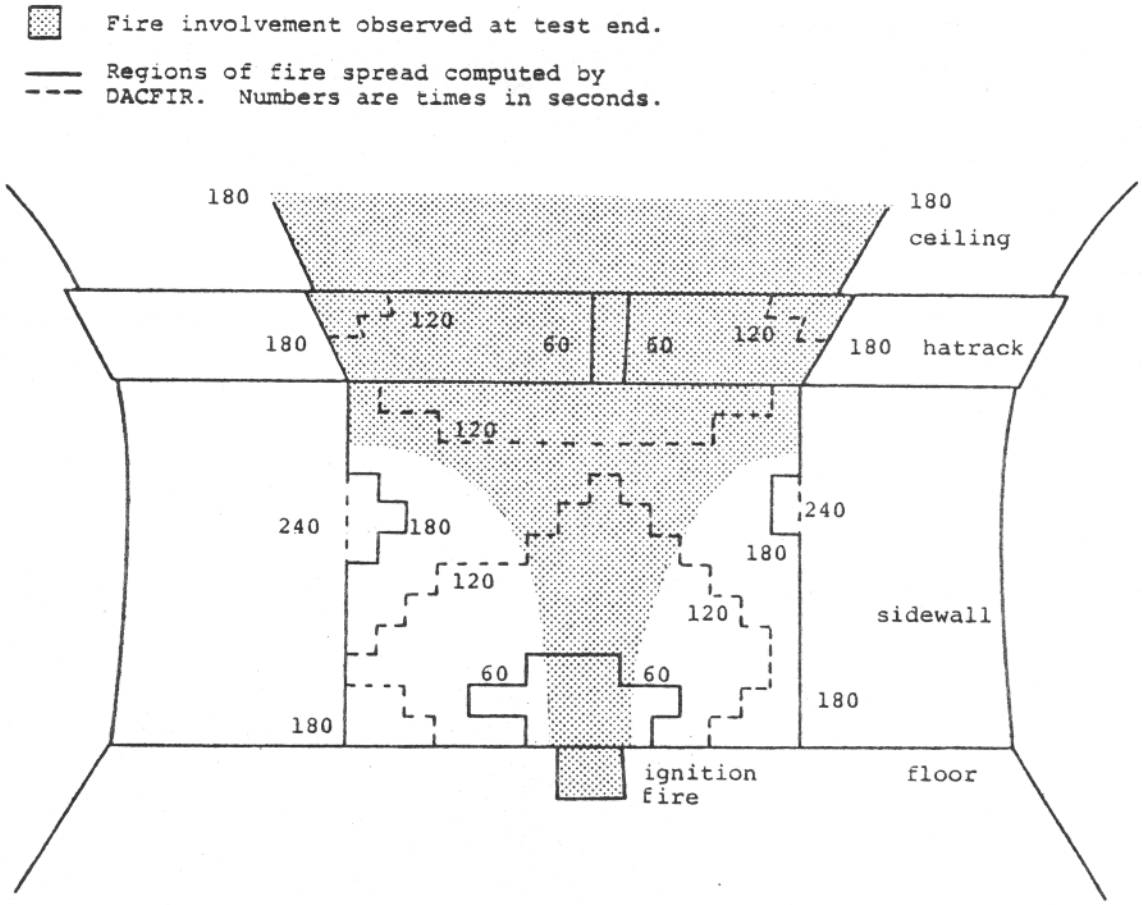

Damage on cabin lining surfaces

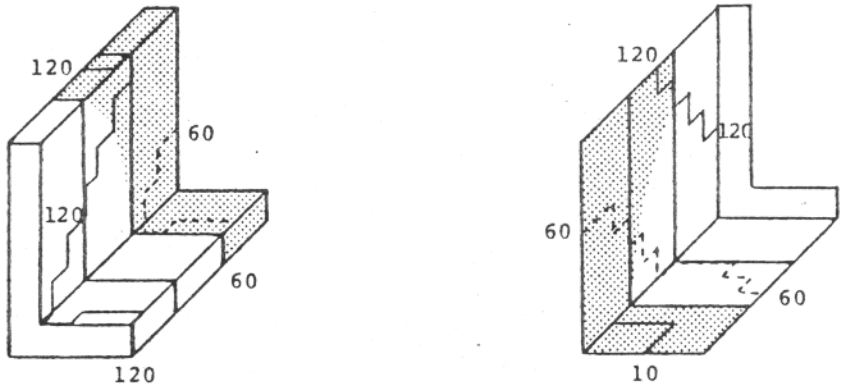

Damage on seat row above ignition fire

Figure 3-20. Computer and Observed Areas of Damage - Case 15P

3.3.3 Case 15A - Improved Materials Set A

Figure 3-21 shows the predicted and observed cabin temperature for this test using improved ceiling and hatrack materials. Since the experimental PVF-aluminum material was not available for laboratory testing, an inert material was specified for the sidewall in the computer simulation. Without the active involvement of the sidewall, the fire as computed by DACFIR was confined to the center seat group, the hatrack, and the ceiling. Figures 3-22 through 3-27 show the comparison of the oxygen and toxic gas levels. The agreement for O_2, CO_2, and HCN is good for most times, while that for CO and HCl is fair or poor before three minutes but improves after that time. HF is not predicted well during the test but this is to be expected since the PVF coated sidewall data was not available. The computed smoke accumulation and the growth of the hot layer differed little from the results for Case 15P as can be seen by comparing Figures 3-28 and 3-29 to Figures 3-18 and 3-19.

Figure 3-30 shows the observed and computed damage sustained in Case 15A. The computed results are confined to the lining surfaces of the hatrack and ceiling by the inert floor and sidewall. Table 3-3 compares the areas of damage in absolute terms and as percentages of each surface exposed. Without the fire spread to the forward and aft seat groups from the sidewall, a closer agreement in the total involvement of seat material was obtained than in Case 15P.

3.3.4 Case 15B - Improved Materials Set B

In this test the seat upholstery and cushioning were of newer, more fire-resistant materials. In addition, the sidewall was made of the same nylon-honeycomb sandwich panel construction as the ceiling and hatrack in this and the previous improved materials test.

Figure 3-31 shows the computed and observed temperature. Here the model did not reproduce the general rise of temperature starting at about 100 seconds. The observed

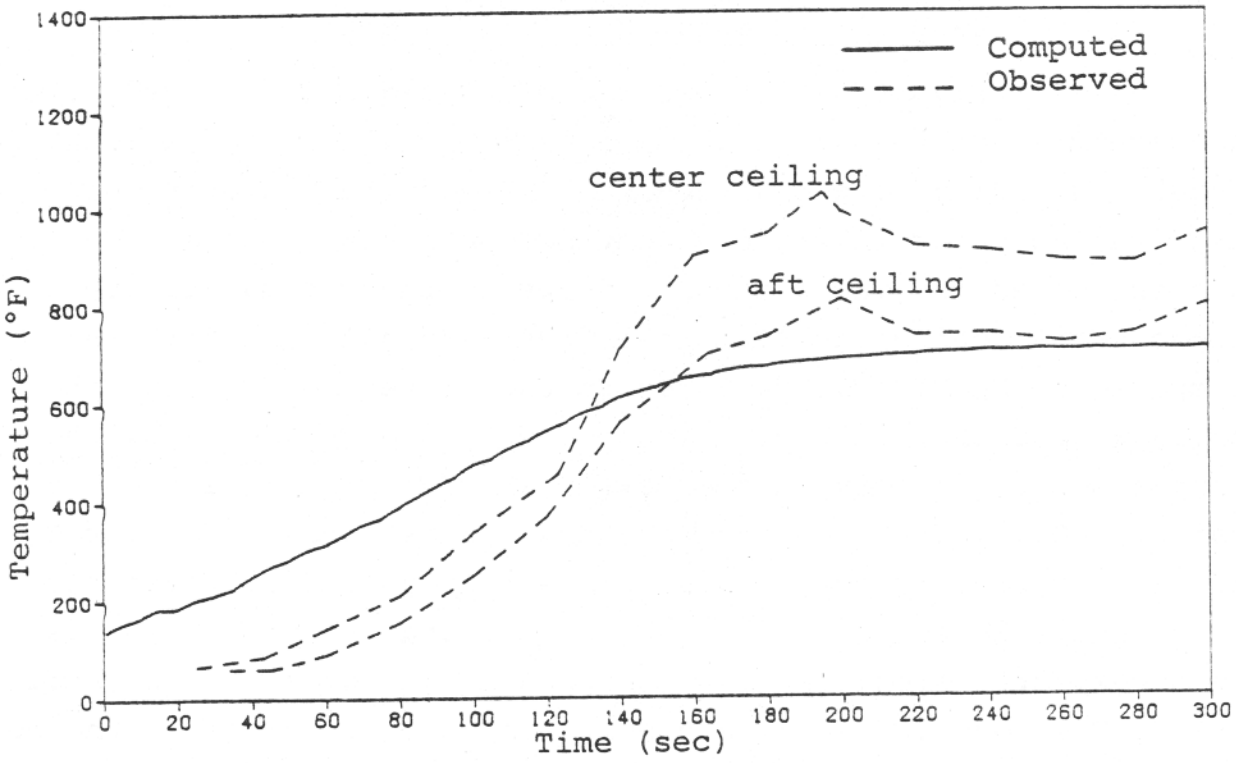

Figure 3-21. Upper Zone Temperature - Case 15A

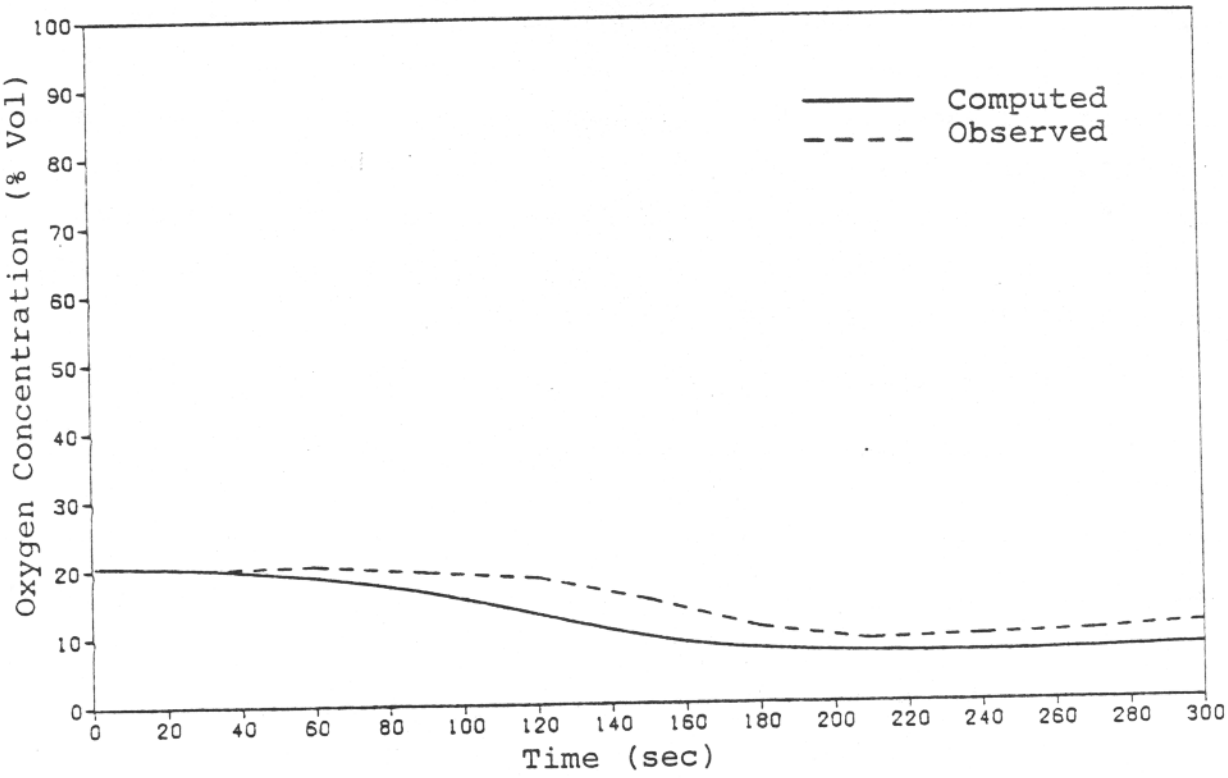

Figure 3-22. Oxygen Concentration - Case 15A

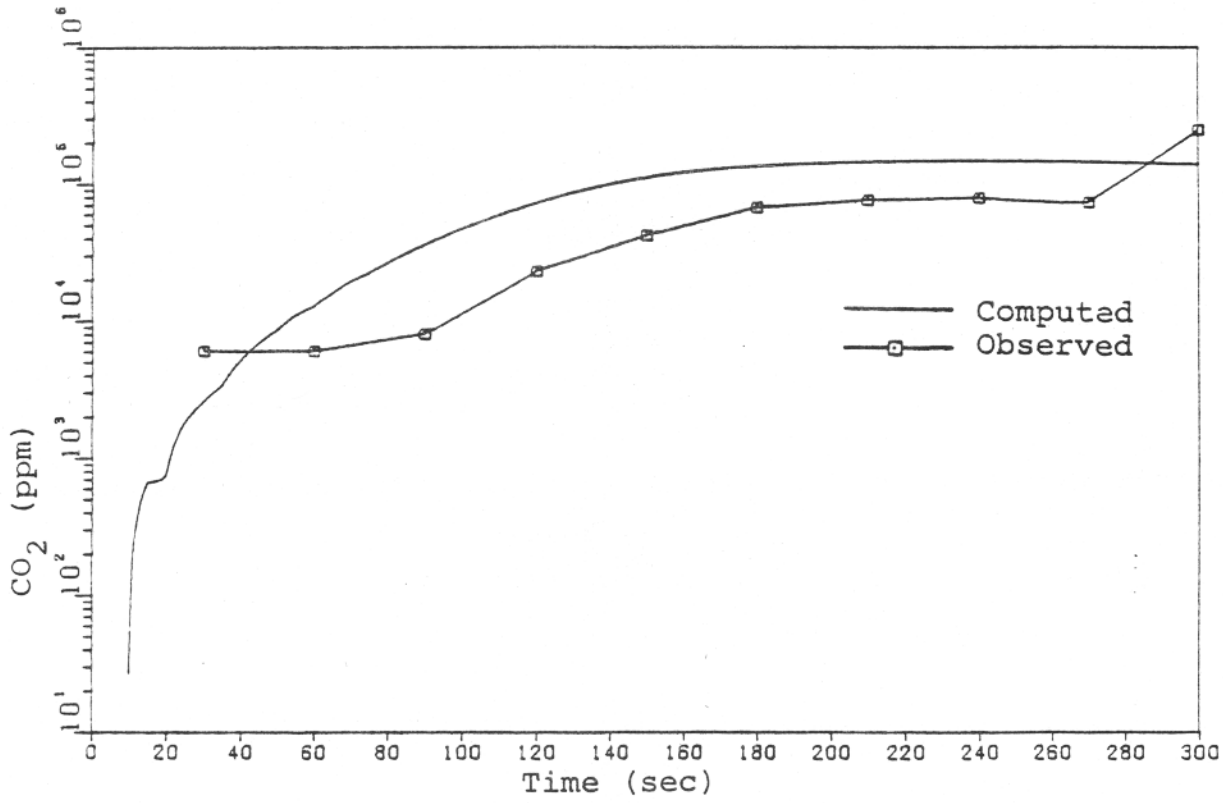

Figure 3-23. Carbon Dioxide Concentration - Case 15A

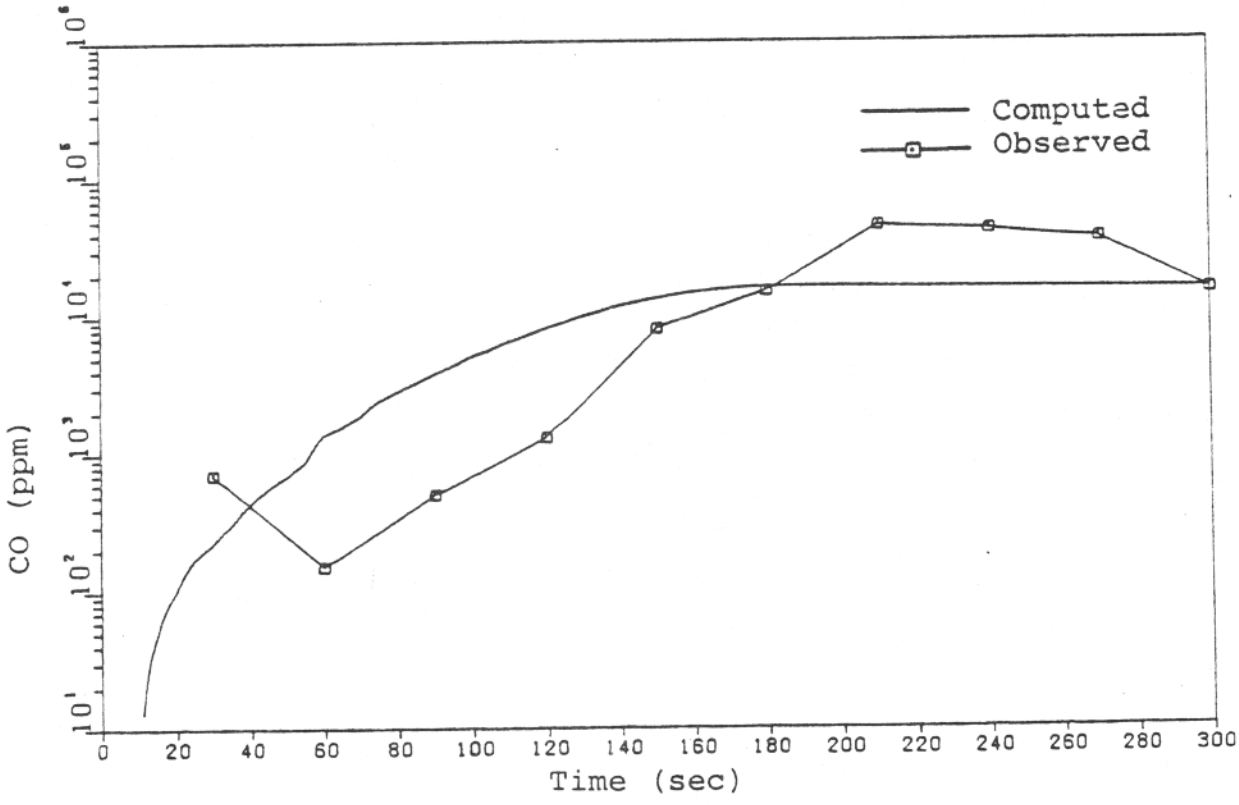

Figure 3-24. Carbon Monoxide Concentration - Case 15A

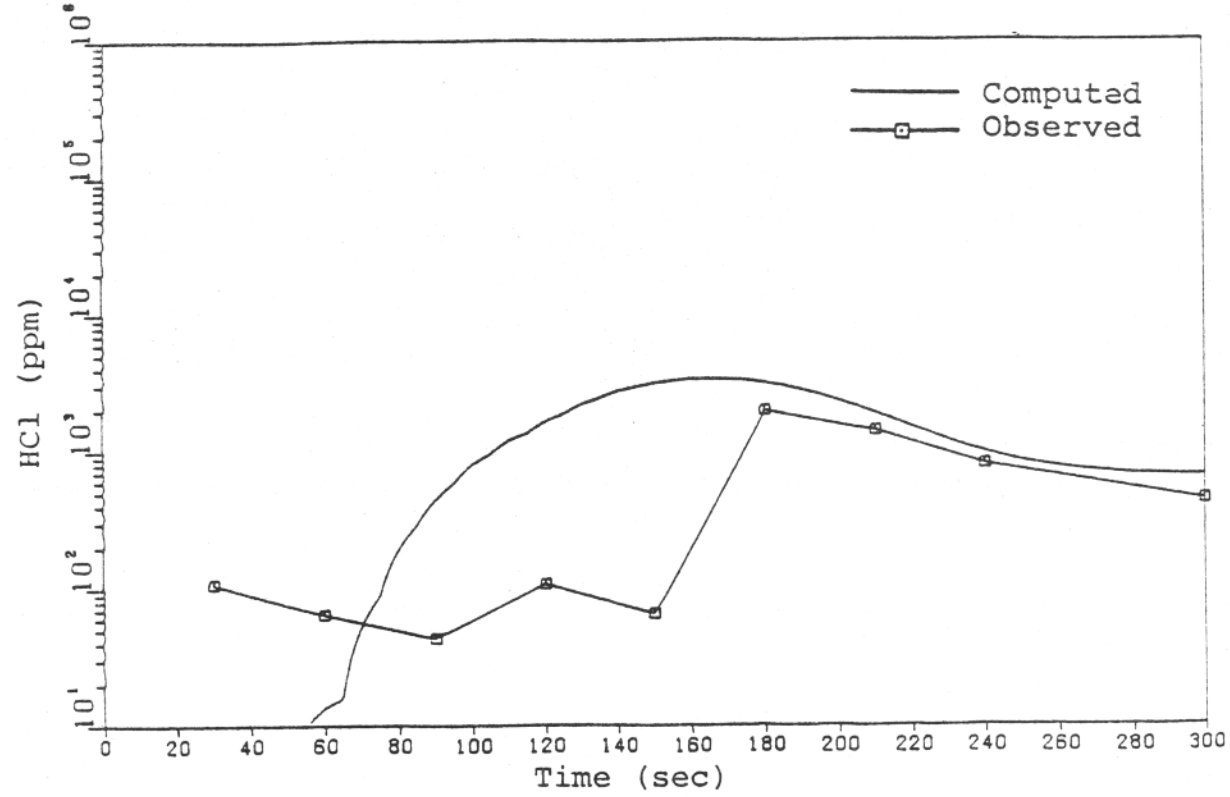

Figure 3-25. Hydrogen Chloride Concentration - Case 15A

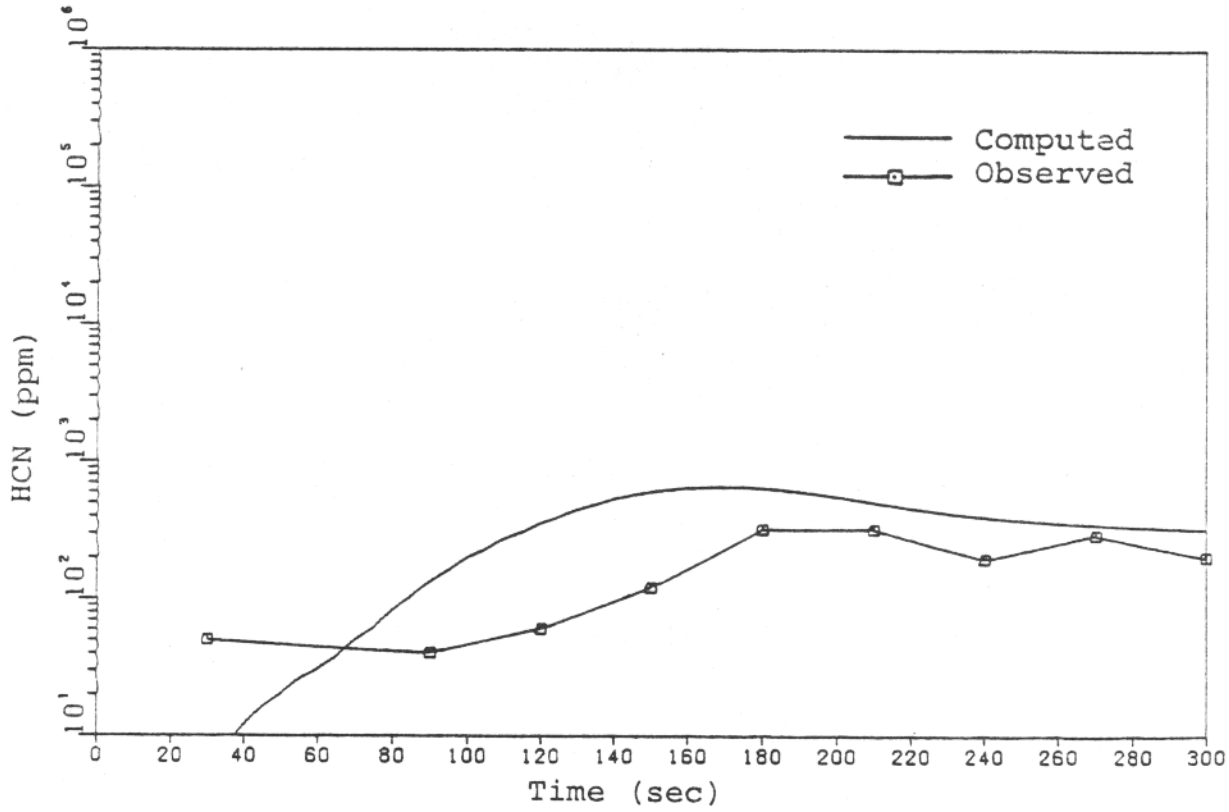

Figure 3-26. Hydrogen Cyanide Concentration - Case 15A

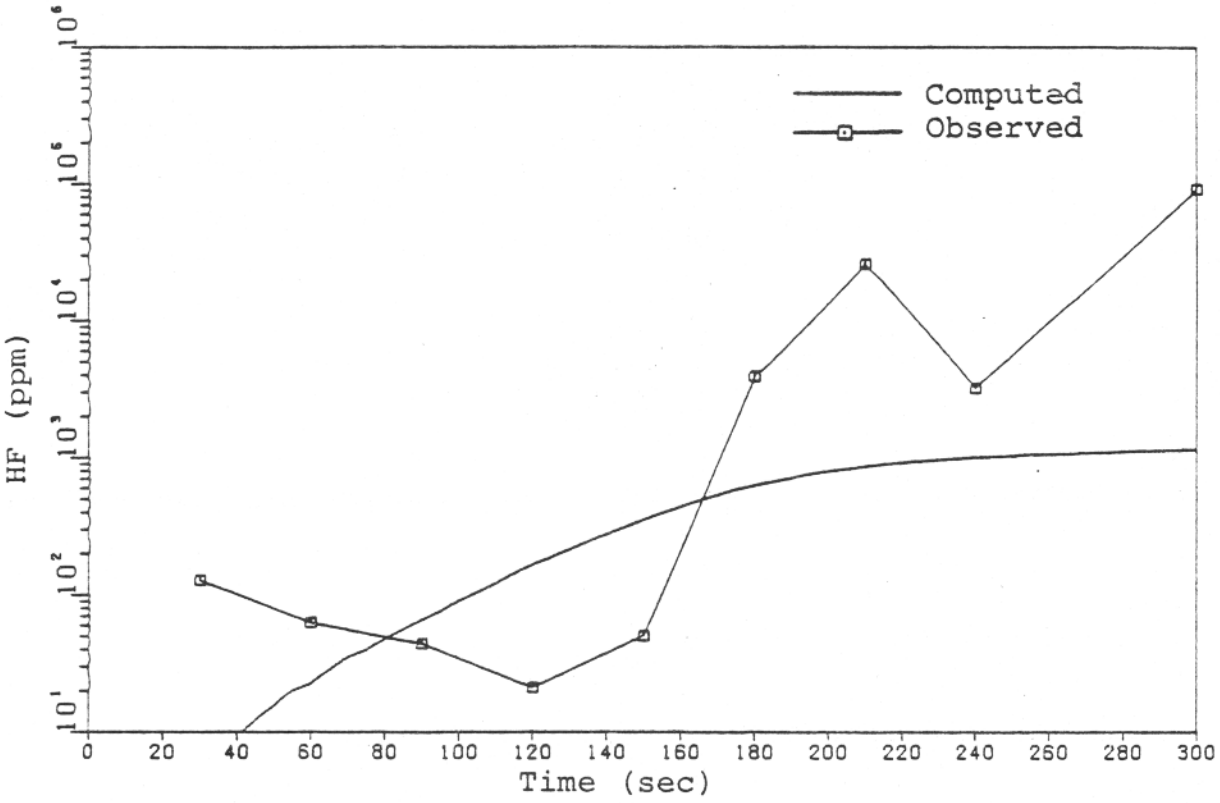

Figure 3-27. Hydrogen Fluoride Concentration - Case 15A

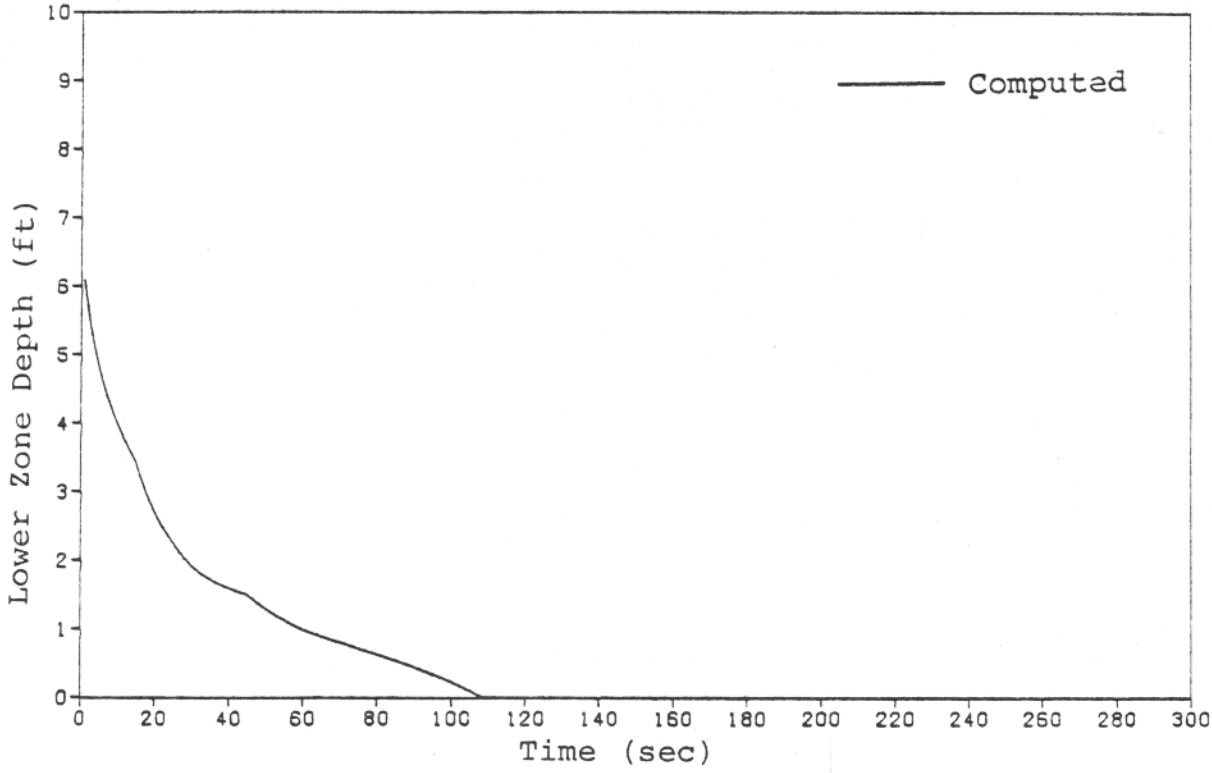

Figure 3-28. Lower Zone Depth - Case 15A

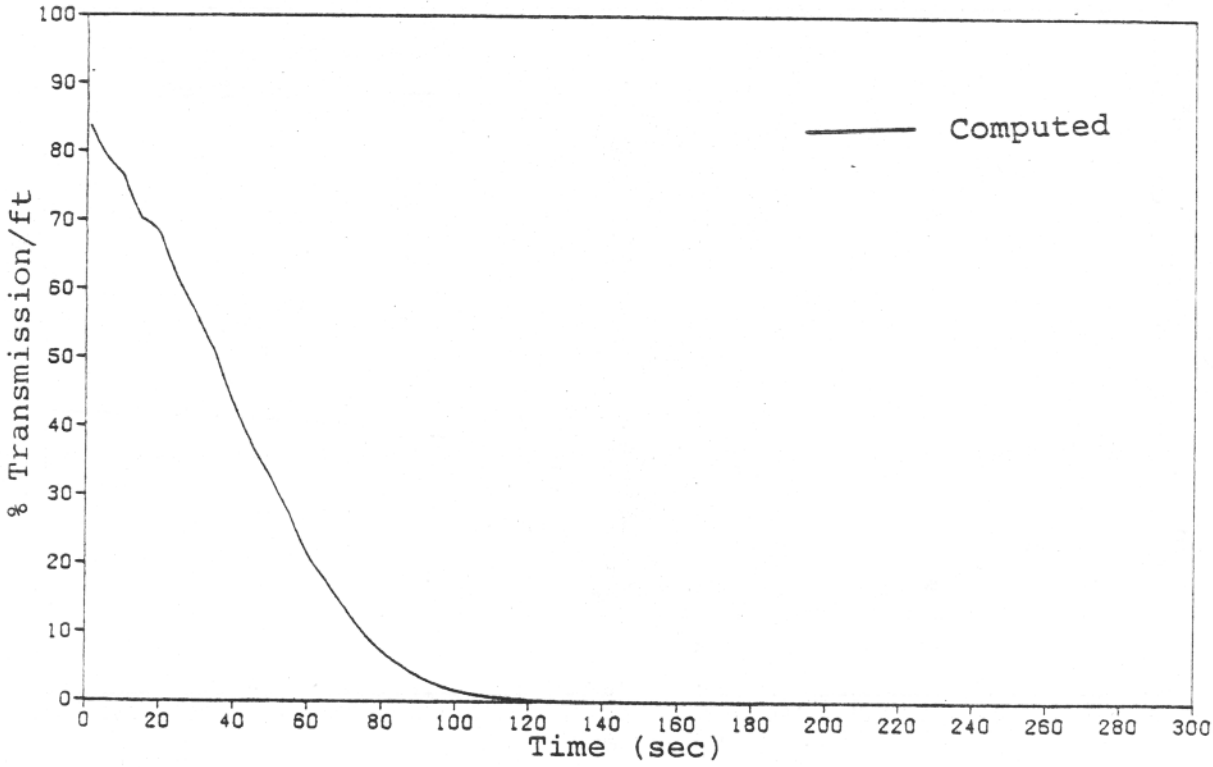

Figure 3-29. Smoke Accumulation - Case 15A

TABLE 3-3

COMPARISON OF SIMULATED AND OBSERVED AREAS OF DAMAGE - CASE 15A

	OBSERVED AREA[1]		COMPUTED AREA	
STRUCTURE	(ft^2)	% TOTAL EXPOSED	(ft^2)	% TOTAL EXPOSED
Sidewall	34.6	40	Material Data Not Available	
Hatrack	32.5	100	33.8	100
Ceiling	59.0	100	86.0[2]	99
Seats	22.4	50[1]	44.5	90

[1] Damaged area within test section considered by model (center 7.5 ft of 15 ft length)

[2] Difference in percent figures due to differences in modeled and actual ceiling area

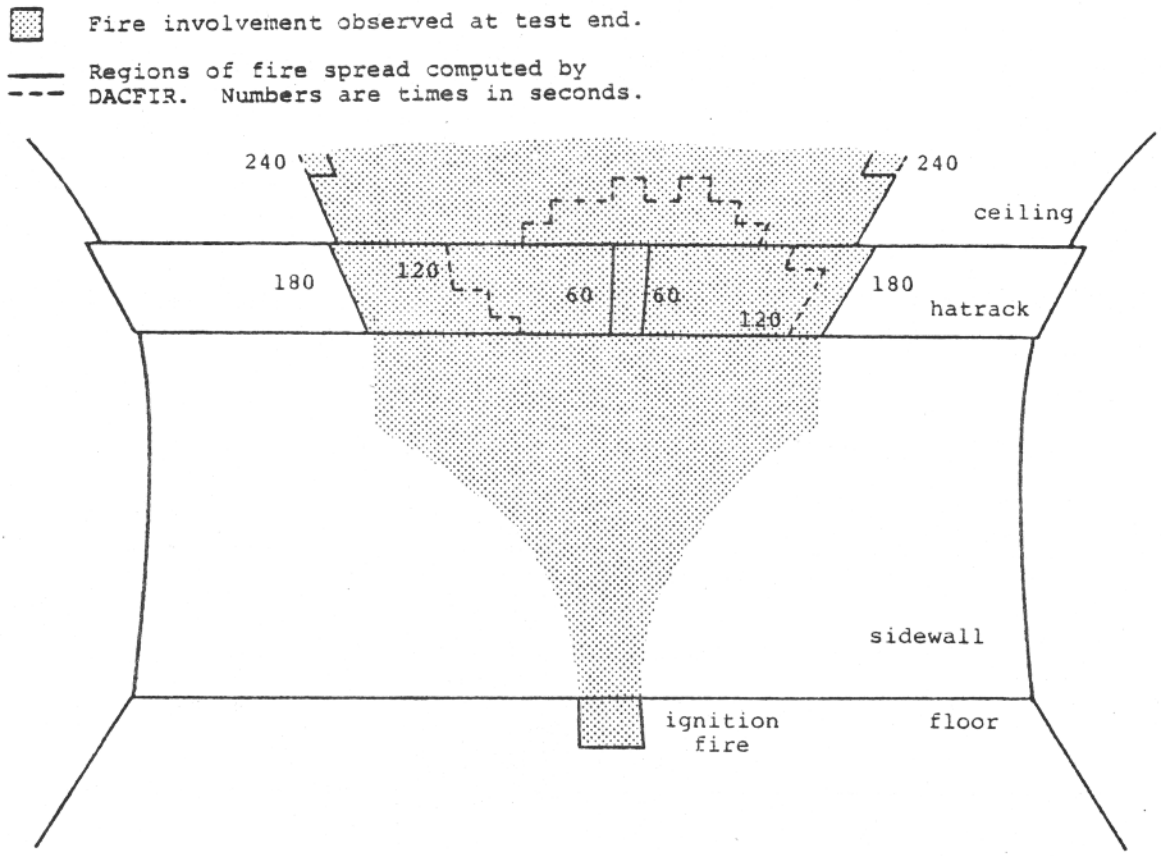

Damage on cabin lining surfaces

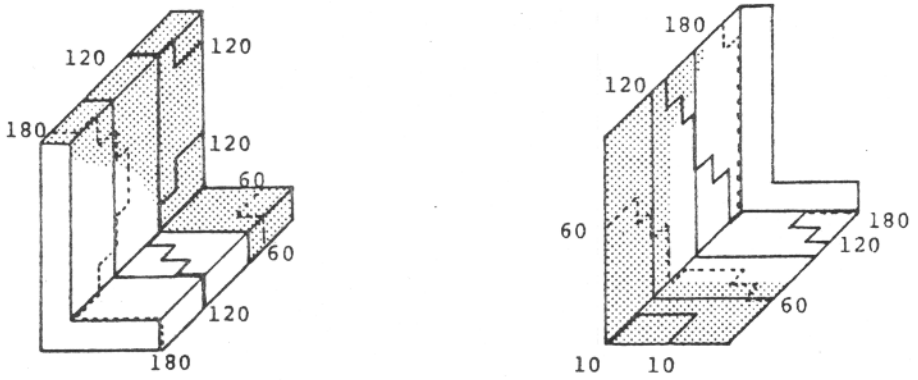

Damage on seat row above ignition fire

Figure 3-30. Computed and Observed Areas of Damage - Case 15A

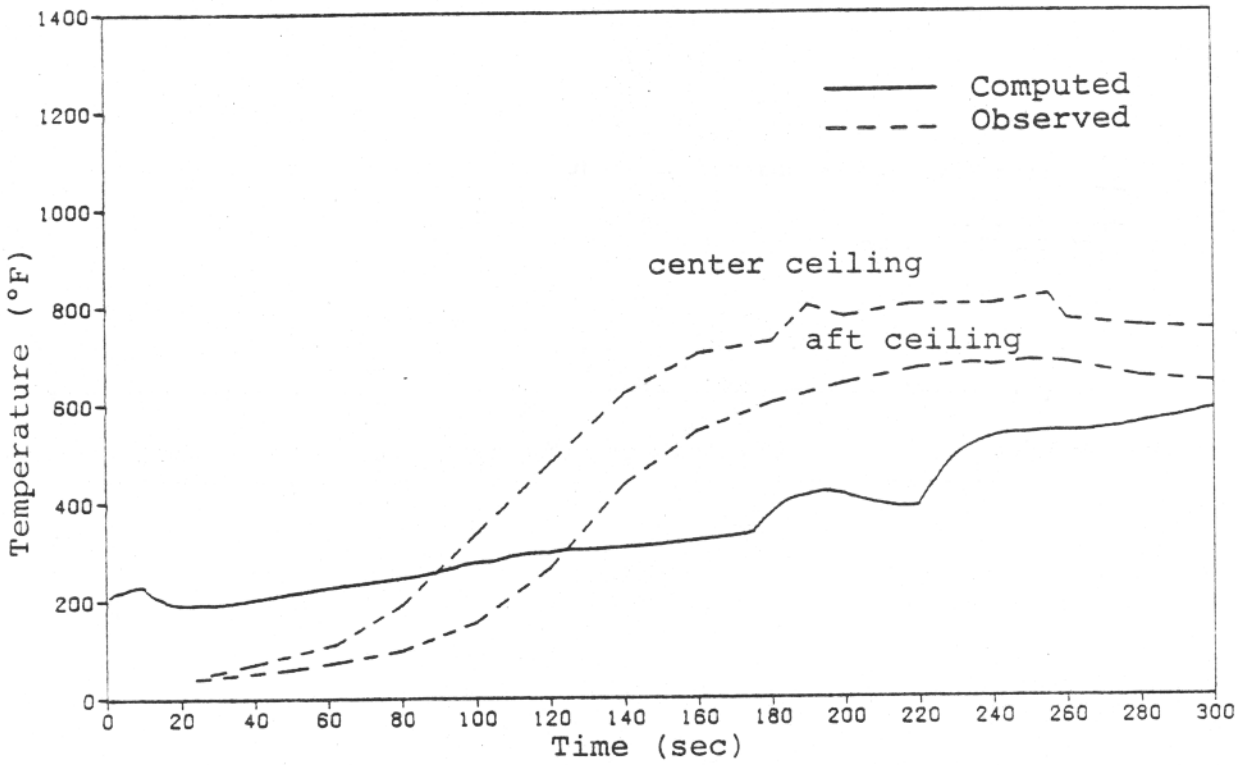

Figure 3-31. Upper Zone Temperature - Case 15B

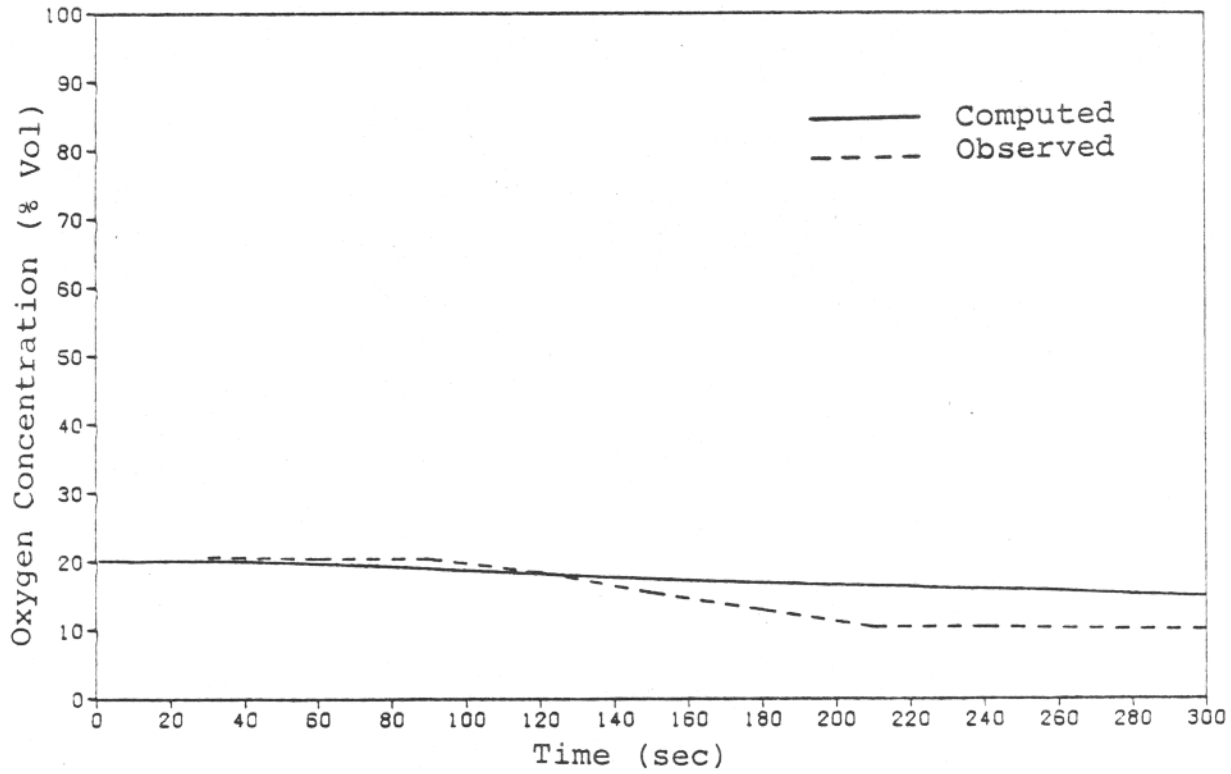

Figure 3-32. Oxygen Concentration - Case 15B

temperature stabilizes after about 200 seconds and only near the end of the test does the computed temperature approach the measured levels. The oxygen and CO_2 concentrations shown in Figures 3-32 and 3-33 are also not in as good agreement as in Cases 15P and 15A. For carbon monoxide, Figure 3-34, the agreement is better, equaling that obtained in 15P and 15A. The match for HCl is difficult to judge. No HCl was detected before 210 seconds but after this time the measured values jump to over 14,000 ppm. Somewhat the same rapid variation in the measured values of HCN and particularly HF is shown in Figures 3-36 and 3-37. The agreement with the computed values can only be judged, at best, fair. The time required for the cabin to fill with the combustion products was somewhat longer, 135 seconds versus about 100 seconds in the earlier tests, as shown in Figure 3-38. Smoke accumulation was also slower, the visibility dropping below one percent at 150 seconds.

In Table 3-4 and Figure 3-40 the pattern of good prediction of involvement on the ceiling and hatrack and over prediction on the sidewall and seats is again evident.

3.3.5 Case 15C - Improved Materials Set C

The third set of improved materials consisted of those used in Case 15B but with glass fiber padding substituted for the polyurethane foam of the seats. Figure 3-41 shows that this substitution resulted in significantly less heat generation. The agreement between the computed and observed temperatures is good, especially near the end of the test. The jagged appearance of the computed temperature curve reflects the successive ignition and burn out of areas of material, particularly the seat upholstery fabric. This effect is noticeable here because of the absence of the constantly growing seat foam fire that was present in the earlier cases. Oxygen consumption was accurately predicted as shown in Figure 3-42. Agreement in the prediction was good for CO_2 but the concentration of the other gases was overestimated as shown in Figures 3-43 through 3-47. Smoke development and the growth of the upper layer,

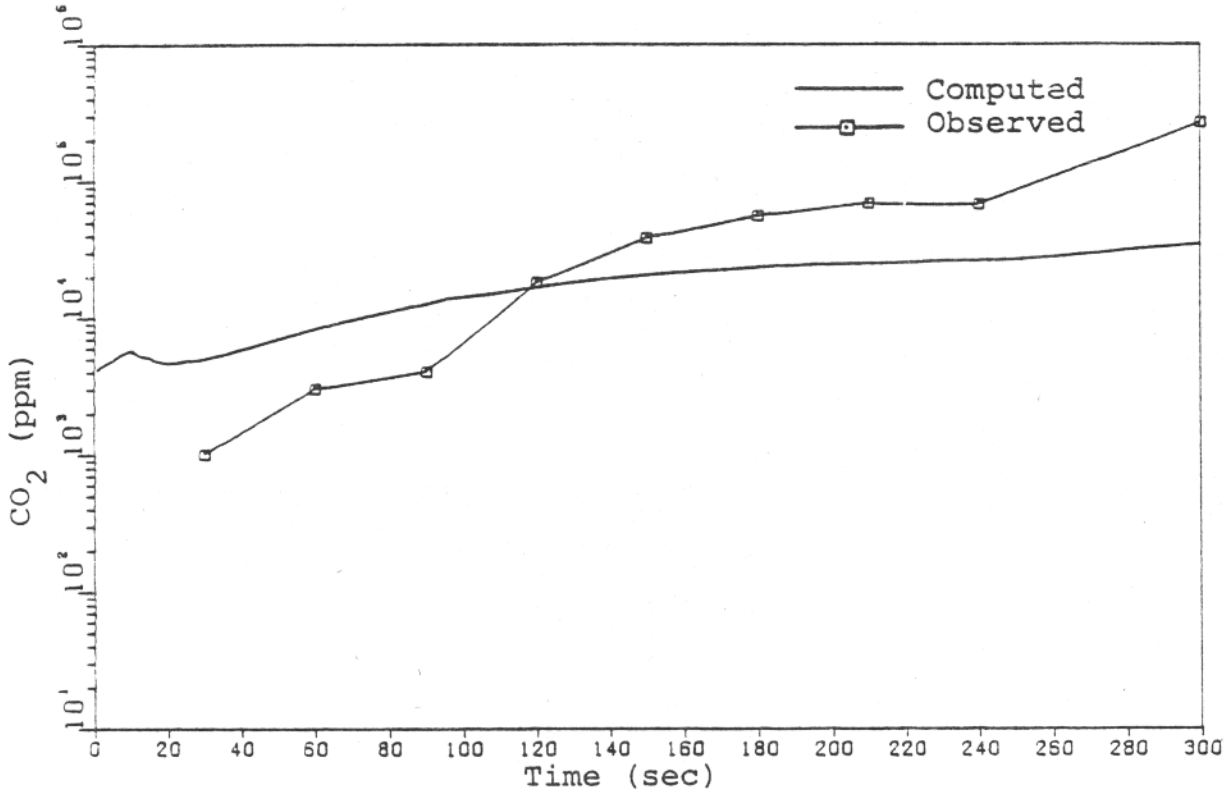

Figure 3-33. Carbon Dioxide Concentration - Case 15P

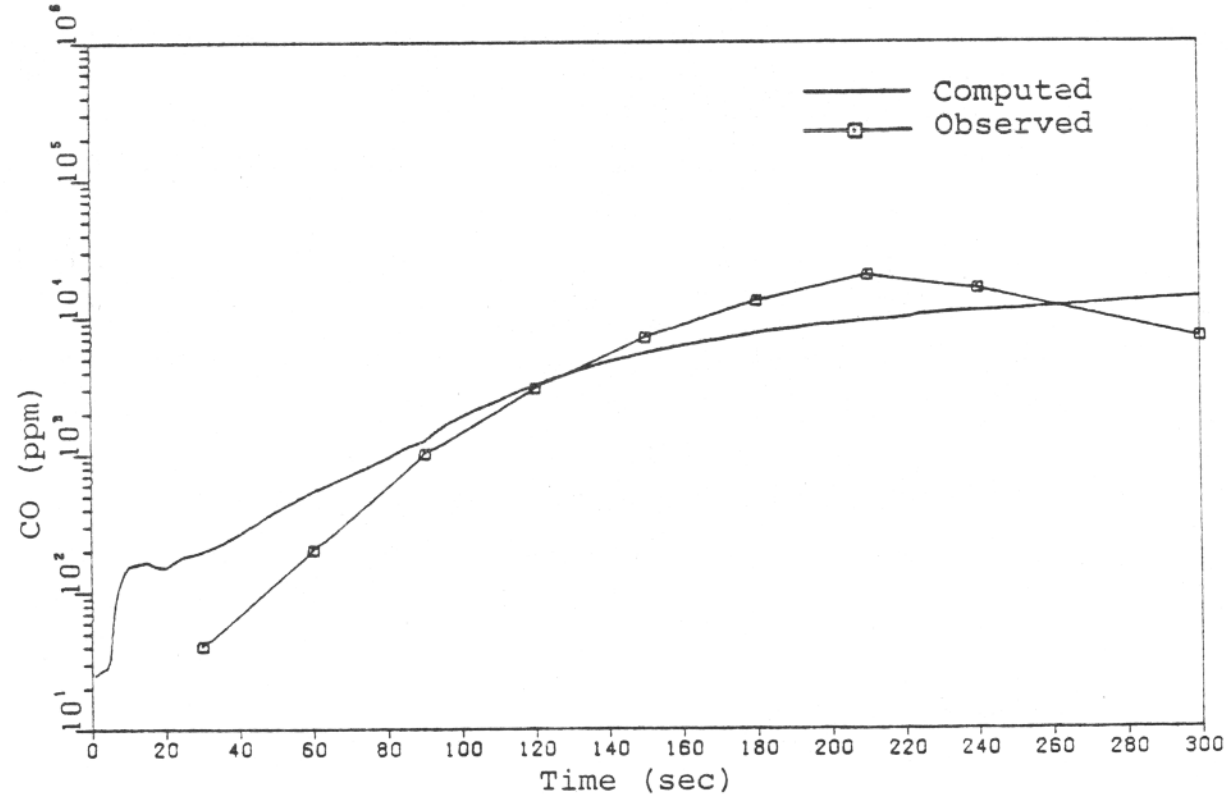

Figure 3-34. Carbon Monoxide Concentration - Case 15B

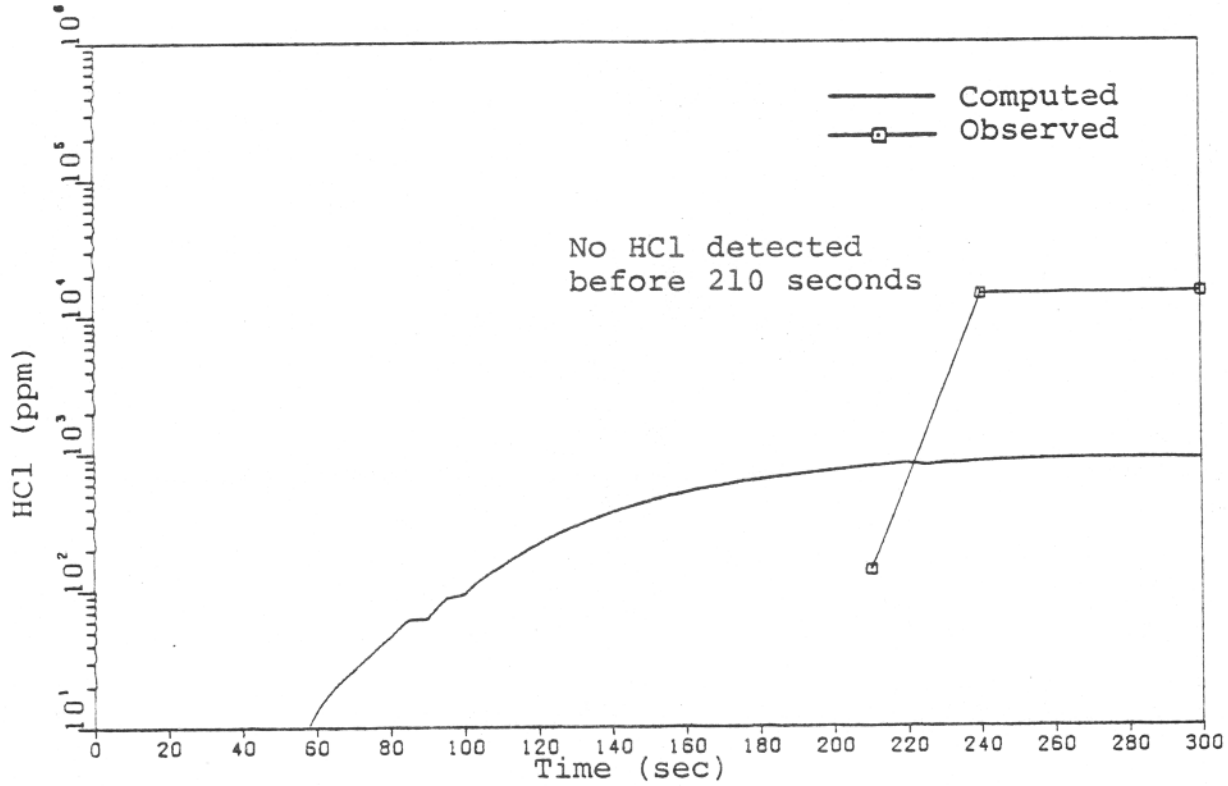

Figure 3-35. Hydrogen Chloride Concentration - Case 15B

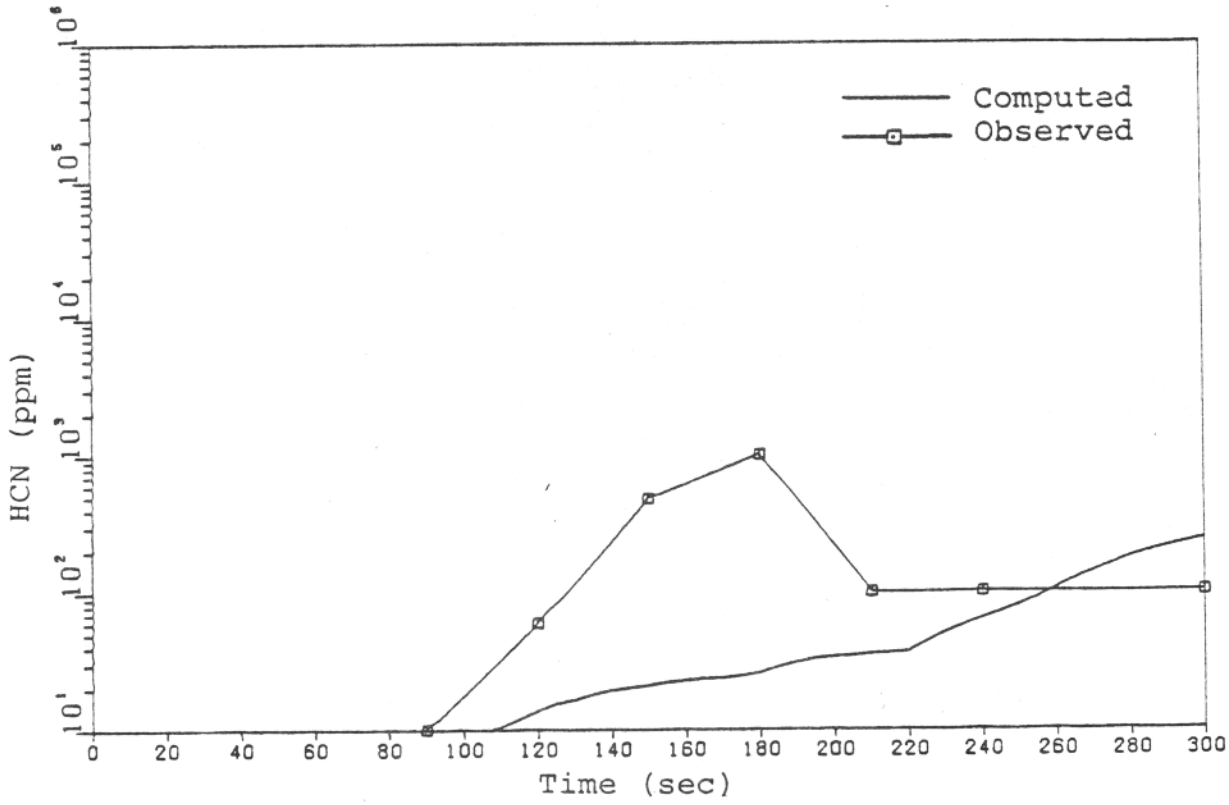

Figure 3-36. Hydrogen Cyanide Concentration - Case 15B

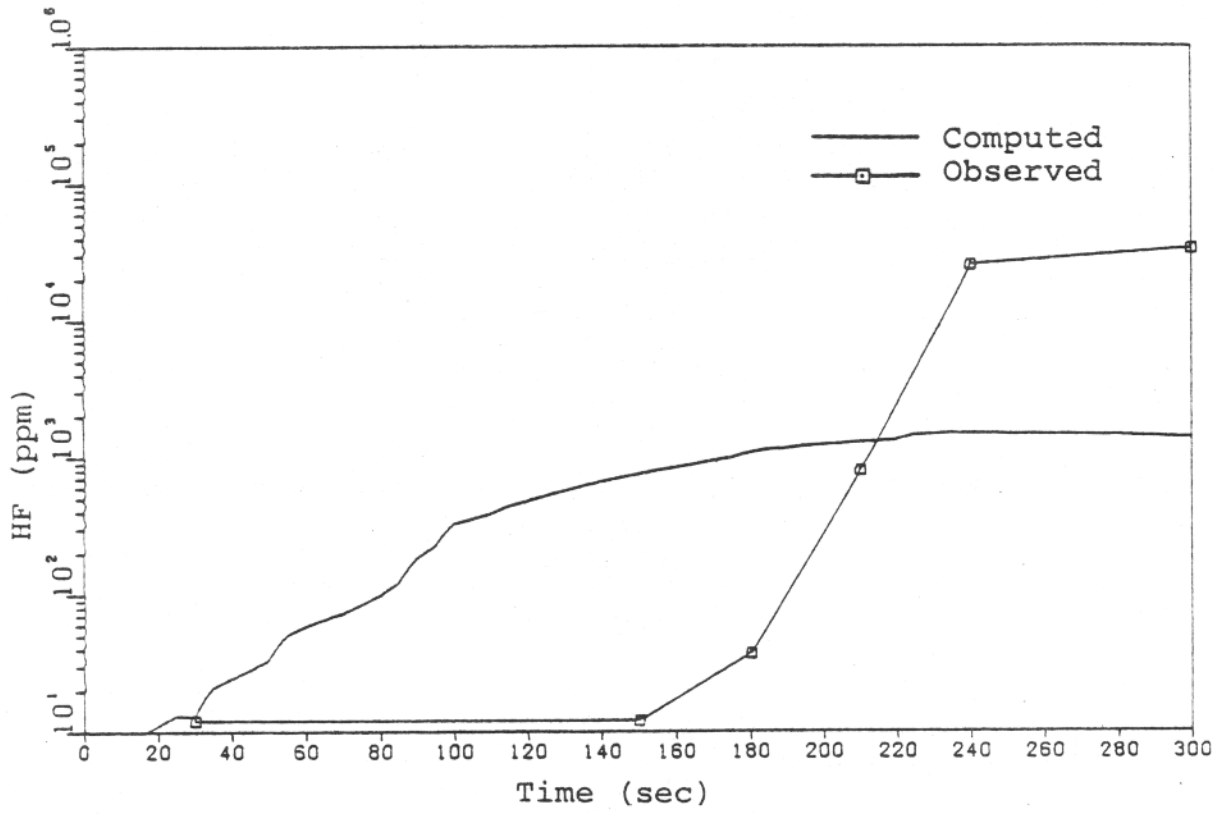

Figure 3-37. Hydrogen Fluoride Concentration - Case 15B

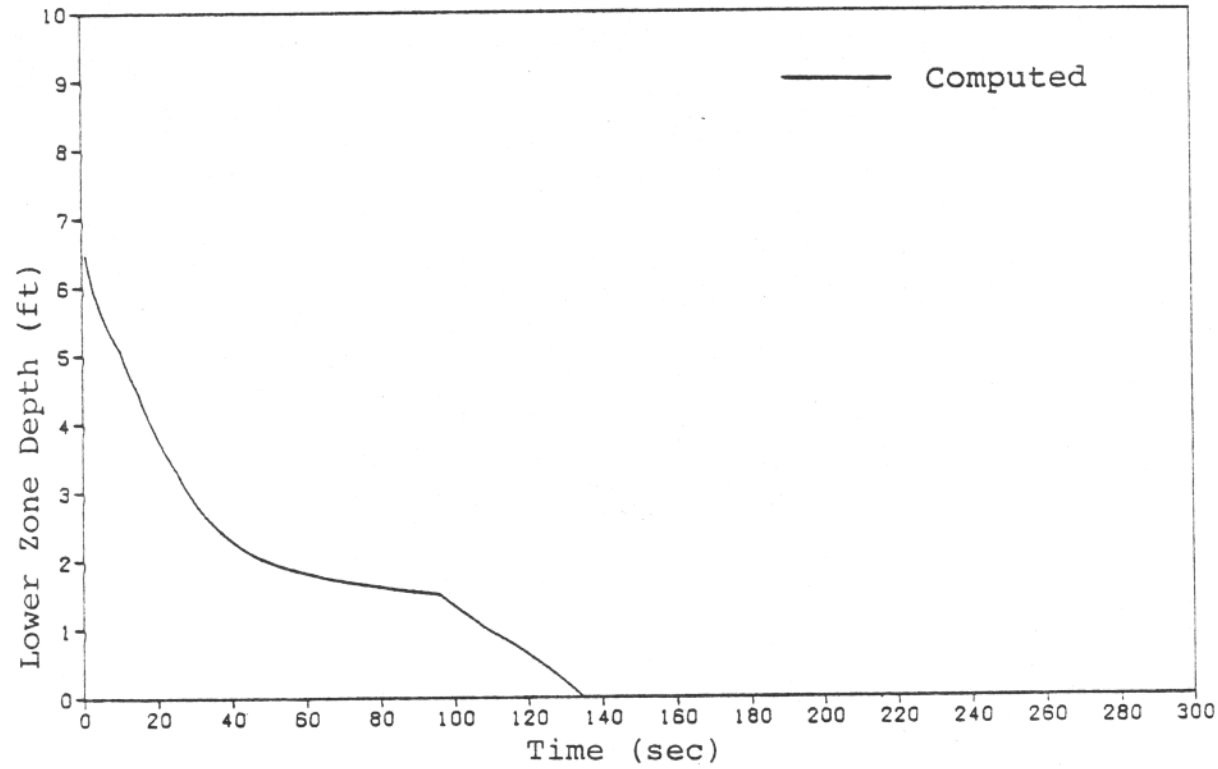

Figure 3-38. Lower Zone Depth - Case 15B

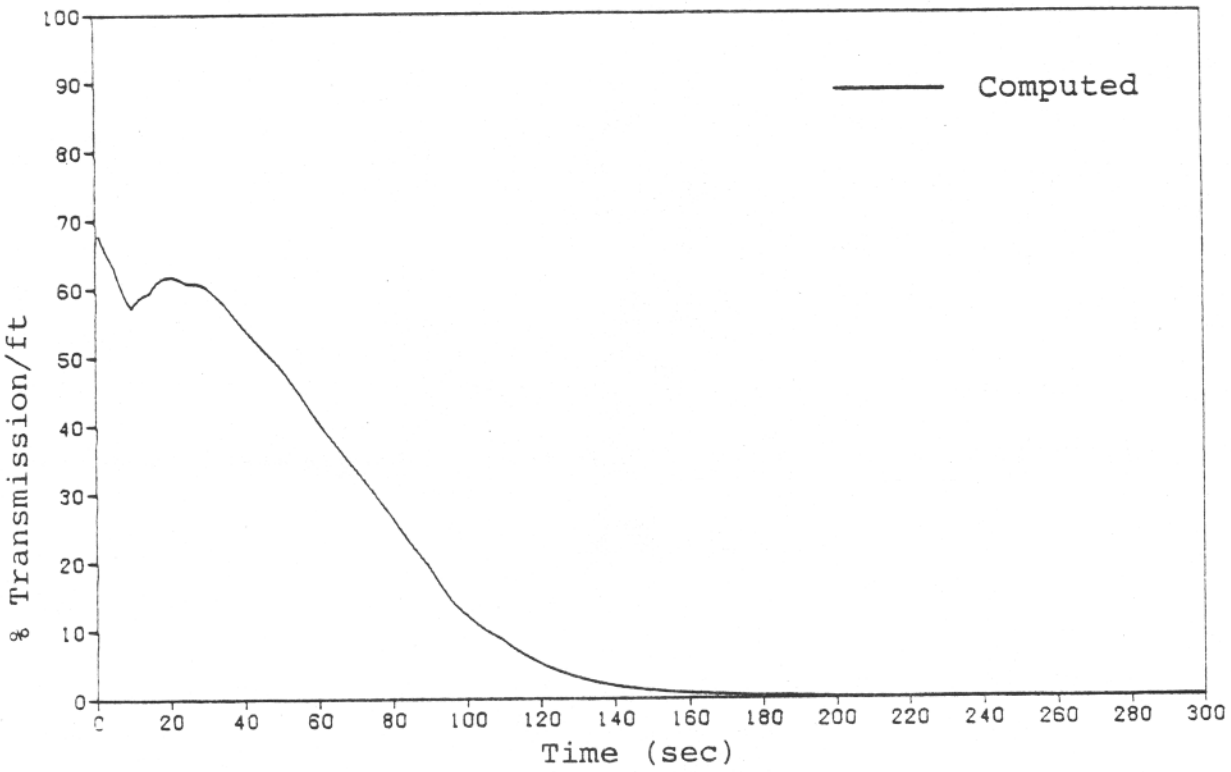

Figure 3-39. Smoke Accumulation - Case 15B

TABLE 3-4

COMPARISON OF SIMULATED AND OBSERVED AREAS OF DAMAGE - CASE 15B

	OBSERVED AREA[1]		COMPUTED AREA	
STRUCTURE	(ft^2)	% TOTAL EXPOSED	(ft^2)	% TOTAL EXPOSED
Sidewall	25.0	29	45.0	100
Hatrack	3.5	5	34.0	100
Ceiling	59.0	100	86.0	100[2]
Seats	15.0	33[3]	60.5	37[4]

[1] Damaged area within test section considered by model (center 7.5 ft or 15 ft length)

[2] Difference in percent figures due to difference in modeled and actual surface areas

[3] Damage on one seat row

[4] Total damage on three seat rows

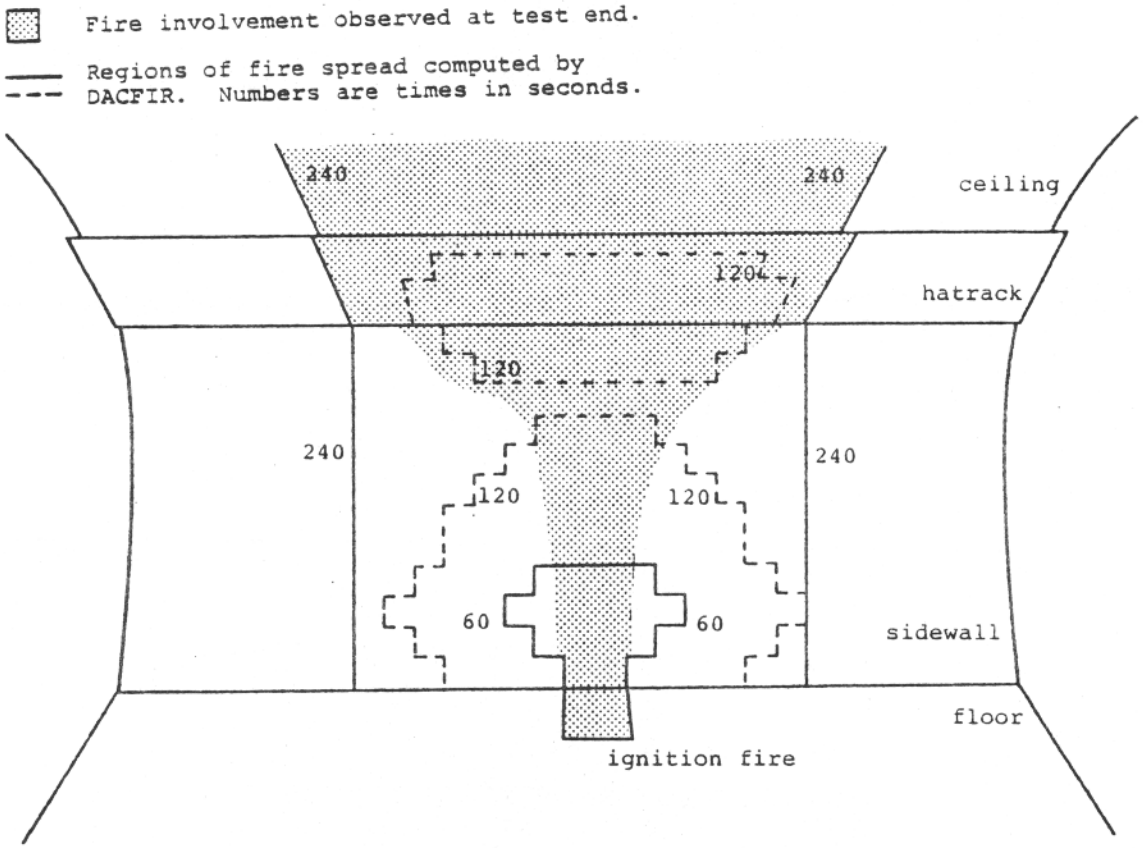

Damage on Cabin lining surfaces

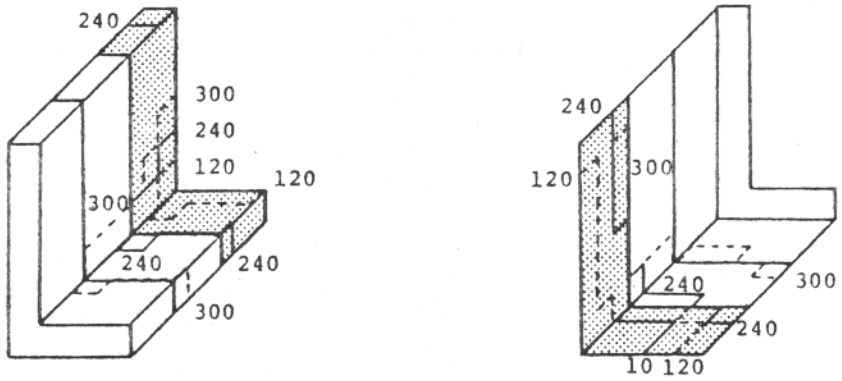

Damage on seat row above ignition fire

Figure 3-40. Computed and Observed Areas of Damage - Case 15B

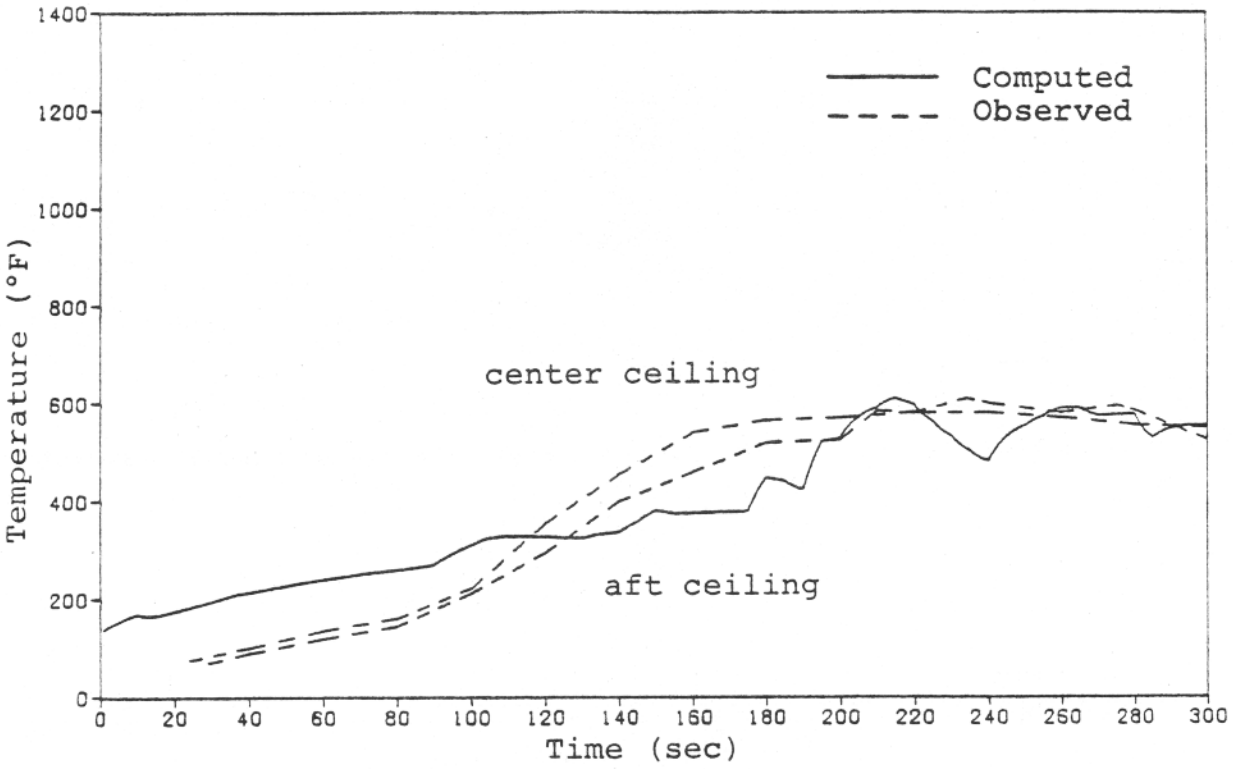

Figure 3-41. Upper Zone Temperature - Case 15C

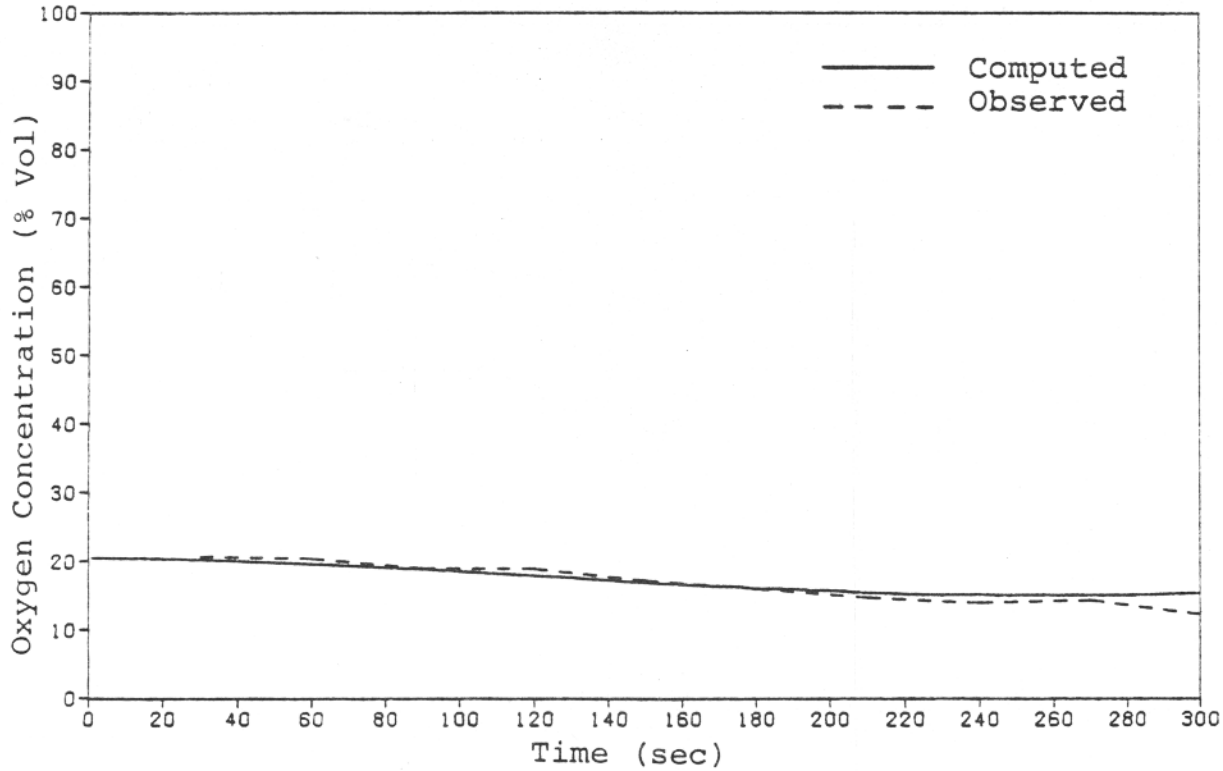

Figure 3-42. Oxygen Concentration - Case 15C

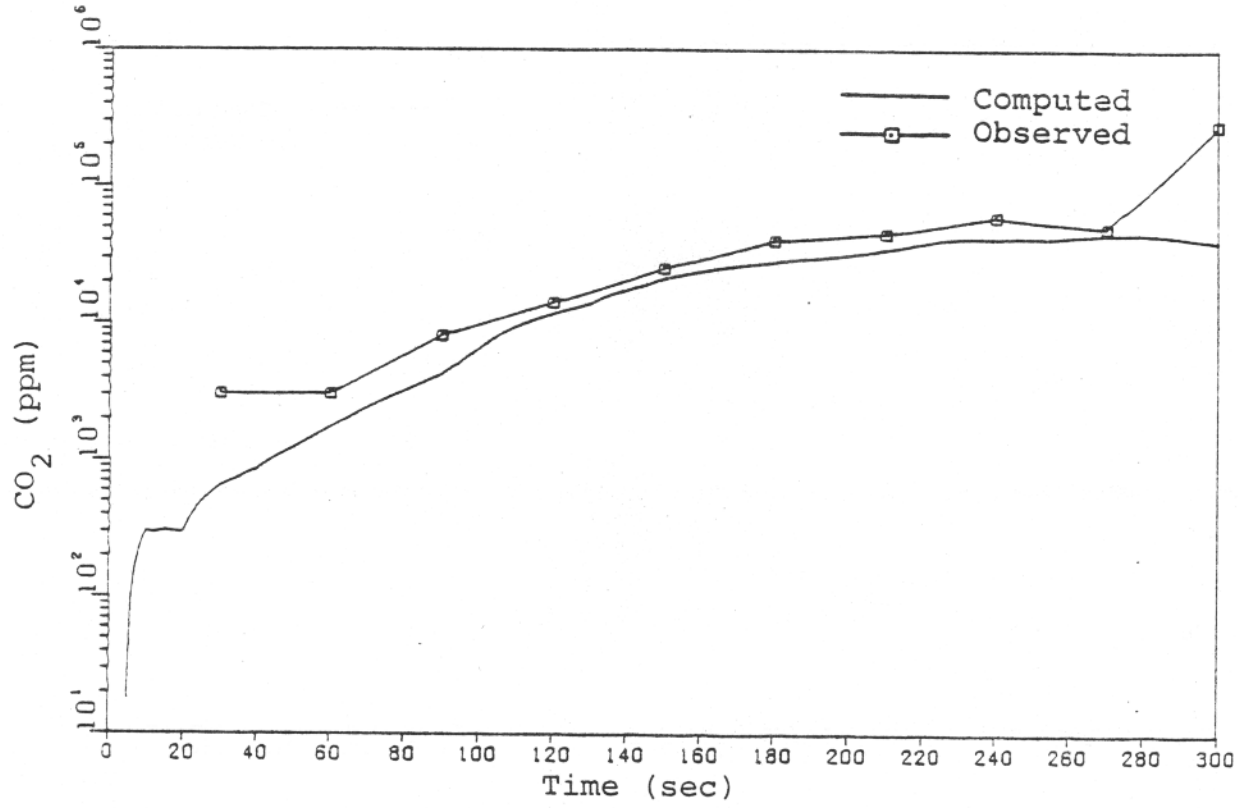

Figure 3-43. Carbon Dioxide Concentration - Case 15C

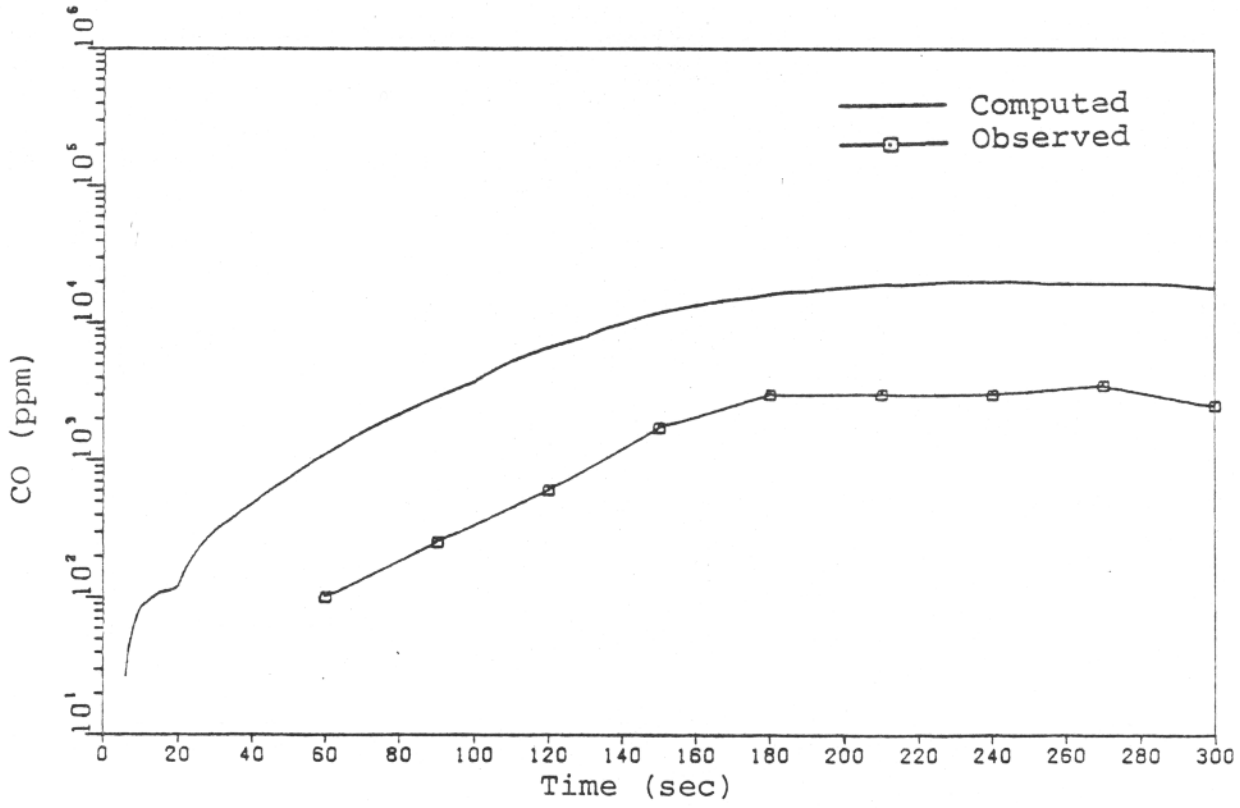

Figure 3-44. Carbon Monoxide Concentration - Case 15C

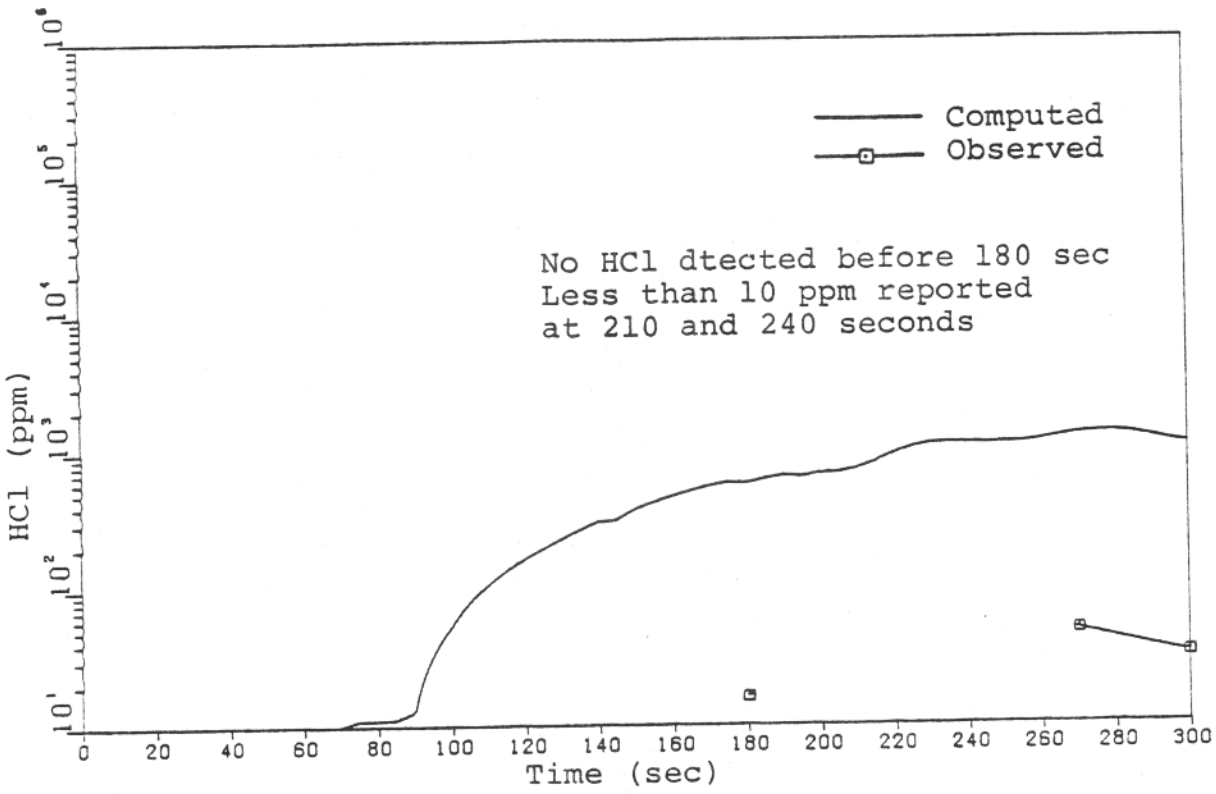

Figure 3-45. Hydrogen Chloride Concentration - Case 15C

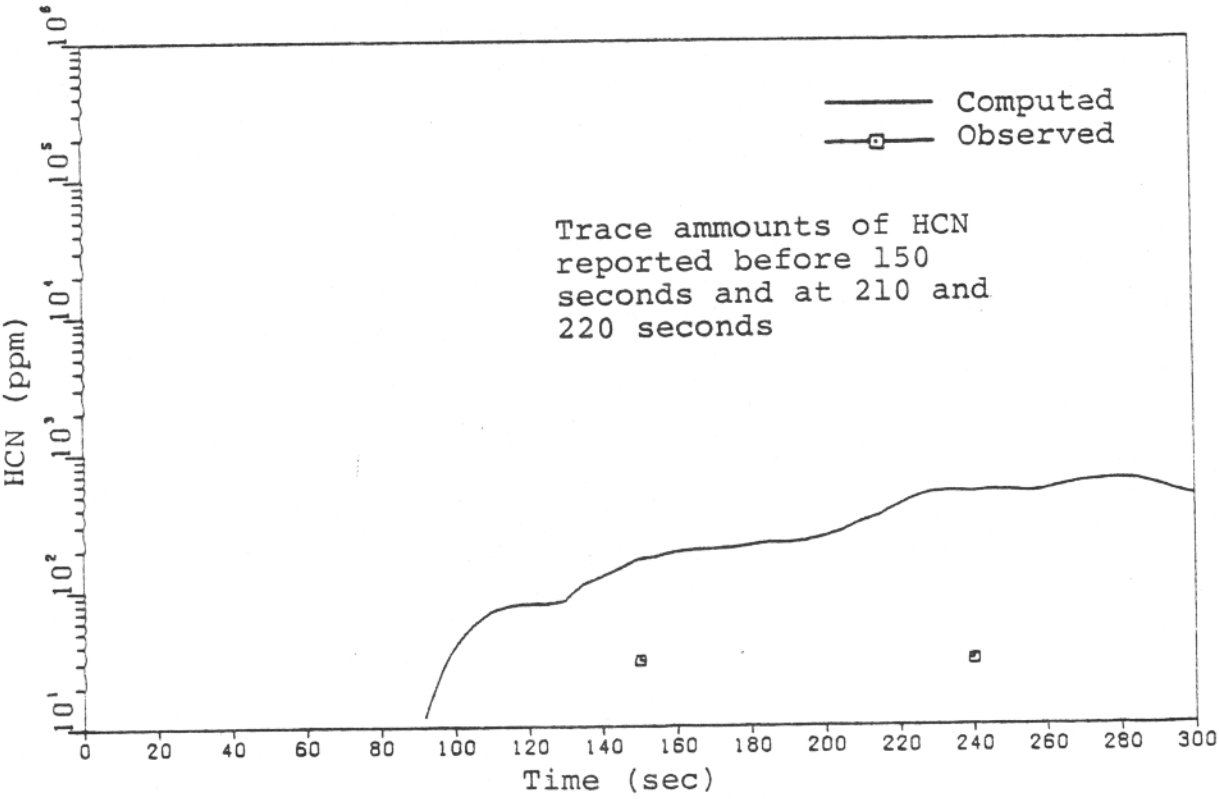

Figure 3-46. Hydrogen Cyanide Concentration - Case 15C

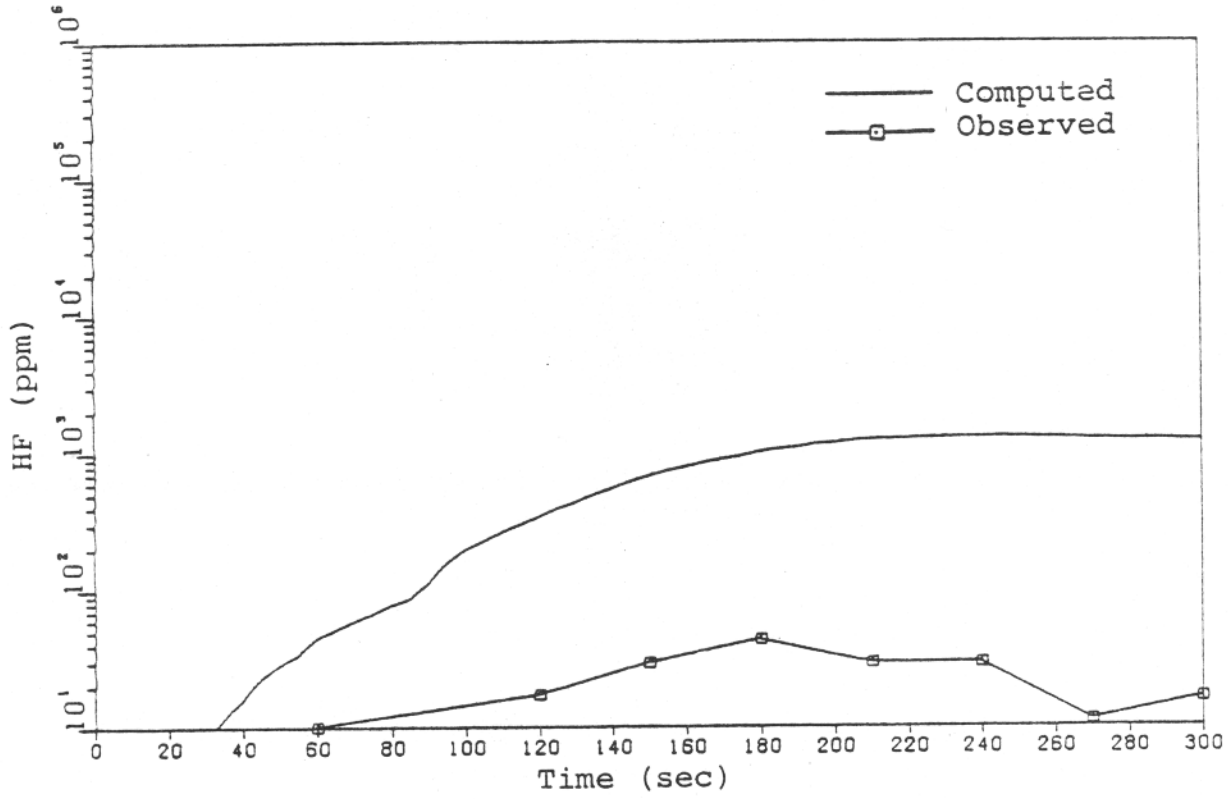

Figure 3-47. Hydrogen Fluoride Concentration - Case 15C

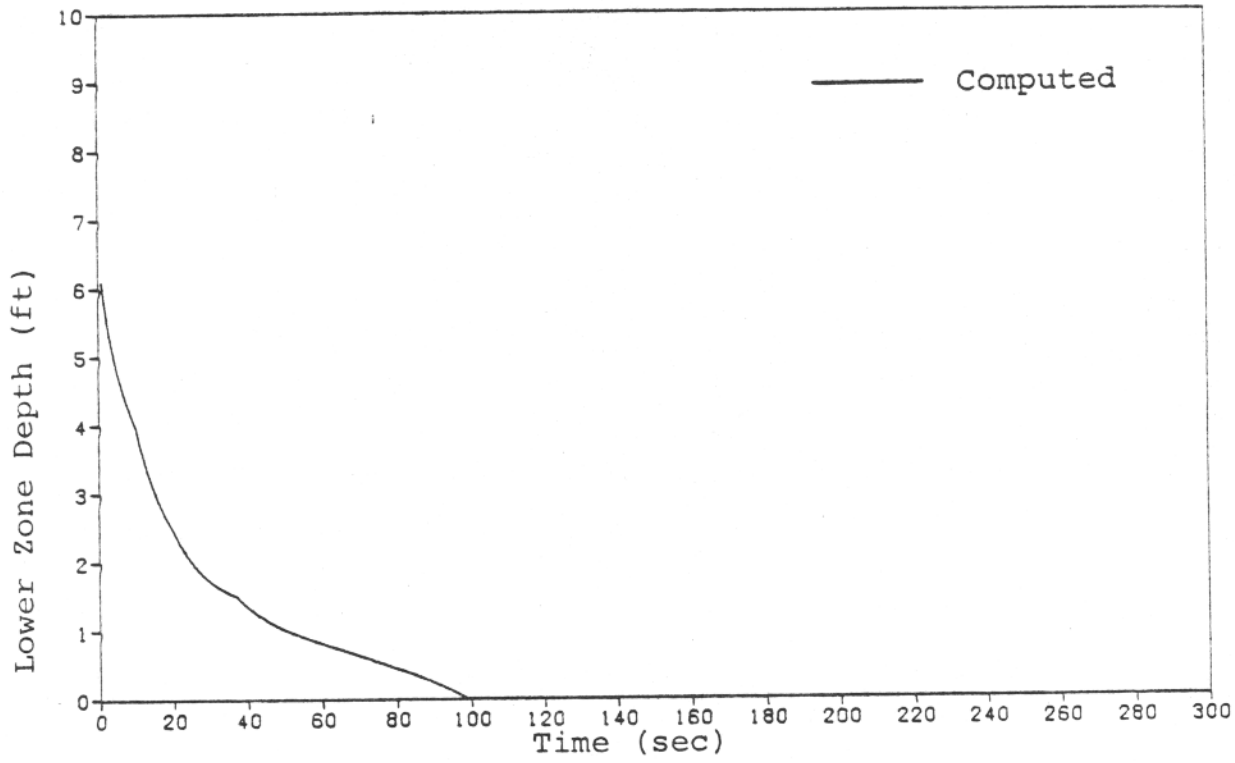

Figure 3-48. Lower Zone Depth - Case 15C

Figures 3-48 and 3-49, resembled the earlier cases. Table 3-5 and Figure 3-50 show the predicted and observed fire spread. In Figure 3-50 the ceiling and hatrack has been shaded to show fire involvement, although in the test only heavy sooting and some melting or burning of the surface coating in small, scattered areas was the only evidence of fire damage on these surfaces.

3.3.6 Case 26P - Present In-Service (1968) Materials

In the 26-foot fuselage fire tests, much more temperature and gas concentration data was available for comparison to the model's predictions. Of the fifty thermocouple channels, four were selected for comparison to DACFIR's computation of the upper zone gas temperature and are shown in Figure 3-51. The broken curves represent readings at 12 inches above the floor on the aft cabin tree, 48 inches above the floor on the forward cabin tree, 48 inches above the floor on the center tree, and 82 inches above the floor (8 inches below the ceiling) on the center cabin tree. All readings are on the fuselage centerline. The solid line is the computed temperature which shows a fair agreement with the 48 inch forward thermocouple except for the period before 80 seconds. The analysis of this test given in [6] indicates that a flash fire occurred around 90 seconds as indicated by the rapid rise of the ceiling thermocouple reading at that time. In contrast to Case 15P, however, the temperature data shows that at least some vigorous burning continued after 90 seconds. Therefore the flash fire was probably restricted to the area near the ignition fire and did not permeate the entire cabin.

Figures 3-52 through 3-58 give the cabin gas composition. Two sets of experimental data are included. Readings at sample port A were taken 48 inches above the floor and directly opposite the fire. Readings from sample port B were taken at the same vertical position and side of the fuselage as A but 20 inches from the forward bulkhead. Equipment failure caused much of the gas data to be lost after

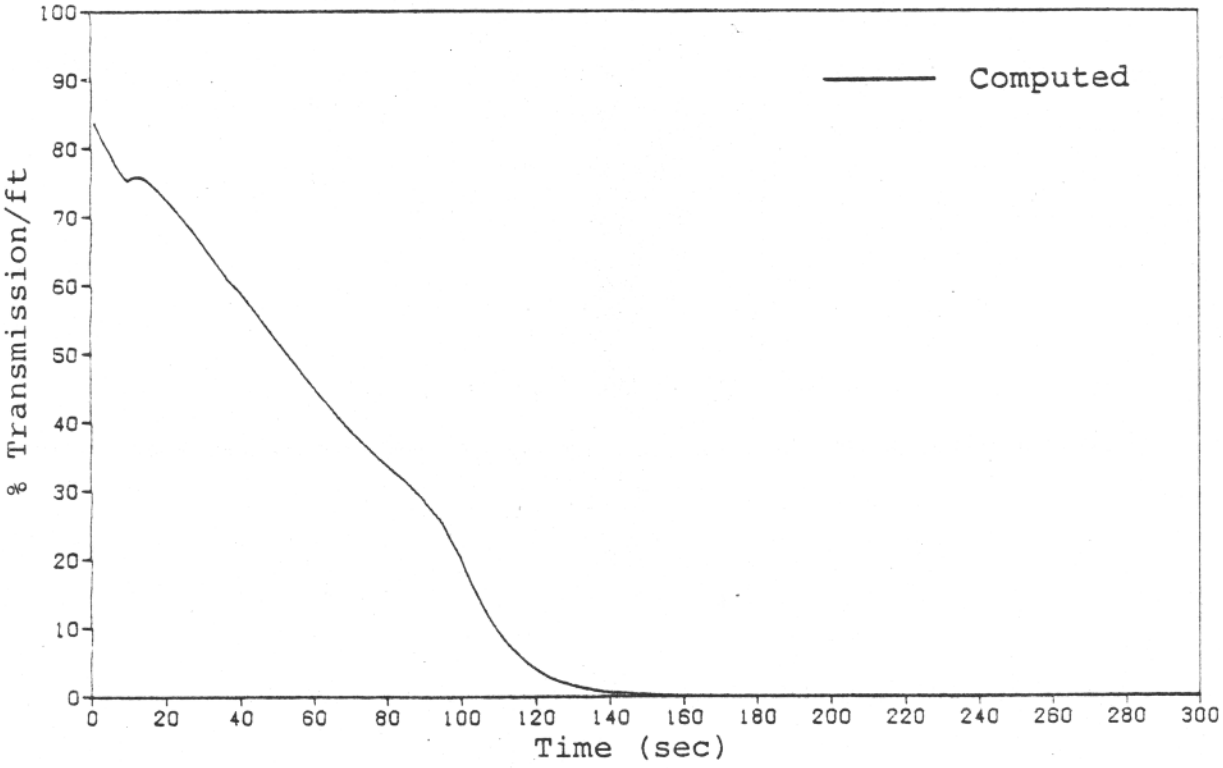

Figure 3-49. Smoke Accumulation - Case 15C

TABLE 3-5

COMPARISON OF SIMULATED AND OBSERVED AREAS OF DAMAGE - CASE 15C

	OBSERVED AREA[1]		COMPUTED AREA	
STRUCTURE	(ft^2)	% TOTAL EXPOSED	(ft^2)	% TOTAL EXPOSED
Sidewall	20.0	23	45.0	100
Hatrack	0.0	0	33.8	100
Ceiling	5.0	4	55.5	64
Seats	19.0	43[2]	124.2	93[3]

[1] Damaged area within test section considered by model (center 7.5 ft or 15 ft length)

[2] Damage on one seat row

[3] Total damage on three seat rows

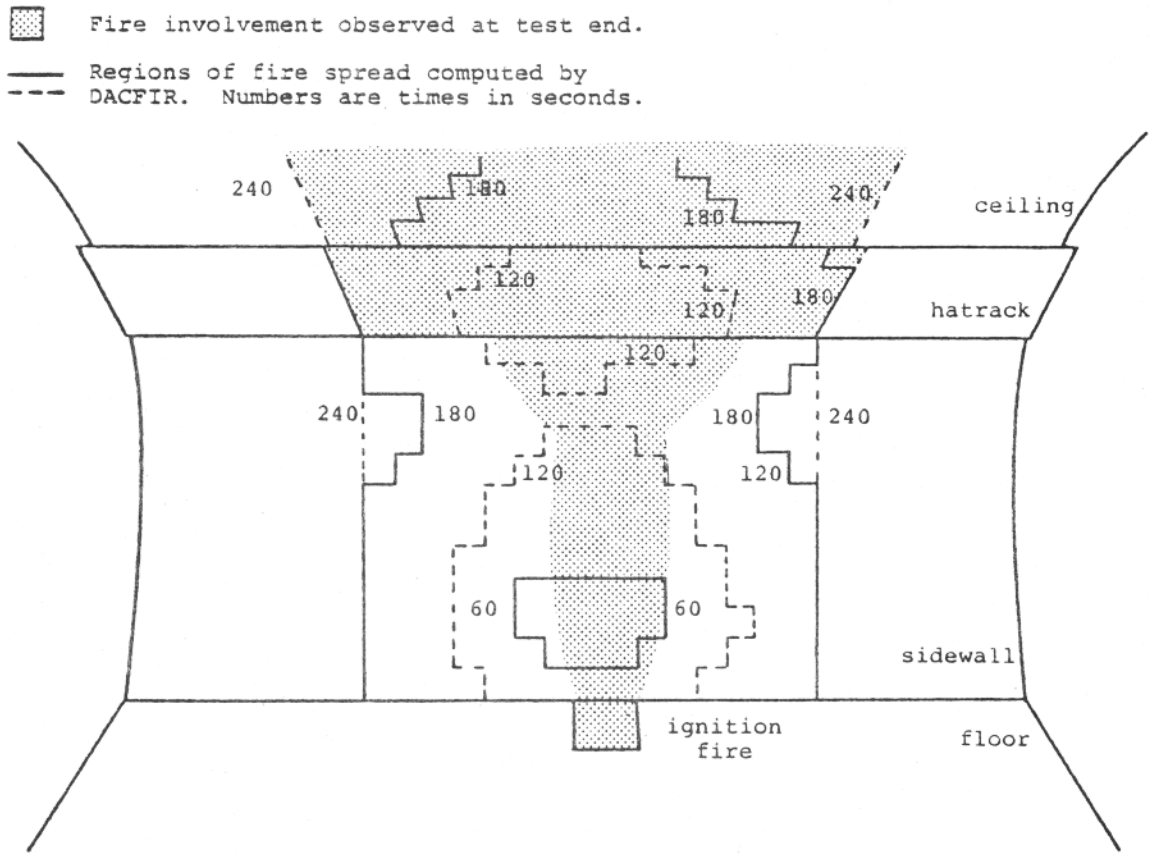

Damage on cabin lining surfaces

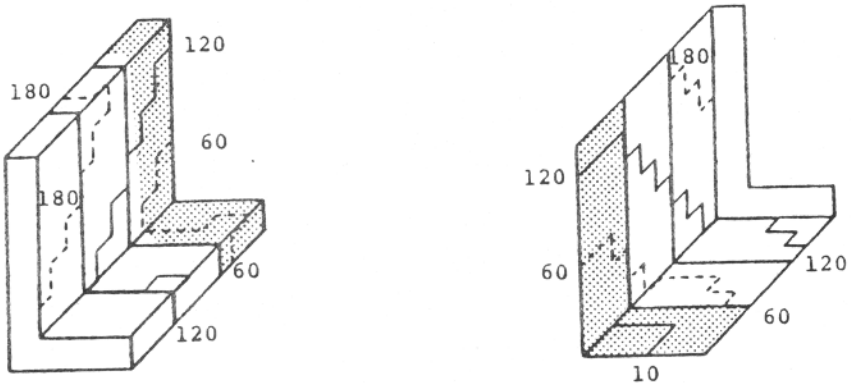

Damage on seat row above ignition fire

Figure 3-50. Computed and Observed Areas of Damage - Case 15C

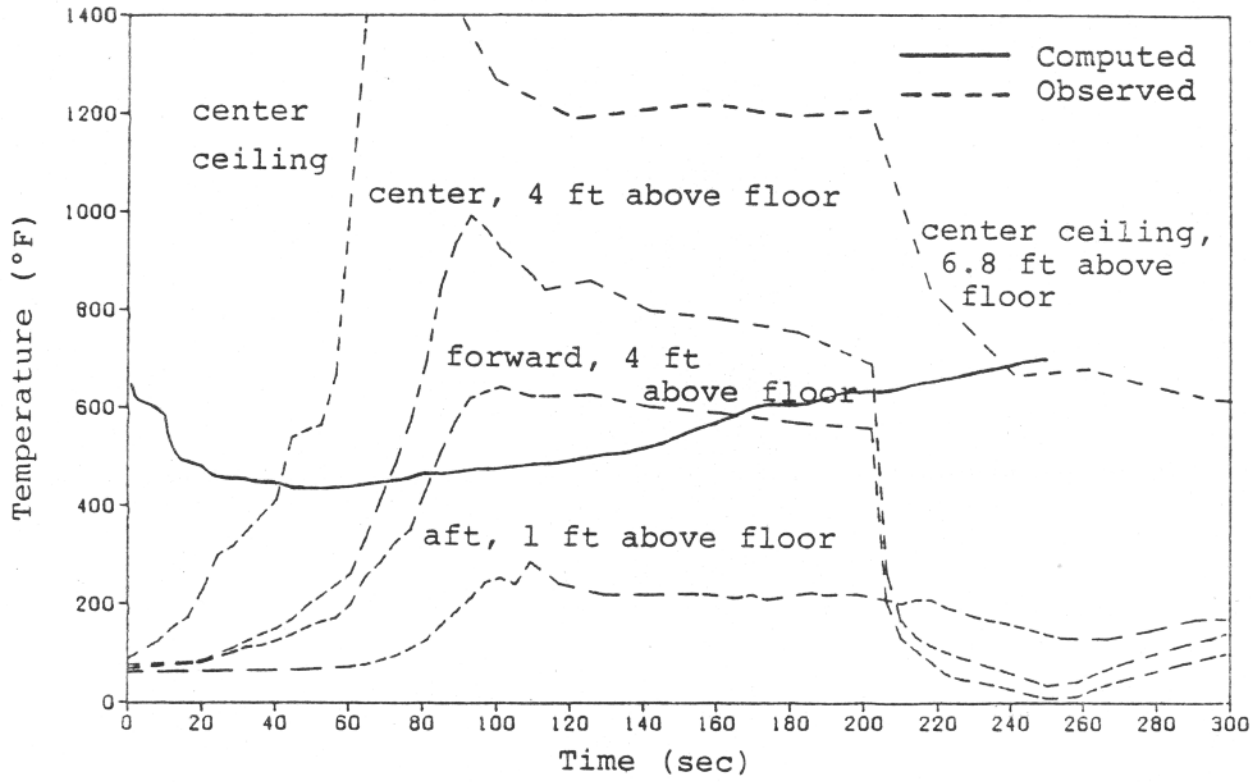

Figure 3-51. Upper Zone Temperature - Case 26P

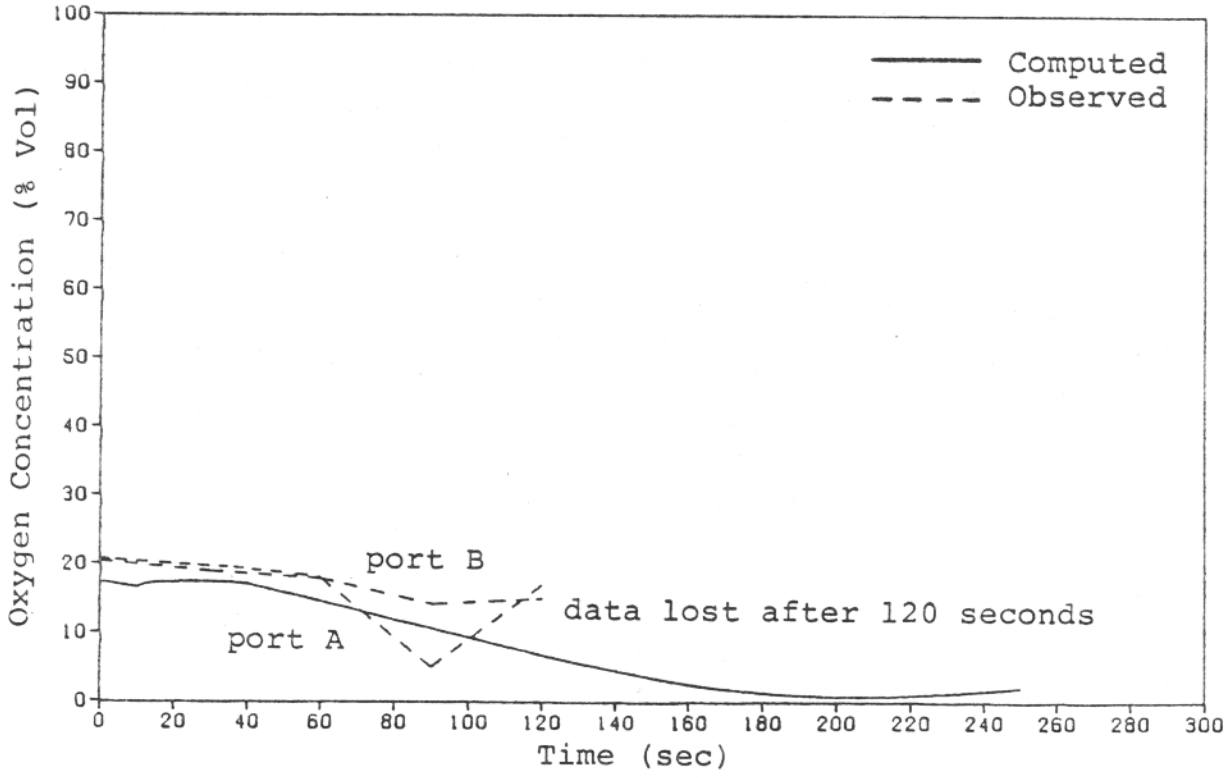

Figure 3-52. Oxygen Concentration - Case 26P

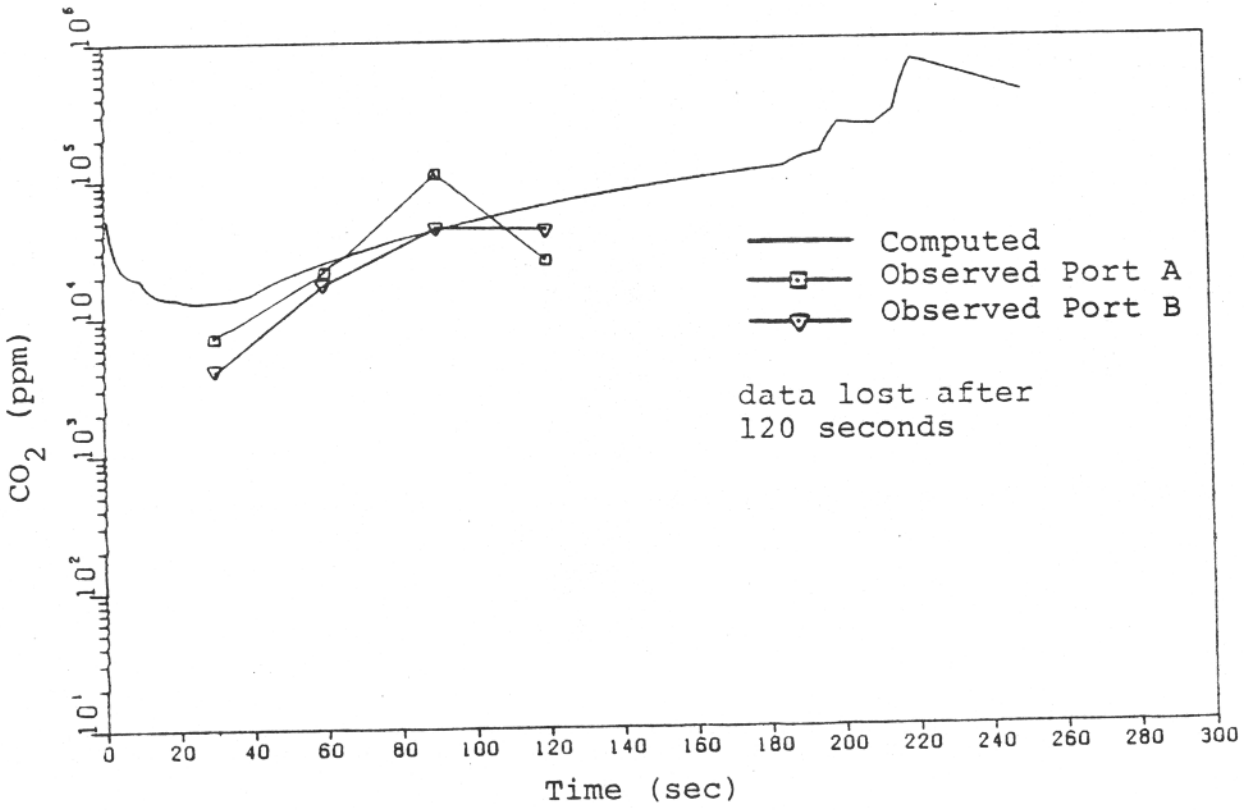

Figure 3-53. Carbon Dioxide Concentration - Case 26P

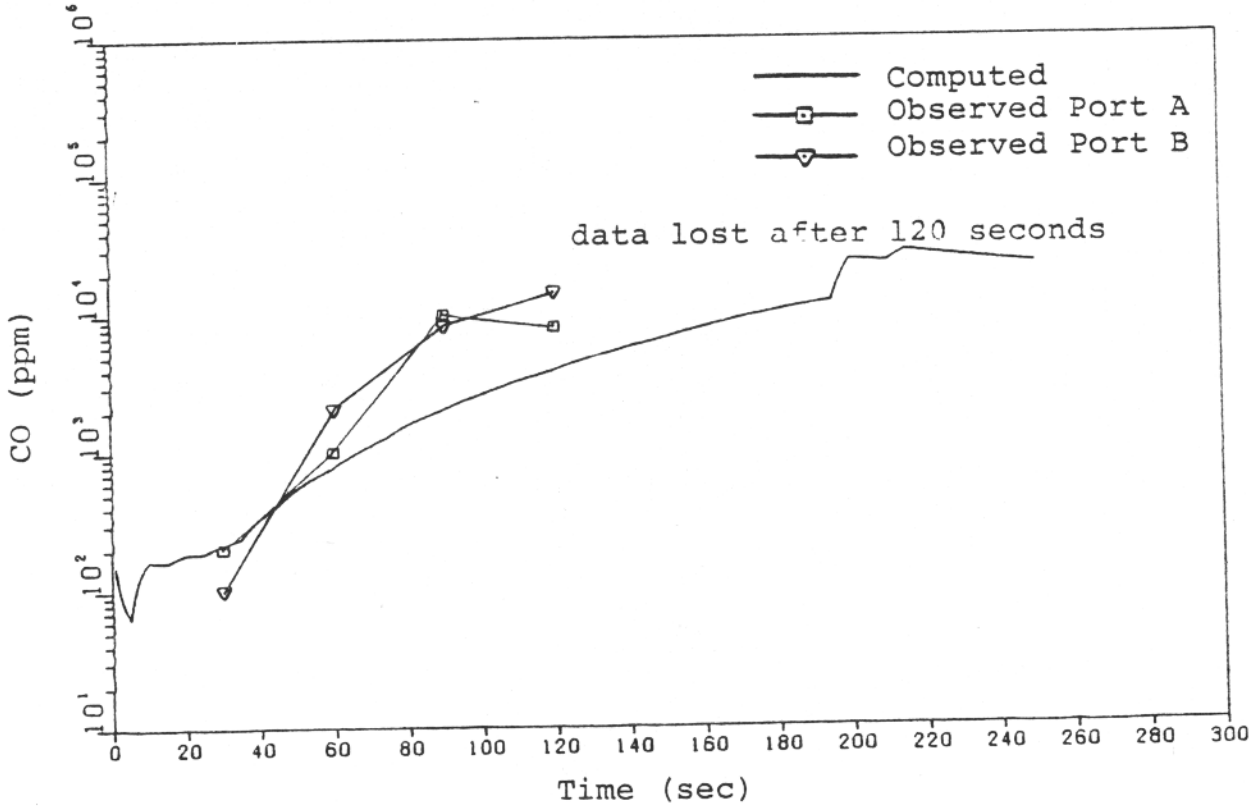

Figure 3-54. Carbon Monoxide Concentration - Case 26P

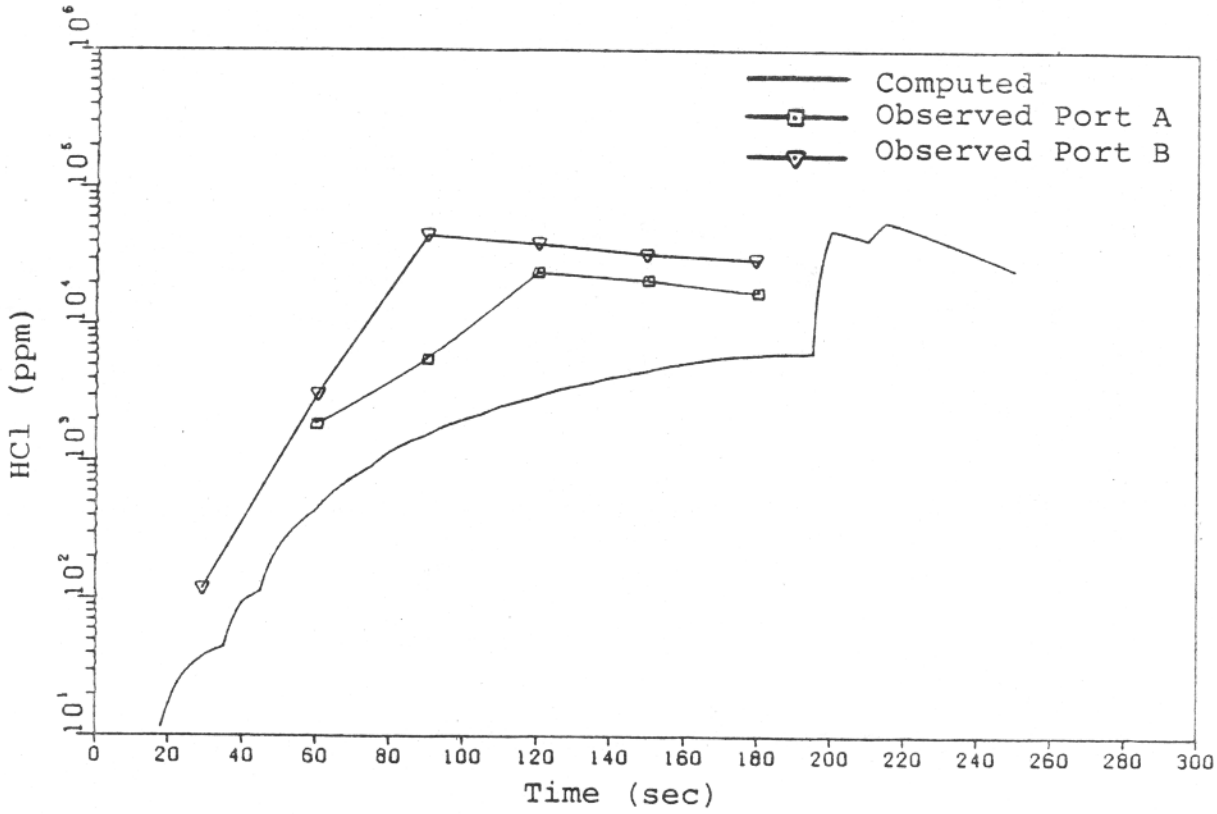

Figure 3-55. Hydrogen Chloride Concentration - Case 26P

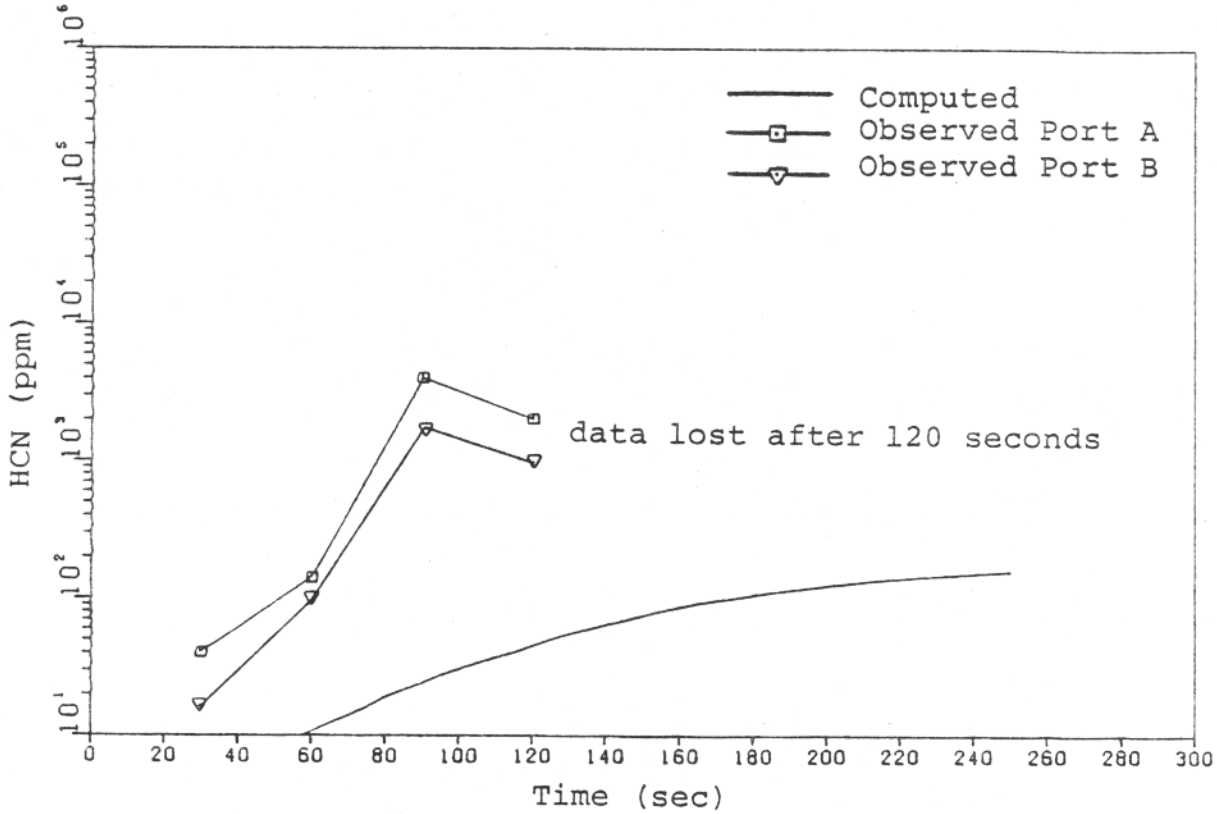

Figure 3-56. Hydrogen Cyanide Concentration - Case 26P

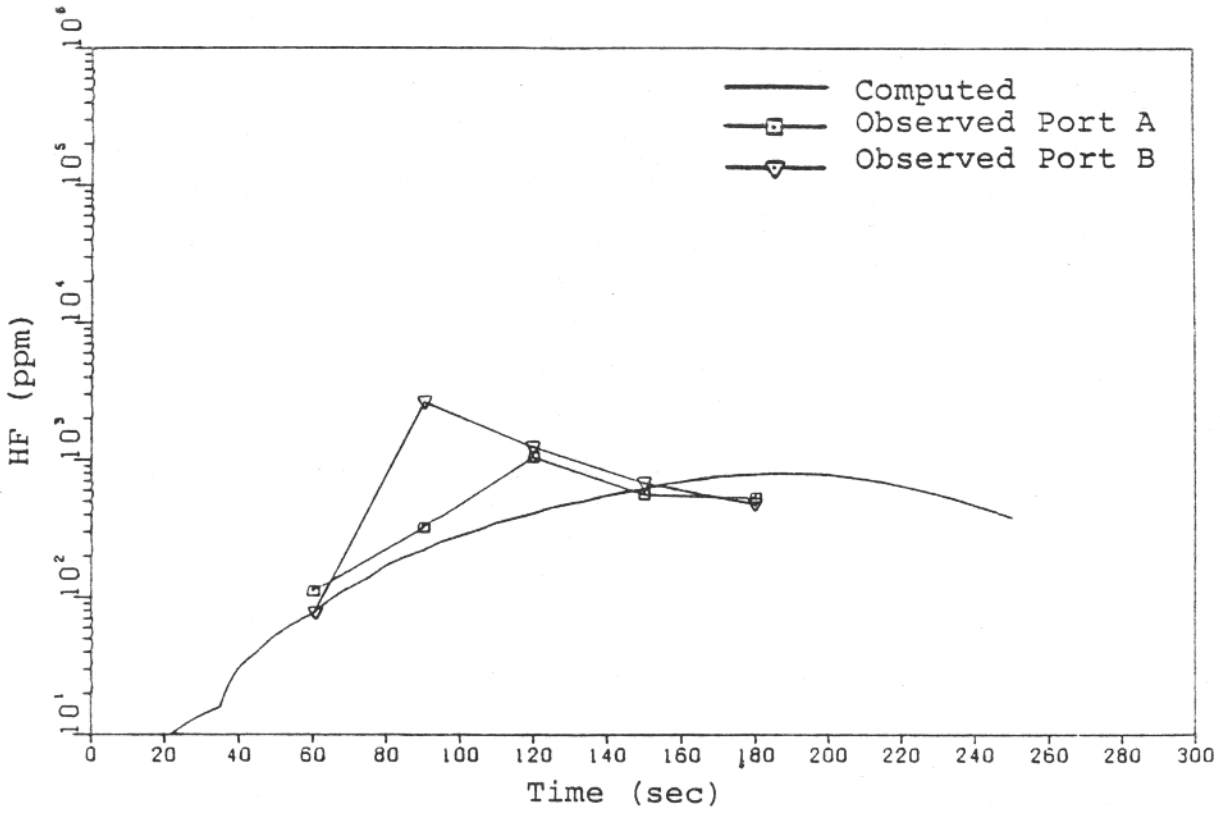

Figure 3-57. Hydrogen Fluoride Concentration - Case 26P

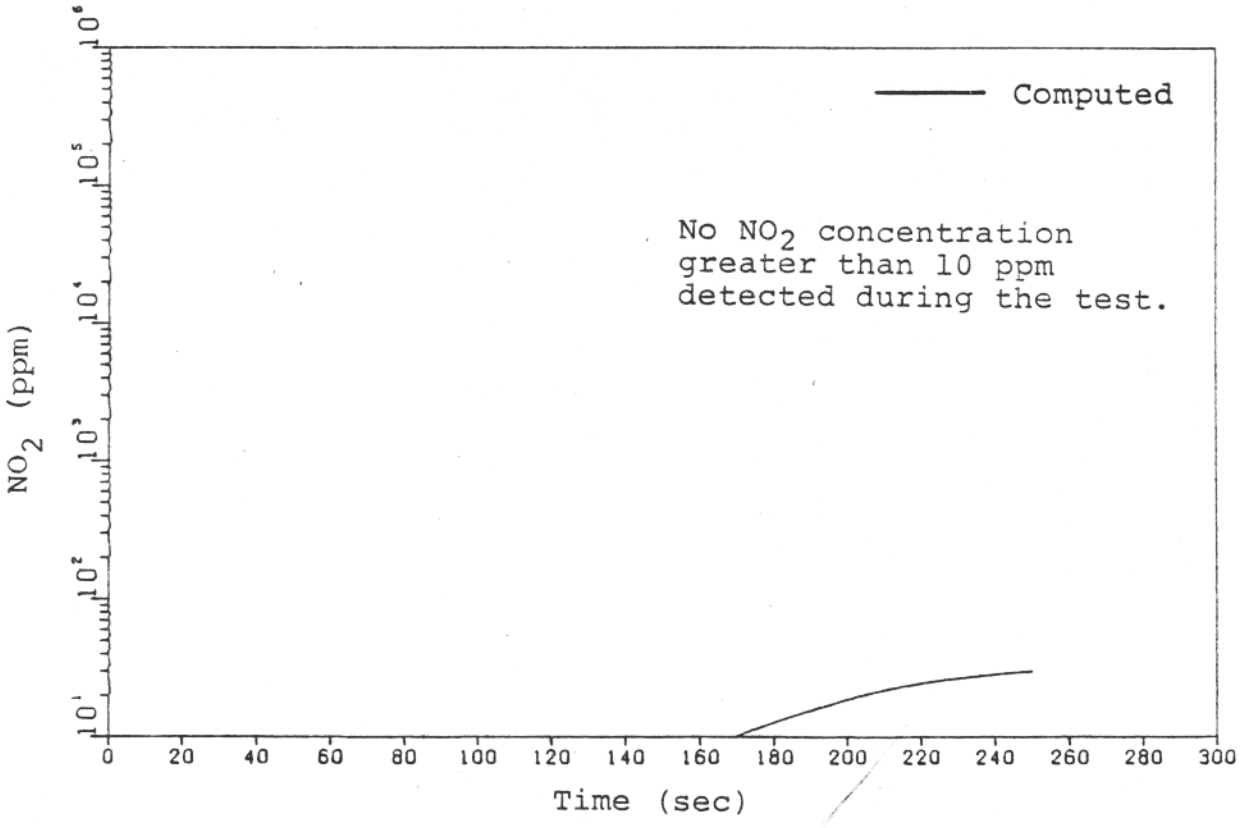

Figure 3-58. Nitrogen Dioxide Concentration - Case 26P

120 seconds. For O_2, CO_2, CO, and HF the agreement of the model and results are fair to good. HCN and HCl are underestimated by an order of magnitude at some points. NO_2 levels were very low in the test, always less than 10 ppm, and the computed value of NO_2 does not exceed about 100 ppm.

Figure 3-59 shows that the computed upper zone depth filled the 2000 cubic foot volume of the cabin at 140 seconds. Figure 3-60 shows that the smoke reduced visibility below 1% at 115 seconds. Table 3-6 and Figure 3-61 show the comparison of fire involvement.

3.3.7 Case 26N - Improved Materials

Figures 3-62 through 3-71 and Table 3-7 give the comparison between the model and test results for Case 26N. In this test improved materials were used. The materials were essentially the same as those of 15B but with the addition of carpet, window reveals and dust panes, and simulated PSU surfaces. The data presented is that from the second attempt at conducting the full scale test; in the first attempt flames from the fuel pan would not enter the cabin due, apparently, to wind conditions [6]. In this second try, the same problem with ignition occurred until the fuel pan wind screen was removed at which point almost all the flames suddenly entered the rupture driven by a six knot wind.

The larger size of the fuel fire and, perhaps, its intensification by the wind is apparently the reason that the temperatures, gas concentrations, and areas of damage in this test are roughly the same as Case 26P even through improved materials were used. The figures do not show the improvement that was observed between Cases 15P and 15B. The DACFIR model, however, demonstrates the improved flammability properties of the furnishings as is shown by the lower computed temperature, Figure 3-62 versus Figure 3-51, and smaller computed flame spread, Figure 3-71 versus Figure 3-61. Since the model does not contain a mechanism for simulating the wind effect on the

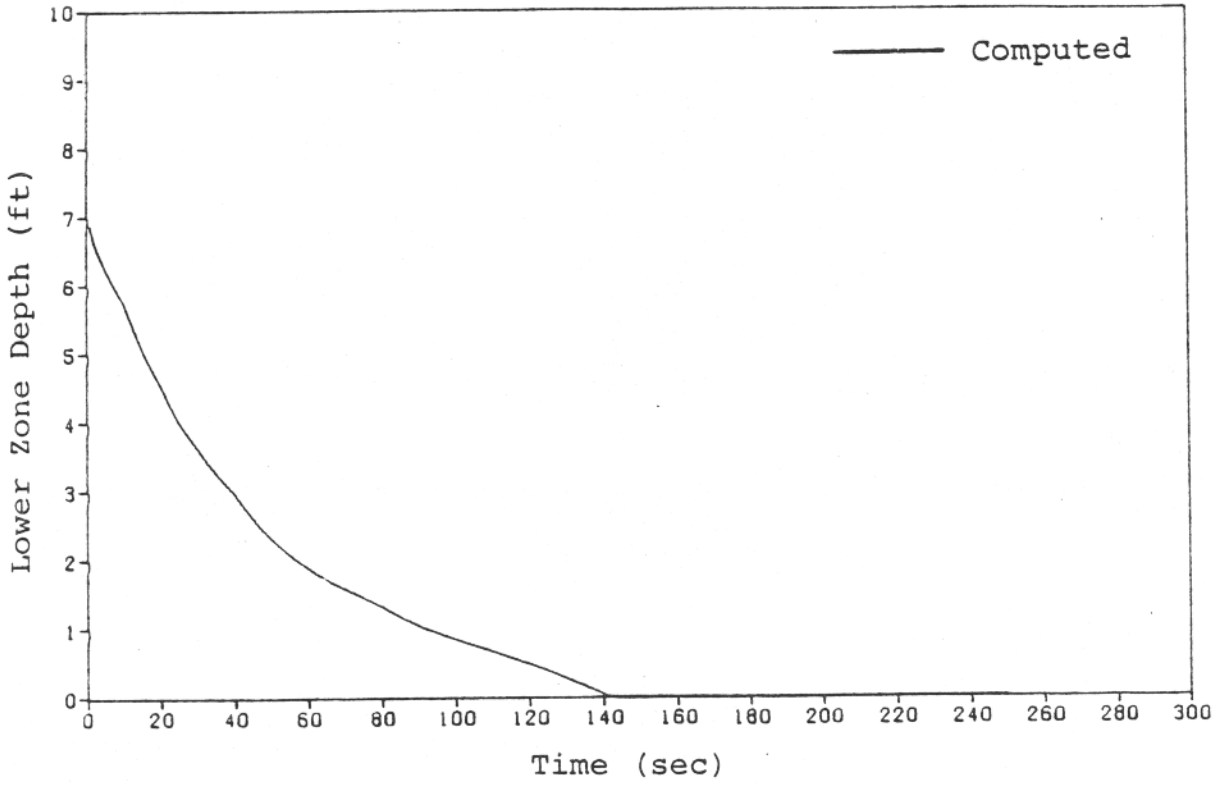

Figure 3-59. Lower Zone Depth - Case 26P

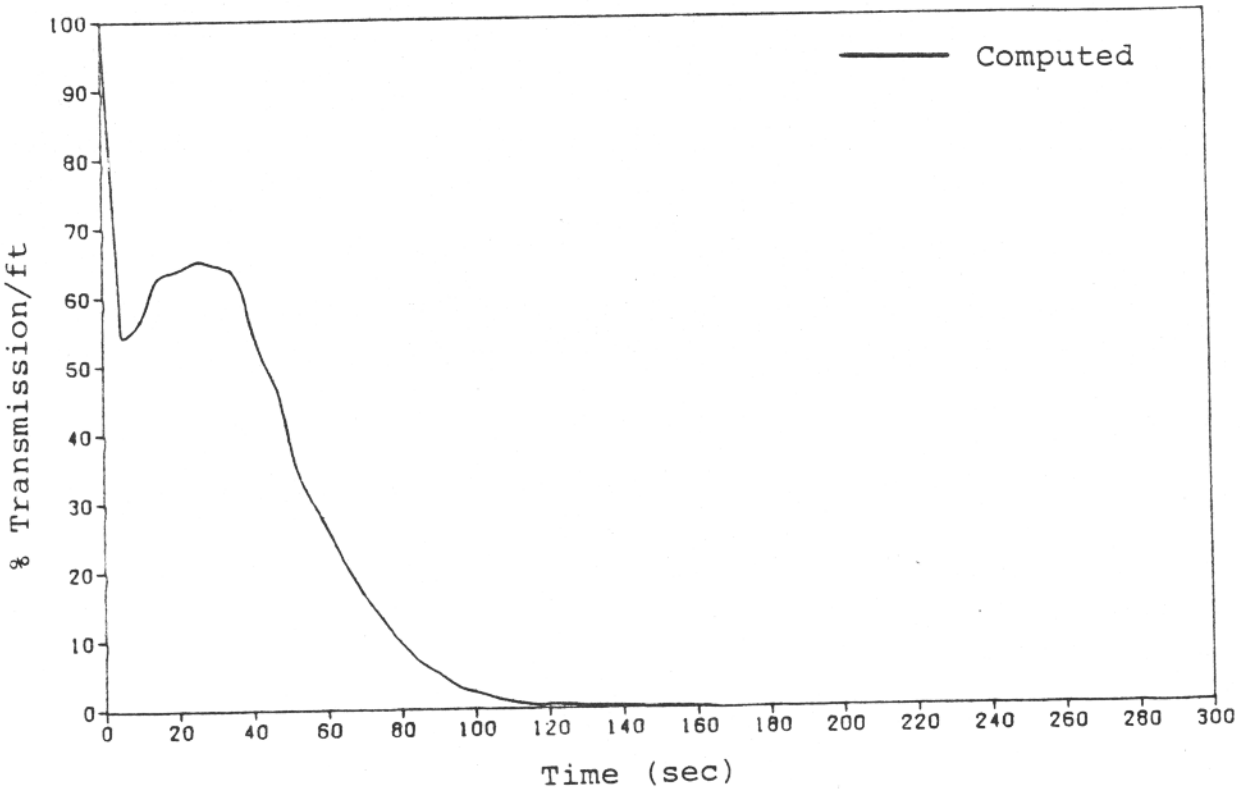

Figure 3-60. Smoke Accumulation - Case 26P

TABLE 3-6

COMPARISON OF SIMULATED AND OBSERVED AREAS OF DAMAGE - CASE 26P

STRUCTURE		OBSERVED AREA[1] (ft^2)	OBSERVED AREA[1] % TOTAL EXPOSED	COMPUTED AREA (ft^2)	COMPUTED AREA % TOTAL EXPOSED
Carpet		2.5	3	14.3	17
Sidewall		25 - 34	30 - 40[2]	43.3	48
PSU		32.5	100[2]	14.3	48
Hatrack Bullnose		10.7	95	2.8	37
Hatrack		32.5	100	6.3	5
Ceiling		75.0	100[3]	13.8	12
Seats	Group				
	1	0	0	0	0
	2	0	0	28.0	51
	3	0	0	0	0
	4	18.5	42	41.8	76
	5	0	0	0	0
	6	0	0	17.5	32

[1] Damaged area within test section considered by model

[2] Damage described as "melting and shrinking" of the vinyl

[3] Much delamination occurred, the amount of actual burning is not known

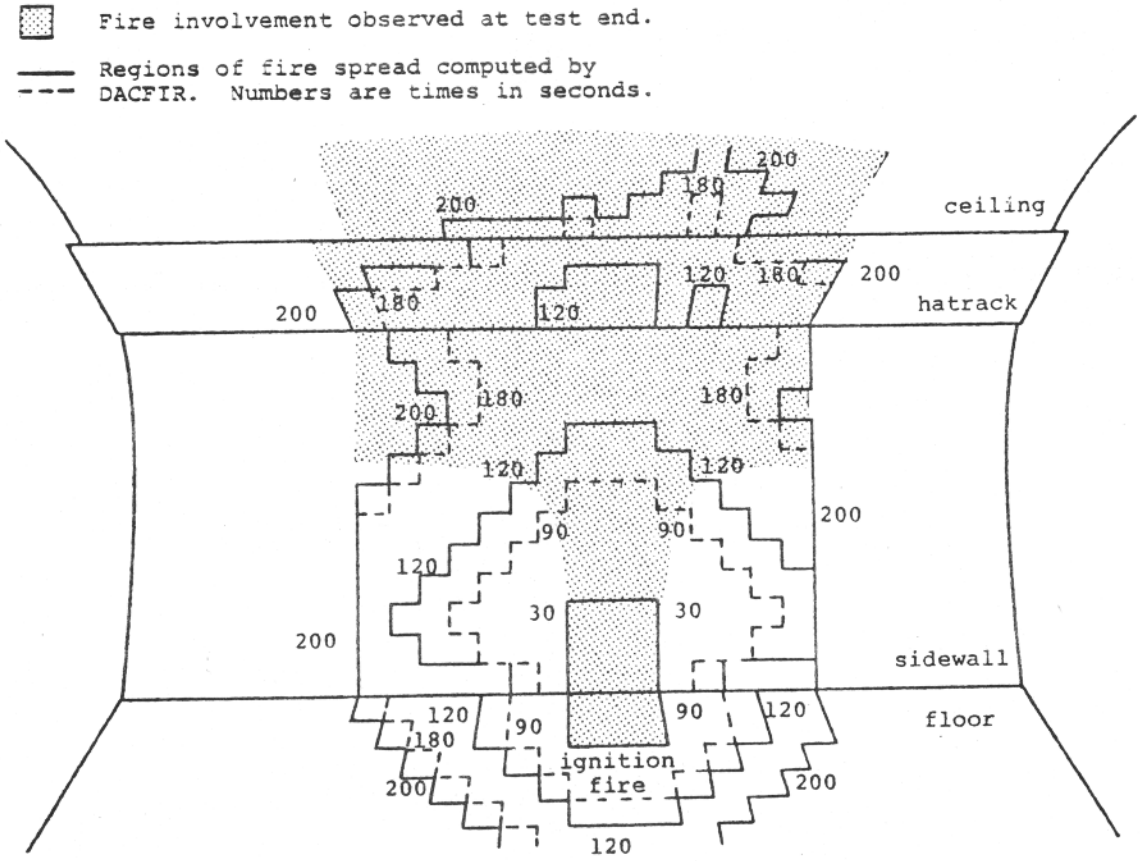

Damage on cabin lining surfaces

Damage on seat row above ignition fire

Figure 3-61. Computed and Observed Areas of Damage - Case 26P

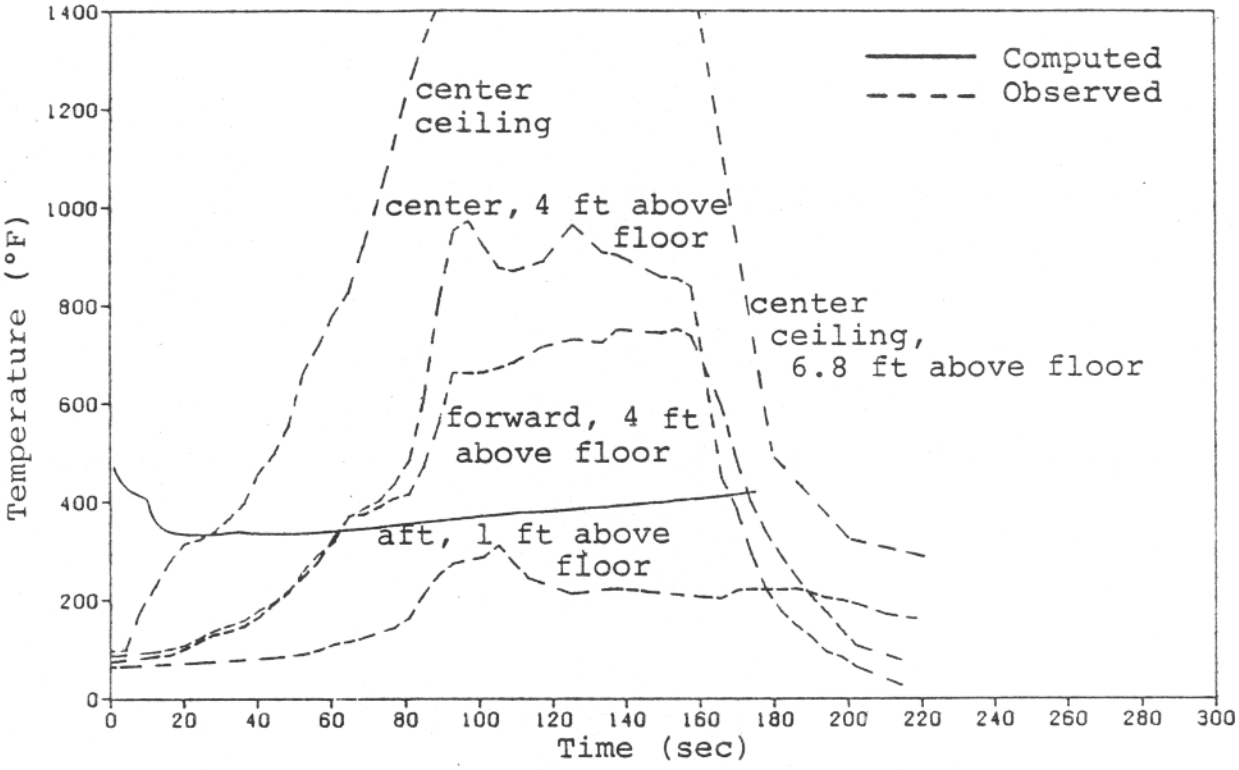

Figure 3-62. Upper Zone Temperature - Case 26N

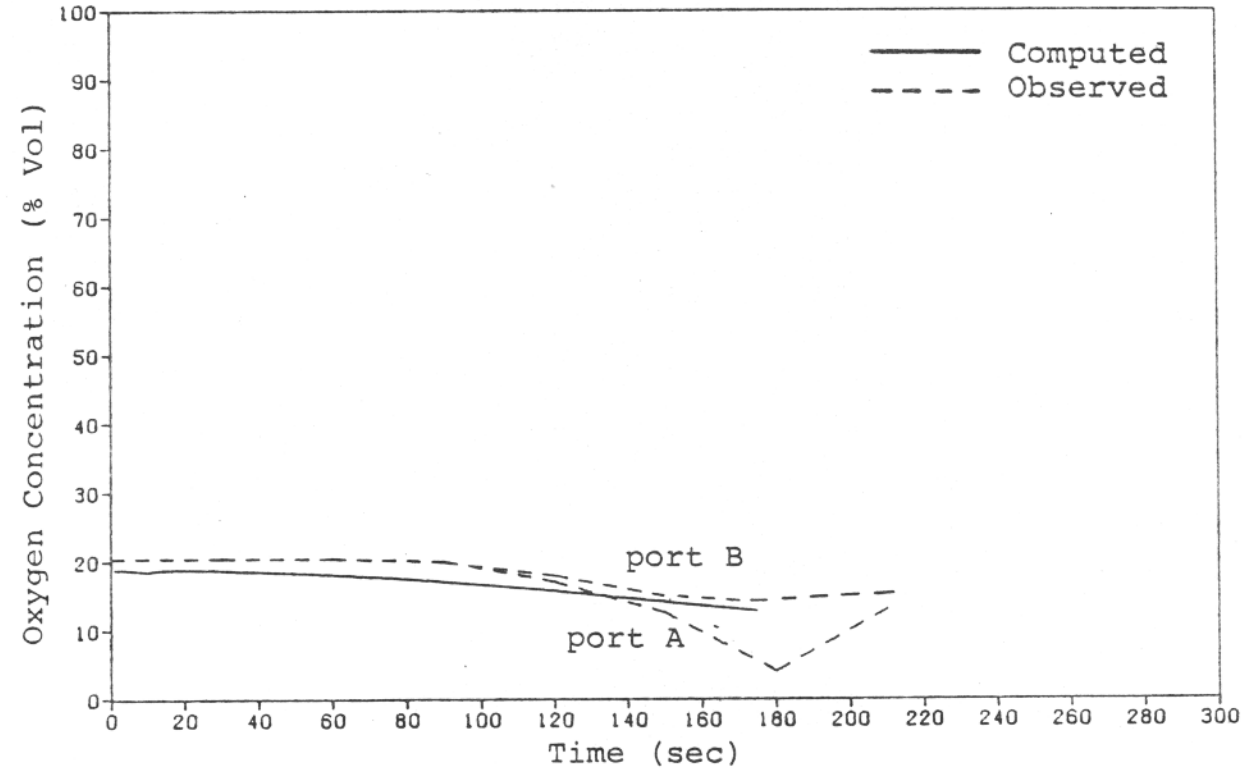

Figure 3-63. Oxygen Concentration - Case 26N

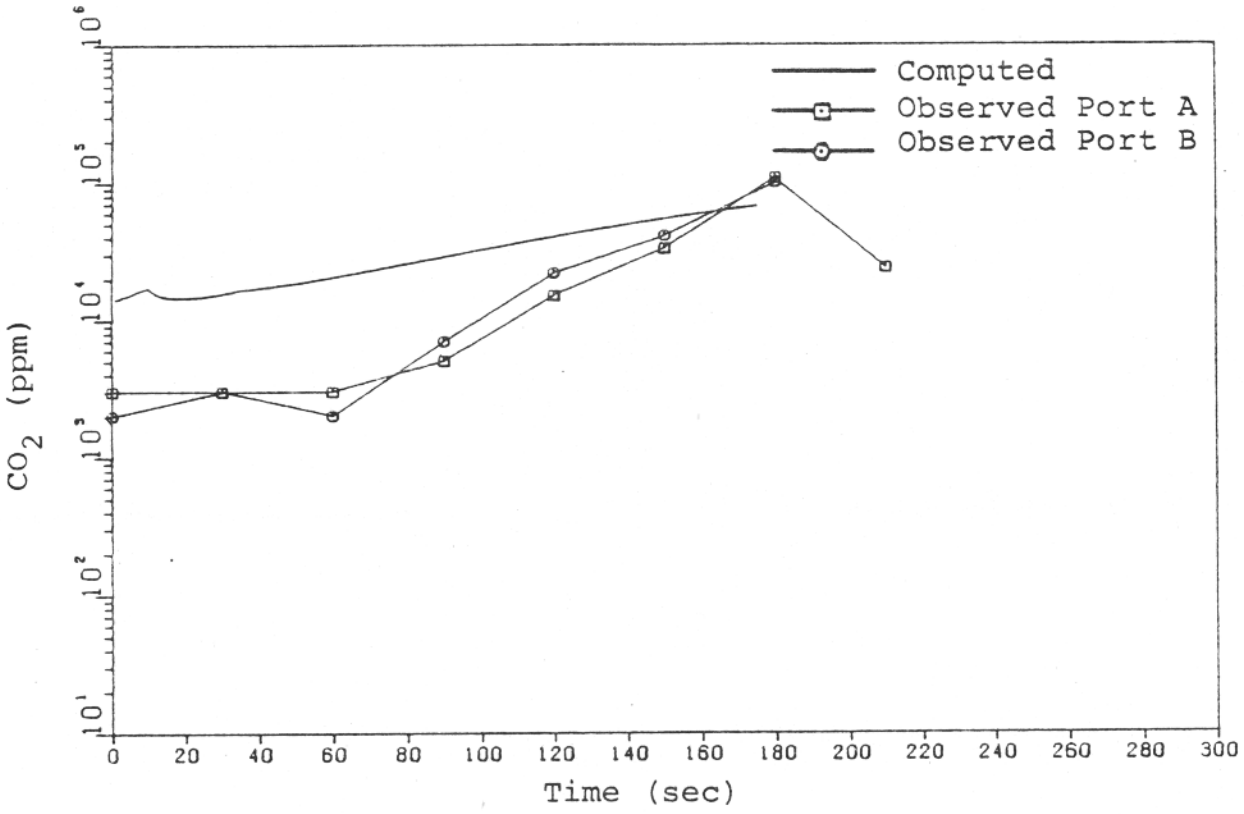

Figure 3-64. Carbon Dioxide Concentration - Case 26N

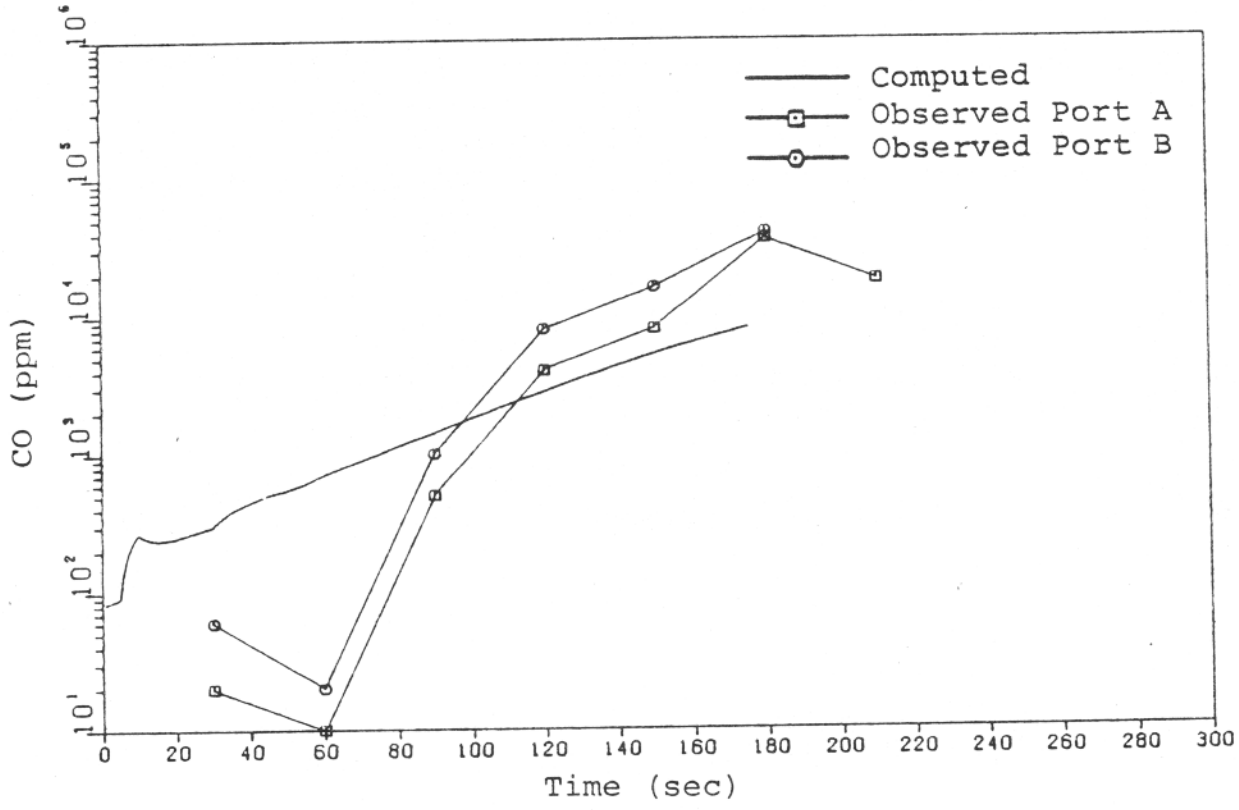

Figure 3-65. Carbon Monoxide Concentration - Case 26N

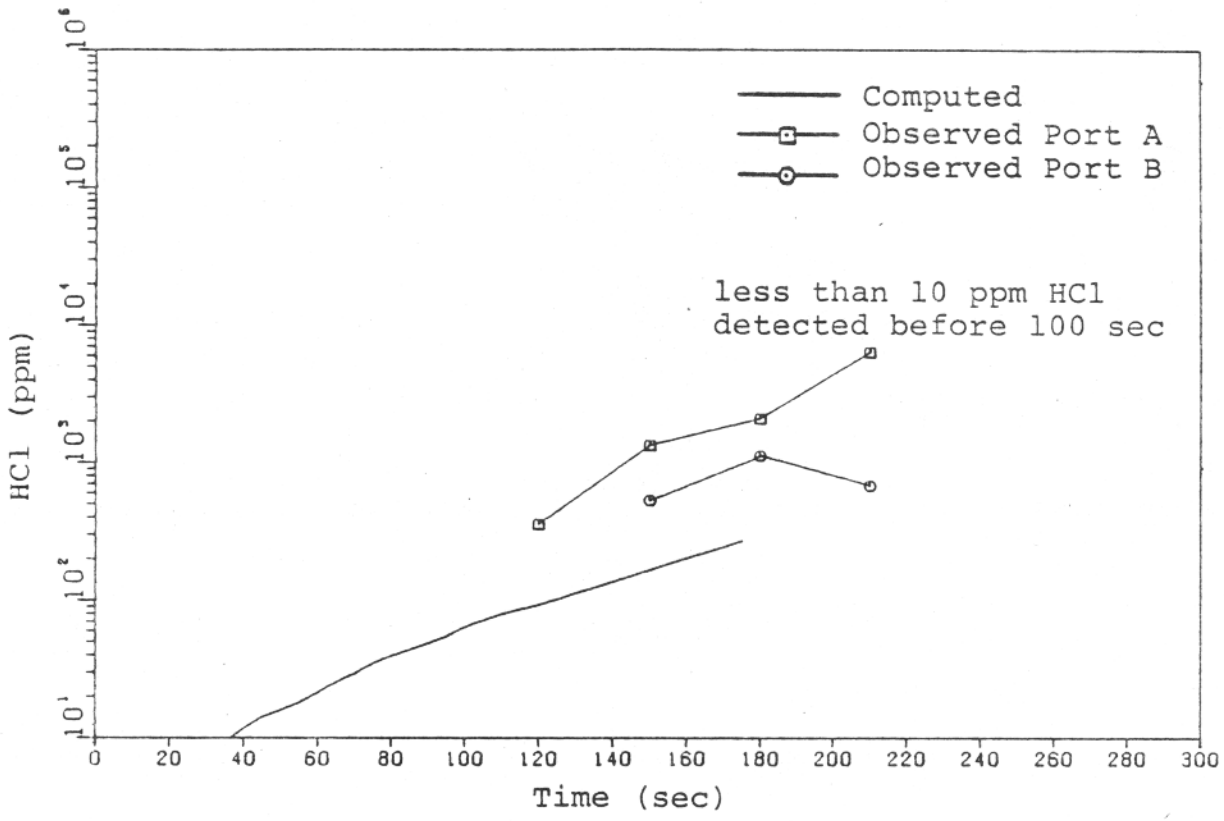

Figure 3-66. Hydrogen Chloride Concentration - Case 26N

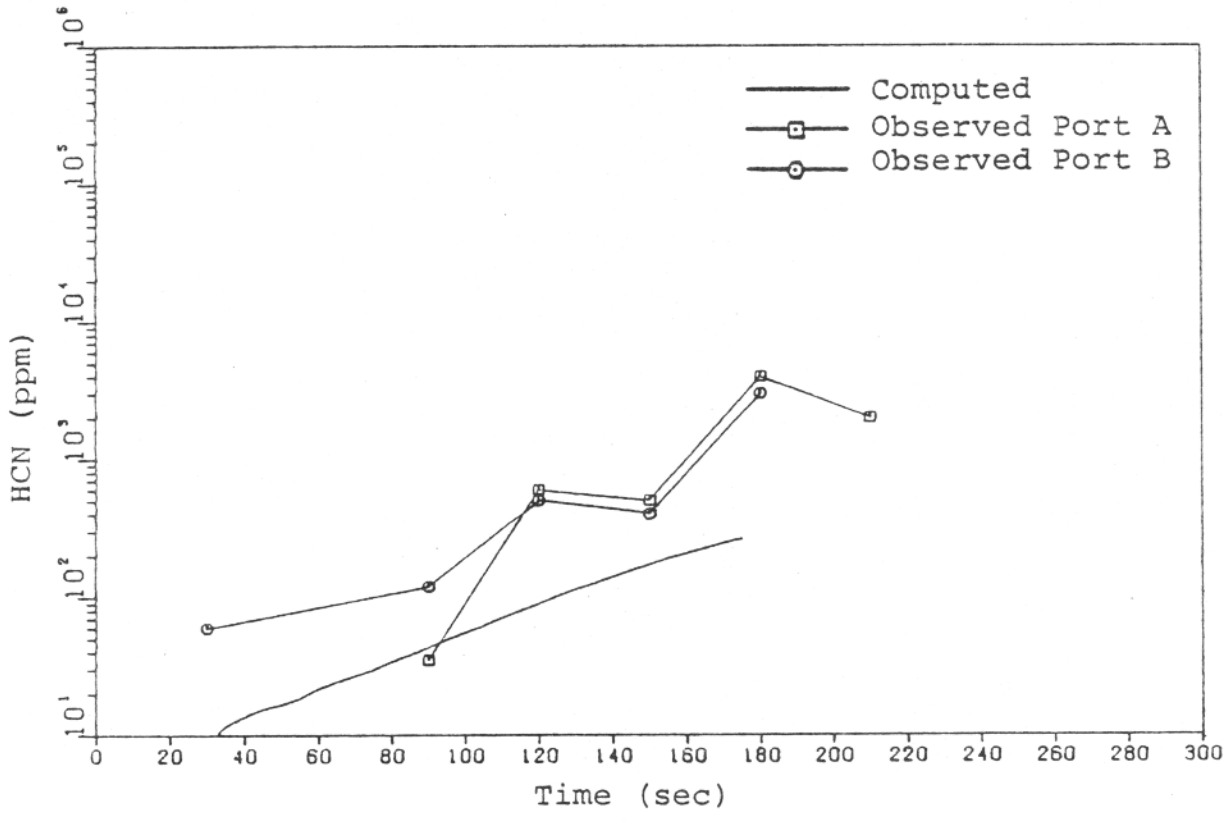

Figure 3-67. Hydrogen Cyanide Concentration - Case 26N

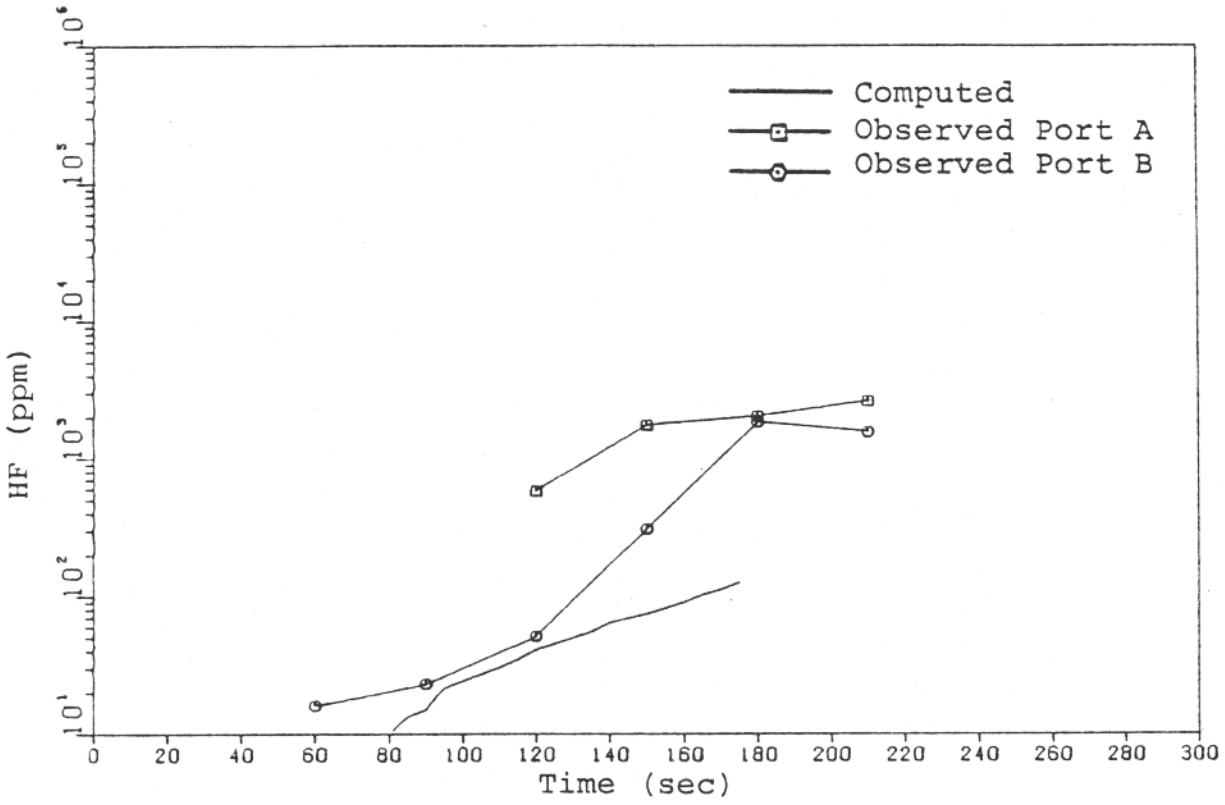

Figure 3-68. Hydrogen Fluoride Concentration - Case 26N

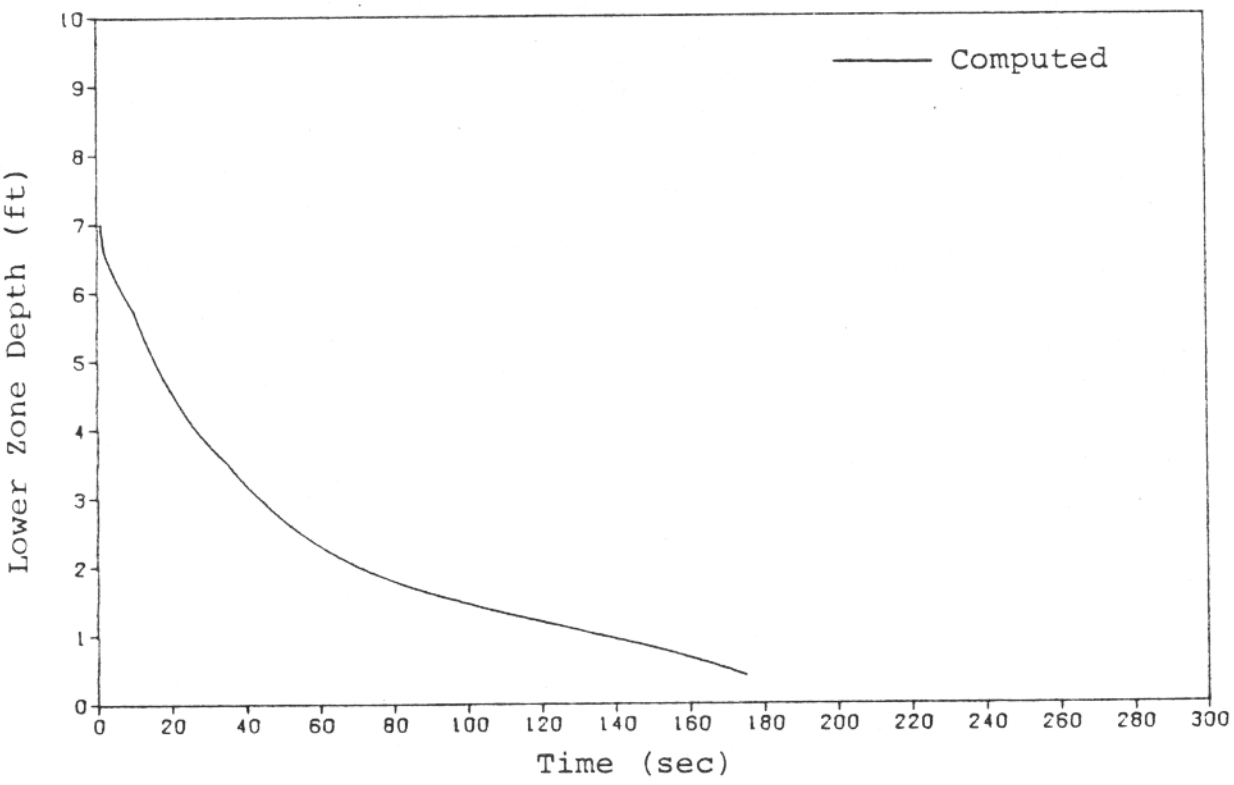

Figure 3-69. Lower Zone Depth - Case 26N

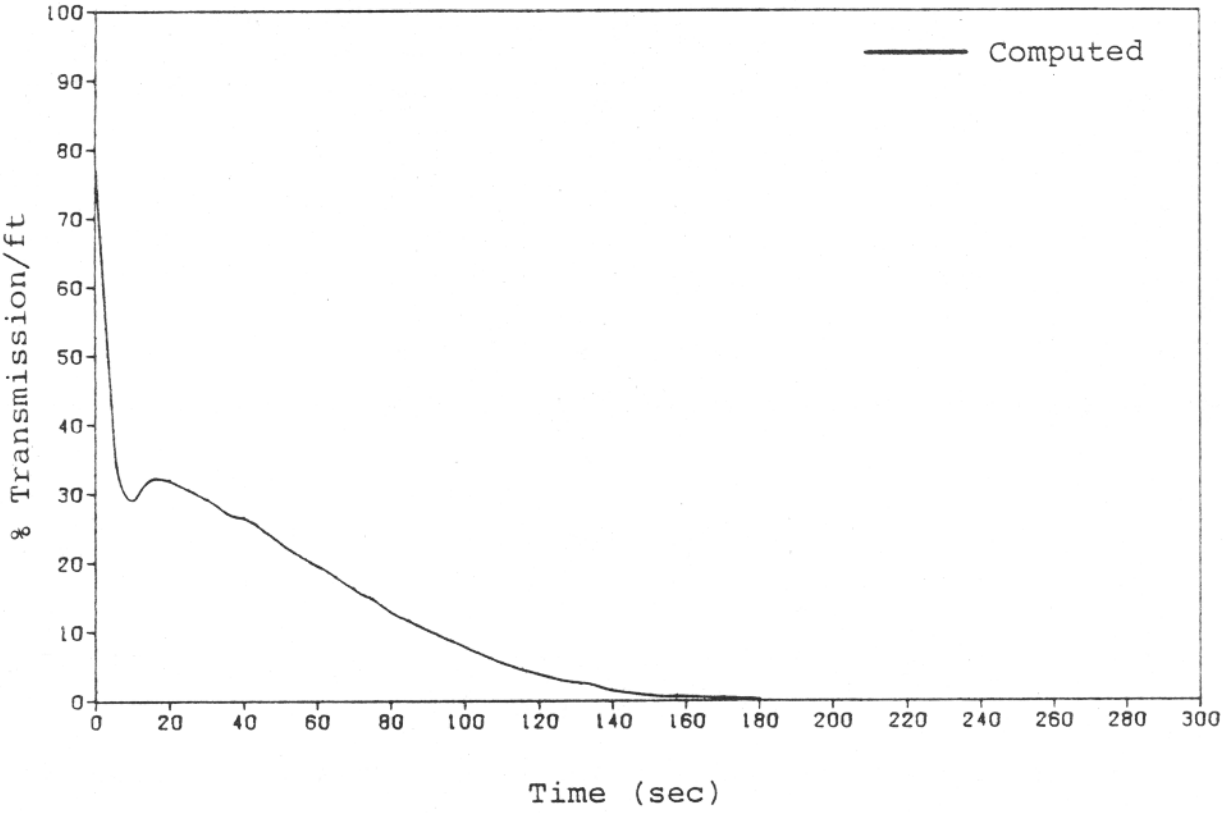

Figure 3-70. Smoke Accumulation - Case 26N

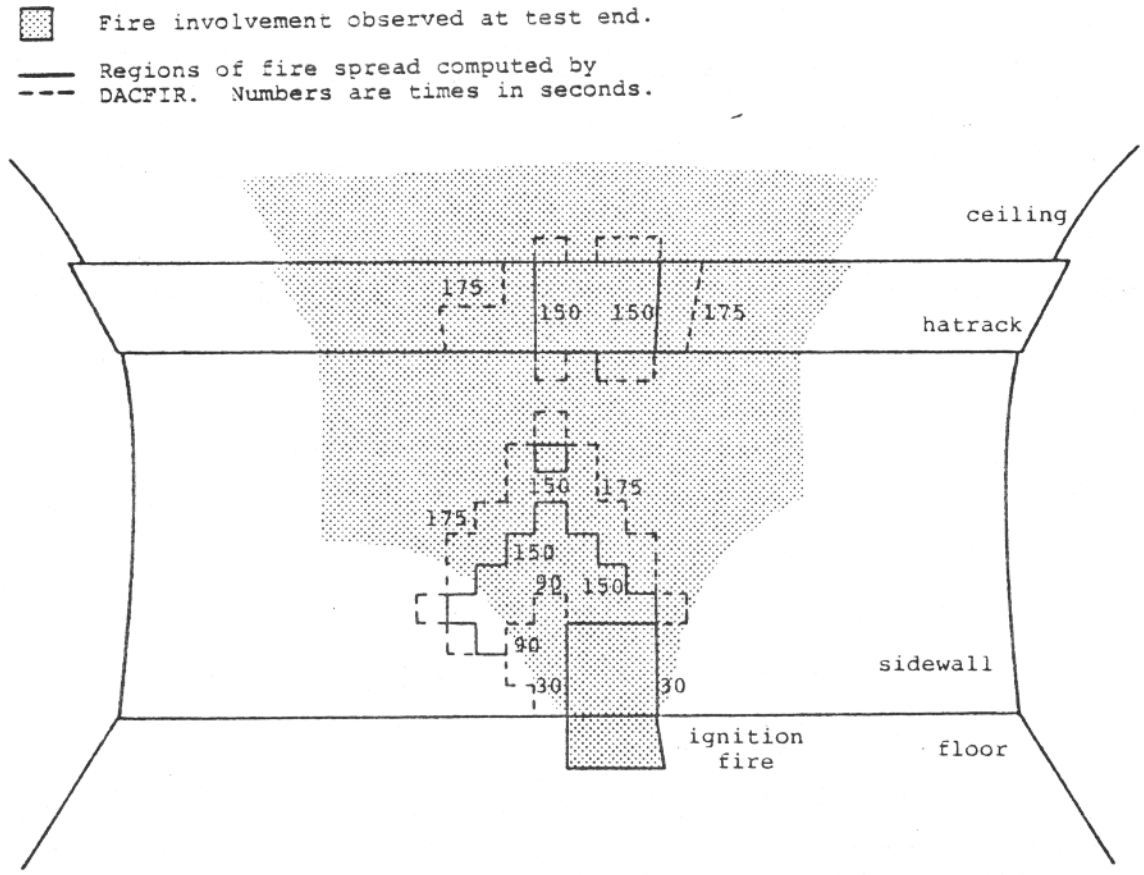

Damage on cabin lining surfaces

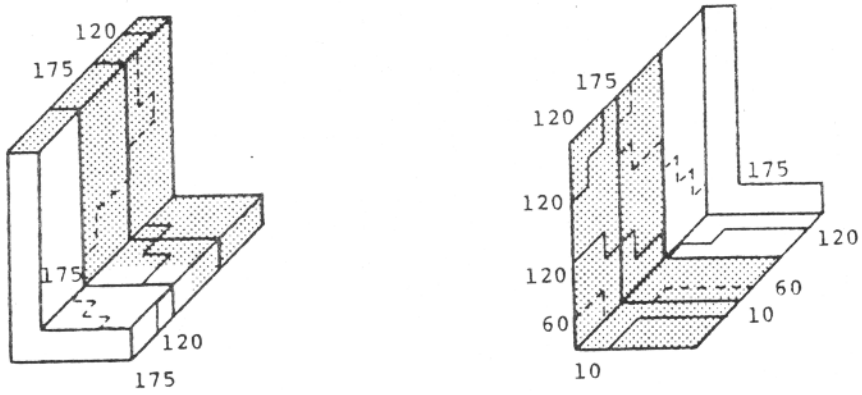

Damage on seat row above ignition fire

Figure 3-71. Computed and Observed Areas of Damage - Case 26N

TABLE 3-7

COMPARISON OF SIMULATED AND OBSERVED AREAS OF DAMAGE - CASE 26N

STRUCTURE		OBSERVED AREA[1] (ft^2)	OBSERVED AREA[1] % TOTAL EXPOSED	COMPUTED AREA (ft^2)	COMPUTED AREA % TOTAL EXPOSED
Carpet		2.0	2	Material Not Available	
Sidewall		25 - 34	30 - 40	13.5	15
PSU-Hatrack Bottom		32.5	100	7.8	52
Hatrack Edge & Top		32.5	100	1.8	2
Ceiling		75.0[2]	100	5.8	7
Seats	Group 1	0	0	0	0
	2	18.0	40	5.5	10
	3	0	0	0	0
	4	40.0	90	29.3	53
	5	0	0	0	0
	6	27.0	60	2.5	5

[1] Damaged area within test section considered by model (center 7.5 ft or 15 ft length)

[2] Delamination occurred, the amount of actual burning in not known

fire, the comparison between the computed and observed results is not strictly valid. It is interesting to note, however, that the agreement for gas concentration is still fair during the period of somewhat steady burning, 100 to 160 seconds as indicated by the temperature readings. For this larger cabin, the computed upper zone did not reach the floor by the end of the run, Figure 3-69. Smoke generation in the model was quite severe as shown in Figure 3-70.

3.3.8 Summary of the Model and Test Comparisons

The agreement between the results of the seven AIA-CDP cabin mock-up fire tests and the predictions of the DACFIR model are summarized in Table 3-8. The table shows that the program was most successful at predicting the order of magnitude of the accumulation of toxic gases. Temperature prediction was generally good for later times in the tests but never very good for the early times. Prediction of the rate of fire spread and material involvement was usually fair or good for the overhead surfaces, the ceiling, hatrack, and upper sidewall, but poor for the lower sidewall, floor, and seats. Overestimation of the spread of flames over these surfaces could be due to the flame radiation model and/or problems with the flame spread rate input data. Since the production of heat, smoke, and toxic gas is a function of the area of each material burning, improvement in the spread prediction should result in improvement in the temperature and gas concentrations computed.

TABLE 3-8

SUMMARY OF MODEL AND TEST COMPARISONS

Agreement Between Predicted and Observed Results

Case	Upper Cabin Temperature			Toxic Gas Concentrations			Extent of Materials Involvement (End of Test)					Notes
	Early*	Middle	Late	Early	Middle	Late	Crpt	Sdwl	Htrk	Ceil	Seats	
15Z	F/F**	G*	G	G	G	G	____	____	____	____	____	CO_2 over predicted
15P	F	G	____	G/F	G	G	____	P	G	G	P	Flash-over after 200 seconds
15A	F	G	G	G	G	G	____	____	G	G	G	Inert sidewall in model
15B	F/P	P	F	G	G	F	____	P	P	G	P	Model predicts extensive fire spread not observed
15C	F	G	G	F	F	P	____	P	P	P	P	O_2, CO_2 prediction good, others poor-results in over prediction of fire spread
26P	P	G	____	G/F	G	____	F/P	F	F	F/P	P	Test terminated at 200 sec. Most gas data after 150 seconds lost
26N	P	F	____	F	F	____	____	F	F	P	F/P	Test terminated after 160 seconds

*Early = First 100 seconds of test
Middle = Second 100 seconds of test
Late = Third 100 seconds of test

**P = Poor
F = Fair
G = Good

SECTION 4
CONCLUSIONS

After consideration of the comparisons of the DACFIR model to the AIA-CDP cabin fire tests, the following conclusions have been reached concerning the performance of the model and the nature of the input data.

4.1 SIMULATION OF SPECIFIC TESTS

The DACFIR model's ability to reproduce the results of the AIA tests has been summarized in Table 3-8. From examination of the table, it can be seen that the model has been moderately successful in predicting the average temperature in the upper portion of the cabin. Better results occur for the smaller cabin size, as might be expected by the assumption of a uniform hot gas zone. The model usually does best at predicting toxic gas accumulation, in the sense of an order of magnitude at least. The model does not seem to do well at predicting damage (areas of fire spread or other thermal damage) except for the overhead surfaces. Overall, the program can distinguish the effects of relatively more flammable or less flammable furnishings.

Specific findings and conclusions about the assumptions and structure of DACFIR and about the laboratory data used as its input are listed below.

1. The assumption of a uniform temperature zone of combustion products (the upper zone) is probably an over-simplification. Significant horizontal and vertical temperature gradients can occur in the cabin as is apparent in Cases 26P and 26N. The model should be refined to account for these variations to better model heat transfer to objects remote from the fire as well as for the effects on passenger evacuation. It should be realized that some thermocouple readings from the burn tests indicate that the thermccouple was within or very close to the flames of the fuel and seat fires and should not be compared to the

average upper zone temperature computed by DACFIR. Nevertheless, a better gas flow and thermodynamics model should be sought. A promising improved model is presented in Appendix A.

2. The burning rate of the seat material as observed in the full scale tests does not appear to be constant over the life of a burning element as is assumed by the program. The burning rate seems to accelerate significantly leading to more rapid release of unwanted quantities and depletion of oxygen. Modification of the DACFIR program to remove the assumption of constant release rates of smoke, heat, and gases (at constnat applied flux levels) is possible. The modifications necessary are straightforward but would increase significantly the volume of input data required. Fortunately, data in the required form is already available from past laboratory test programs.

3. With regard to the laboratory test data, it was determined that there appears to be a significant effect in the heat release rate measurements of the thermal inertial of the OSU analyzer. This was indicated by the disagreement of the time to ignite and time to burnout measured visually and from the heat release curve. If the thermal inertia effects can be removed from the heat release data, the result could be more vigorous heat release rates which would make the model show more rapid burning development, as seems to be the case with the seat materials in the tests.

4. The DACFIR model consistently over predicts the rate and extent of flame spread, particularly on vertical surfaces. The problem may be due to one or both of the following factors. The method of measurement of the flame spread velocity as a function of applied heat flux in the OSU analyzer may not be reliable, or the radiation feedback intensity calculation used in the model to select the flame spread velocity may be over estimating the radiant level at the edge of the flame. In addition, the representation in the model of

seat rows as a continuous bench-like arrangement allows fires to spread over an entire row without hindrance, whereas in the tests the breaks between individual seats seem to stop or slow the fire spread.

5. The behavior of the ignition source requires further study. The importance of the ignition source is demonstrated by the outcome of Case 26N where the ignition source size and the effect of the wind overcame whatever improvement was to be obtained by the new materials. Proper understanding of the furnishing materials' effect on the cabin environment during a fire requires a better understanding of the character of the ignition source.

6. For the more vigorous fires, oxygen depletion affects fire behavior in the later stages of the test. While the DACFIR model computes oxygen depletion, the mechanism coupling the lower level of oxygen to fire behavior is not included due to lack of an available quantitative relationship.

4.2 UNDERSTANDING OF THE TESTING/MODELING PROCESS

The development, comparison, and refinment of the DACFIR model has proven to be a great aid in organizing and evaluating the results from full-scale tests. By attempting to model a full-scale test mathematically, the fire and its development must be viewed as a system of coupled, interdependent processes. Each process - the flame, the materials' thermal degradation, the gas dynamics, etc. - must be understood to the precision necessary for the whole mathematical system to reproduce the full-scale results. In building and testing the complete model, the relative importance of each part can be found. This knowledge can then be applied to the design of new tests to determine which situations (scenarios) are important, what processes must be carefully controlled, and what measurements and accuracies are required.

APPENDIX A
AN IMPROVED CABIN GAS DYNAMICS MODEL

INTRODUCTION

The comparison of the DACFIR model to the AIA-CDP fire tests indicates that the simple, two zone treatment of interior gas dynamics may not predict well the observed temperature field in cabin fires for certain situations. It is apparent that significant vertical and horizontal temperature gradients can exist within the region of smoke and gas accumulation if the cabin is much longer than its width. Since actual cabins have a greater length to width ratio than the mock-up cabins used in the comparisons, a method is needed to improve the model's gas dynamics.

Few researchers have dealt directly with the flow of hot gas under a horizontal ceiling. Among those that have are Alpert [1] and Hwang, et al.[2] Alpert analyzed the ceiling jet resulting from the weakly buoyant fire plume striking a flat ceiling. His model assumes an infinite ceiling extent and uses an axisymmetric geometry. Hwang and his co-workers studied the phenomenon of reverse flow, i.e., jet flow against a ventilating current, in mine shaft fires. They formulate a quasi-steady, two-dimensional model applicable to fire gas flows in tunnel-like geometries. Naturally, this is suggestive of the aircraft problem and has motivated the work detailed below.

The feasibility of applying a horizontal jet flow model to aircraft fires was investigated in the simplified case of a single plume generating a jet unconfined by end walls. Theoretical predictions have been compared to results from a series of cabin fire tests conducted in a B737 fuselage at Johnson Space Center of the National Aeronautics and Space

---

[1] Alpert, R.L., "Turbulent Ceiling-Jet Induced by Large-Scale Fires", Combustion Science and Technology, 1975, Vol. 11, pp. 197-213.

[2] Hwang, C.C. et al., "Reverse Stratified Flow in Duct Fires: A Two-Dimensional Approach", Sixteenth Symposium (International) on Combustion (1976), p. 1385.

Administration (NASA-LBJ). A description of the model and the results of this first test are given below.

THE CEILING JET

Figure A.1 presents the features of the jet model. The vertically rising plume from a fire near the cabin floor strikes the flat and level ceiling. Plumes in the DACFIR model are axisymmetric. The problems of determining the flow patterns in the turning region - where the plume gas turns and eventually assumes a more or less parallel flow away from the fire - are not thought worth the considerable effort for solution at present. Therefore, we assume that the plume flow into the turning region is immediately redirected and redistributed into a starting flow for the ceiling jet uniform across the cabin width. In this model the cabin is assumed to be rectangular in cross section. The figure shows the assumed velocity profile in the ceiling jet. The maximum gas velocity and minimum density (and thus the maximum temperature) occur at the ceiling. The decrease in velocity and increase in density through the jet is taken to be semi-gaussian with the lower edge of the jet selected as the point where the velocity has fallen to five percent of its maximum value. The jet exchanges momentum and heat with the ceiling by shear and convective heat transfer. At the lower edge, turbulent entrainment of the cooler air on which the jet floats carries in mass, momentum, and energy. The cool lower air may be flowing toward the fire driven by the entrainment of the plume and also, if applicable, by a ventilation system.

Following Hwang, et al., the integral formulation for the equations of motion of the ceiling jet are:

(1) Continuity $$\frac{d}{dx}\int_o^h \rho v dy = \alpha\rho_\infty(\bar{V} + V_\infty)$$

(2) Energy $$\frac{d}{dx}\int_o^h \rho v C_p T dy = C_p T_\infty \rho_\infty \alpha(\bar{V} + V_\infty) - q_w$$

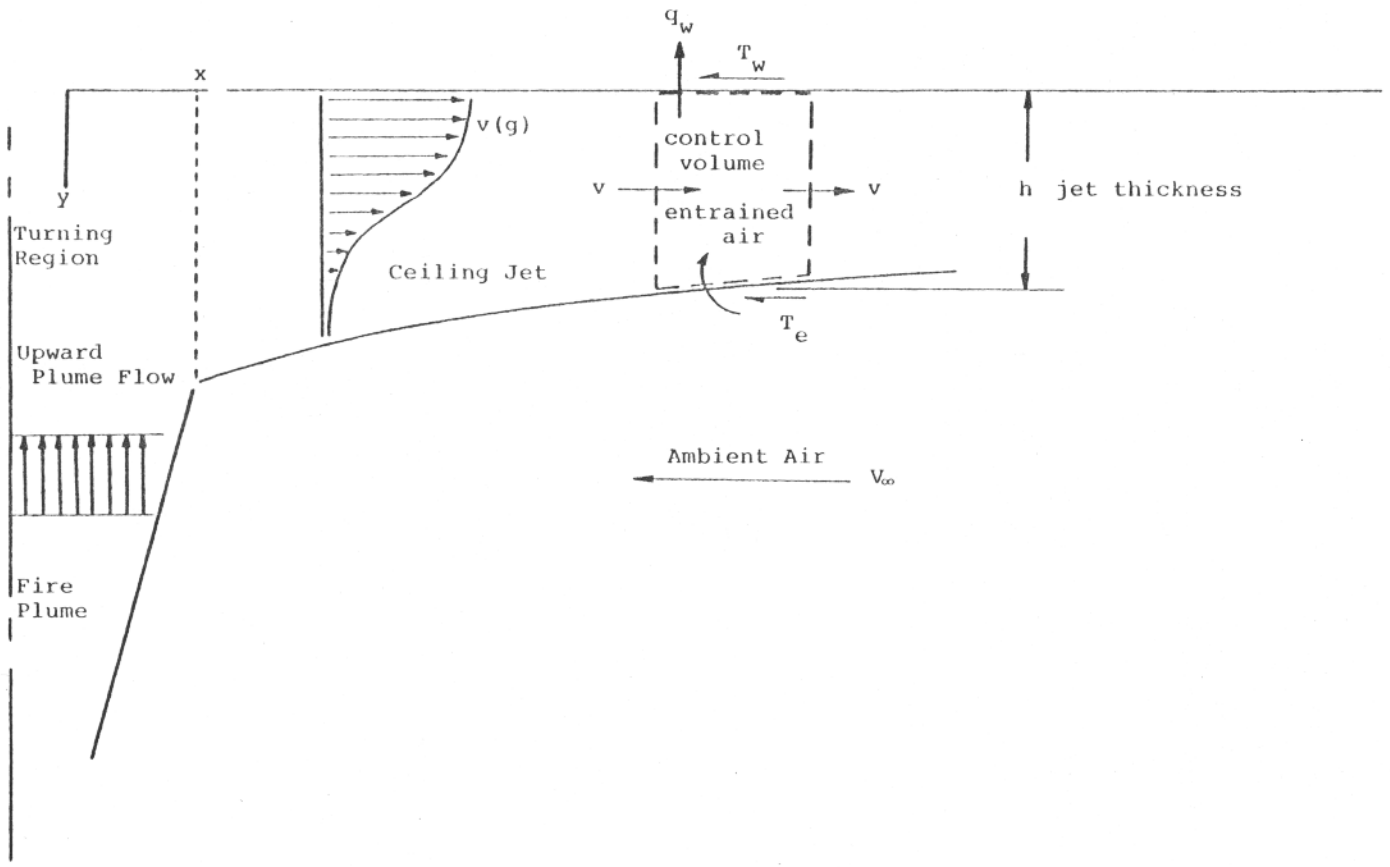

Figure A.1. Flows in The Ceiling Jet Model

(3) Momentum (in the horizontal direction)

$$\frac{d}{dx}\int_o^h \rho v^2 dy = -\alpha\rho_\infty V_\infty(\bar{V} + V_\infty) - \frac{d}{dx}\int_o^h yg(\rho_\infty-\rho)dy - \tau_w - \tau_e - \int_o^h (\frac{\partial P}{\partial x})_\infty dy$$

The coordinate system of this model has its origin at the ceiling impact point with X the horizontal coordinate (positive X directed against the ambient flow) and Y the vertical coordinate (positive Y directed downward).

The variables are density (ρ), velocity (v), and thickness (h) of the ceiling jet layer. Other quantities are:

- α entrainment parameter, a constant for this model;
- C_p specific heat of lower air (ventilation flow) and of the combustion products (assumed constant);
- $(\frac{\partial P}{\partial x})_\infty$ pressure drop in ventilation flow;
- g gravity;
- q_w convection heat loss to the ceiling;
- τ_e shear stress at layer interface;
- τ_w wall shear stress at the ceiling;
- T temperature; and
- $\bar{V}$ characteristic velocity of the jet.

The subscript (∞) denotes ambient conditions.

Once profiles for density and velocity are specified, the integrals in equations (1) - (3) may be evaluated and the resulting set of ordinary differential equations solved.

The semi-guassian profiles assumed are:

$$v = v_m \exp(-y^2/\ell^2) \qquad \rho = \rho_\infty - \Delta\rho = \rho_\infty - \Delta\rho_m \exp(-y^2/\ell^2)$$

where ℓ is the profile half width. To relate ℓ to the jet thickness h, the thickness is defined to be at the point on the velocity profile where the velocity has fallen to five percent of its maximum value. This gives

$$\ell = h/\sqrt{3}$$

With these substitutions, equations (1) - (3) may be restructured into the following set:

$$(1a)\quad (\rho_\infty H_1 - \Delta\rho_m H_1)\frac{dv_m}{dx} - v_m H_2 \frac{d\Delta\rho_m}{dx} + \frac{1}{h}(\rho_\infty v_m H_1 - \Delta\rho_m v_m H_1)\frac{dh}{dx} = \alpha\rho_\infty(V_\infty + \bar{V})$$

$$(2a)\quad H_1\frac{dv_m}{dx} + v_m \frac{H_1}{h}\frac{dh}{dx} = \alpha(\bar{V} + V_\infty) - q_w/(C_p T_\infty \rho_\infty)$$

$$(3a)\quad 2v_m h(\rho_\infty H_2 - \Delta\rho_m H_2)\frac{dv_m}{dx} + (gH_3 - v_m^2 H_2)\frac{d\Delta\rho_m}{dx}$$

$$+ (\rho_\infty v_m^2 H_2 - \Delta\rho_m v_m^2 H_2 + g\Delta\rho_m h^2/3)\frac{dh}{dx}$$

$$= -V_\infty \rho_\infty \alpha h(V_\infty + \bar{V}) - hg\Delta\rho_m H_4 - \tau_w h$$

where

$$H_1 = \sqrt{\pi}/2\ \{\text{erf}\ (\sqrt{3})/\sqrt{3}\ \}h$$

$$H_2 = \sqrt{\pi}/2\ \{\text{erf}\ (\sqrt{6})/\sqrt{6}\ \}h$$

$$H_3 = h^2/6$$

$$H_4 = \sqrt{\pi}/2\ h/\sqrt{3}\ \text{erf}\ (\sqrt{3})$$

where erf is the error function, $\text{erf}\ x \equiv \frac{2}{\sqrt{\pi}} \int_0^x e^{-t^2}\ dt$

and $$q_w = h_c(T - T_w)$$

$$\bar{V} = v_m$$

$$\tau = \tau_w + \tau_{w_\infty} = \frac{1}{2} C_f(\rho_\infty V_\infty^2 + \Delta\rho_m v_m^2)$$

where T_w is the wall temperature, h_c is the convection coefficient (assumed constant), T is the jet temperature ($=\rho_\infty T_\infty/\rho$), and C_f is a friction factor, taken as $C_f = 0.008$.

Thus the set is linear in the derivatives and may be integrated easily.

The solution produces a longitudinal density gradient; hence the desired temperature gradient. Since a density profile is assumed, a vertical gradient is also calculable. Consequently, it is possible to impose a grid on the cabin interior and thereby obtain a set of temperatures from which the temperature at a given point may be interpolated.

In addition, application of conservation of species allows the calculation of smoke and toxic gas concentration gradients:

$$(4) \qquad \frac{d}{dx} \int_o^h \rho v Y_i dy = \alpha\rho_\infty(\bar{V} + V_\infty)\ Y_{\infty i}$$

where Y_i is the mass fraction of i^{th} gas or smoke in jet layer, and $Y_{\infty i}$ is the mass fraction of i^{th} gas or smoke in ambient layer.

If uniform mixing within the hot layer is assumed, along with the previous density and velocity profiles, equation (4) becomes

$$(4a) \qquad H_1 v_m(\rho_\infty - \Delta\rho_m) \frac{dY_i}{dx} + Y_i H_1(\rho_\infty - \Delta\rho_m)\frac{dv_m}{dx} - v_m H_1 \frac{d(\Delta\rho_m)}{dx}$$

$$+ \frac{1}{h}\frac{dh}{dx} v_m H_1 (\rho_\infty - \Delta\rho_m) = \alpha\rho_\infty Y_{\infty i} (V_\infty + \bar{V})$$

INITIALIZATION BY RISING FIRE PLUMES

To initialize the ceiling jet, the Steward-Fang plume is used to calculate upward mass and heat flows from a fire in the lower

cabin. If in the turning region (where upward flow impinges the ceiling and is turned horizontal) heat and momentum loss are assumed negligible, then the conservation laws imply the following simple relations between plume and initial jet values.

(5) Mass $$\pi r_p^2 \rho_p v_p = 2W \int_o^{h'} \rho_j v_j dy$$

(6) Momentum $$\pi r_p^2 \rho_p v_p^2 = 2W \int_o^{h'} \rho_j v_j^2 dy$$

(7) Energy $$\pi r_p^2 C_p T_p \rho_p v_p = 2W \int_o^{h'} C_p T_\infty \rho_\infty v_j dy$$

(8) $$z - h' = y_o$$

where z is the cabin height, h' is the initial jet thickness, y_o is the distance to the jet layer from the floor, and W is the width of the turning region. Subscripts p and j indicate plume and jet values respectively. The factor of two occurs in the right-hand side of equations (5), (6), and (7) since it is assumed that the upward flow divides equally between the positive and negative X directions.

With the assumed jet profiles of density and velocity, equations (5) - (7) become:

(5a) $$\pi r_p^2 \rho_p v_p = W \sqrt{\pi}(\rho_\infty - \Delta\rho_m) \text{ erf } (\sqrt{3})/\sqrt{3}\ h' v_m$$

(6a) $$\pi r_p^2 \rho_p v_p^2 = W\sqrt{\pi}(\rho_\infty - \Delta\rho_m) \text{ erf } (\sqrt{6})/\sqrt{6}\ h' v_m^2$$

(7a) $$\pi r_p^2 v_p^2 = W\sqrt{\pi} \text{ erf } (\sqrt{3})/\sqrt{3}\ h' v_m$$

The set (5) through (8) is solved iteratively using an initial estimate of h' to obtain the starting values for the jet thickness, velocity and density.

With the model in this form, comparisons were made with one of the NASA-LBJ "Design Fire" tests in the 737 fuselage[3]. Starting with an assumed mass loss and heat release rate for the 24 X 24 inch square pan of Jet-A used in the test, computations were made for the hot gas flow from the ceiling impact point to a position 30 feet down the fuselage. A ventilation flow velocity of 8 ft/min was used which corresponds to the 475 cfm ventilation rate used in the burn test.

Initial results of the comparison indicated that the entrainment constant for the ceiling jet was too small to account for the temperature decrease with distance observed at NASA-LBJ. Some adjustment of the constants in the Steward-Fang plume model were also necessary to bring the temperature at the plume impact point up to the observed value. After these adjustments, the performance of the model is shown in Figure A.2.
In the figure, the computed gas temperatures at the ceiling and four inches below the ceiling are shown by the solid and broken curves respectively. Two curves of each type are shown, one for the flow against the ventilation current ("upwind") and one for flow in the same direction as the ventilation current ("downwind"). The square and circular symbols are thermocouple readings from NASA-LBJ test number 17. The square symbols are values downwind from the flow and the circles are upwind readings. All thermocouples were four inches below the ceiling.

The figure shows that the computed temperature at the ceiling agrees very well with the measured temperature four inches below the ceiling. Except for one point, the computed temperature four inches below the ceiling is consistently lower than the measurements. Despite this discrepancy in the vertical direction, the measured and computed horizontal temperature changes are in excellent agreement. Although only one case was analyzed and some room for improvement has been noted, the results shown here are encouraging.

---

[3] Tustin, E. A., et al, "Development of Fire Test Methods for Airplane Interior Materials," Boeing Commerical Airplane Co., NASA-CR, in preparation.

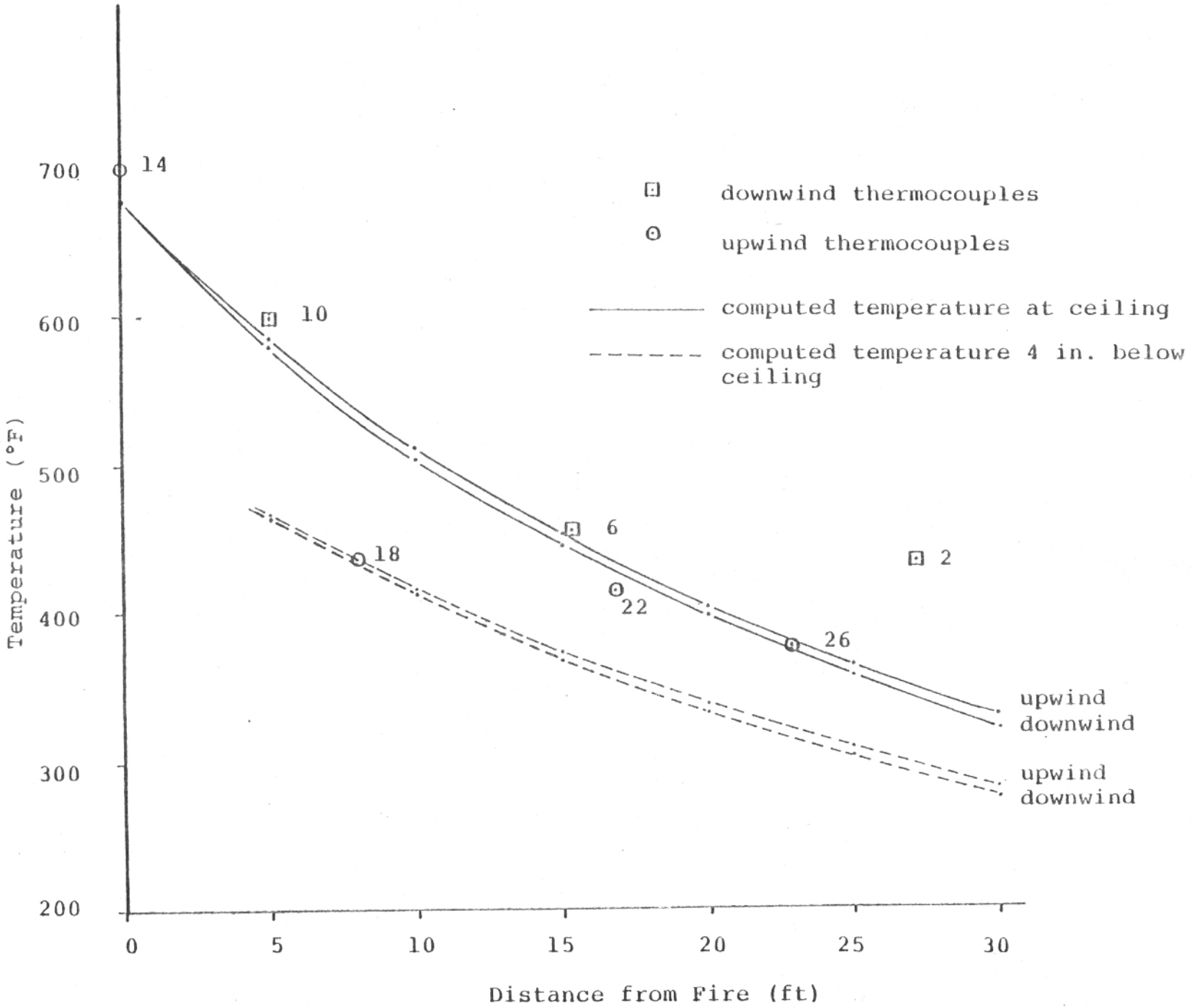

Figure A-2. Comparison of Horizontal Gas Flow Model to NASA 737 Fire Test 17 (2-1-77)

APPENDIX B
LABORATORY DATA COLLECTION

This appendix consists of the final technical report on the laboratory test data collection program conducted in support of the DACFIR validation effort.

A very large amount of data was collected consisting of flame spread rates; time constants; smoke, heat, and gas release rates; and weight loss measurements. Since many of the cabin materials tested are either no longer in widespread use or were experimental at the time of the full scale tests, it was not deemed justified to present the data in this report. The data can be made available to interested parties by contacting the authors or the FAA technical monitor.

UNIVERSITY OF DAYTON

RESEARCH INSTITUTE

(UDRI)

DATA REQUIRED BY UDRI FOR DACFIR SIMULATION

Final Technical Program Report

Covering the Period from

August 1, 1976 to April 9, 1977

BOEING COMMERCIAL AIRPLANE COMPANY

P. O. BOX 3707

SEATTLE, WASHINGTON 98124

Prepared by R. D. Lechner

R. D. Lechner

Approved by W. A. Walker

for R. A. Anderson

APRIL 9, 1977

FINAL REPORT

TITLE: Data Required for DACFIR Simulation

Testing by The Boeing Company in response to the University of Dayton P.O. #RI-77086 dated 7-9-76 for "Verification of the DACFIR Modeling Concepts Using Data from Past Burn Tests" has been completed. Incremental shipments of the total information, photographs, 16-mm color films, and data have been made from time to time in care of Mr. Charles MacArthur, University of Dayton.

DACFIR LABORATORY TEST PROGRAM

SUMMARY

The testing reported herein is in response to the work requested in the University of Dayton Research Institute P.O. #RI-77086 dated 7-9-76.

Location of some of the materials used in the 1968 fire testing program was responsible for a large part of the delay in getting the laboratory work completed. Many of these materials are no longer used, some were never used, and others have become obsolete with material suppliers. Therefore, while some materials were not available for testing, a best effort possible on the part of Boeing has been followed in obtaining data to satisfy the intent of the program.

DESCRIPTION OF MATERIALS

All of the 31 materials requested in the University of Dayton Research Institute's letter dated 10 August 1976 were accumulated and tested in the National Bureau of Standards (NBS) and Ohio State University (OSU) test chambers, except the following:

Material No. 3 -- Enameled aluminum with Tedlar surface film

Material No. 24 -- Muslin-covered polyurethane, upholstered in cotton fabric

Material No. 28 -- Olive drab Nomex

These materials could not be located or reasonably simulated.

However, it should be noted that duplicate materials were not tested. Therefore, there are no data transmitted for the following:

Material No. 5 and Material No. 12 (same as No. 4)

Material No. 10 (same as No. 8)

The materials tested, description, material use (tests), and specimen construction were as indicated in table I.

OSU COMBUSTION ANALYZER TESTING

All materials were tested at four heat flux levels (5.0, 3.5, 2.5, and 1.5 watts/sq cm), with orientation(s) as indicated in the University of Dayton letter. Due to the limitations of materials, time, or anticipated results, only one specimen was tested at the lower two heat flux levels. Three specimens per material were tested at the two higher heat flux levels.

The following is the test procedure used for the OSU testing:

- Specimen weighed - Recorded
- Specimen inserted into chamber - Time noted
- Start of smoke (visual) - Time measured (seconds)
- Start of flame (visual) - Time measured (seconds)
- Spread of flame (visual) - Time measured (seconds)
- End of flame (visual) - Time measured (seconds)
- End of smoke (visual) - Time measured (seconds)
- Specimen removed from chamber - Time noted
- Specimen weighed - Recorded
- Strip chart - Recorded heat and smoke curves

The smoke and heat curves were digitized with a direct link to a CDC 6600 computer.

CALCULATIONS AND MEASUREMENTS

The following calculations and/or measurements were obtained from tests made in the OSU combustion analyzer:

- Time to flame (t_f) HRC -- Time between specimen insertion and the time the heat release rate curve begins to rise above the zero level.
- Time to flame (t_f) visual -- Time between specimen insertion and visual appearance of flame.
- Flame spread rate -- Time required for flames to travel from the point of flame application to a specific edge of the specimen. In the case of horizontal test position for flaming condition, a single point of flame was always applied at the center of the specimen and the rate of spread was taken over the 5-inch distance to the farthest edge. For vertical test, a multiple flame was applied at edge or top or bottom and the rate of spread was taken over the 6-inch distance to the opposite edge.
- Time to char (t_{fc}) visual -- Time between first appearance of flame and flame out or ceased smoking.
- Time to char (t_{fc}) HRC -- Unobtainable. (In the interest of reducing overall test time, the chamber was not permitted to return to the zero level before removal of specimen from chamber.)
- Total heat released (h_t) (Btu) -- Computed from the heat release rate curve generated by the OSU combustion analyzer.

- Total smoke released in the flaming state (D_{sf}) and in the smoldering state (D_{ss}) -- Computed from the smoke release curves generated by the OSU combustion analyzer. Also, a determination was made of the maximum value of the specific optical density from the smoke curve.
- Weight loss rate = $\frac{\text{weight before - weight after}}{\text{time to burn}} = \frac{\text{grams}}{\text{minute}}$

SIZE OF SPECIMENS FOR OSU TESTS

- Horizontal tests -- 4 inches x 10 inches
- Vertical tests -- 6 inches x 6 inches (except in the case of Material No. 14, in which the specimen size was 3 inches x 3 inches).

TOXIC GAS EVOLUTION TESTING

The materials listed in table I were burned or pyrolyzed in an NBS Smoke Chamber. The specimen configuration (nominal 3-inch square), combustion chamber volume (516 liters), pilot flame size, chamber temperature, and sample exposure conditions were all as described for the standard NBS Smoke Density test (ref. 1: NBS Technical Note 708, "Interlaboratory Evaluation of Smoke Density Chamber," T. G. Lee, National Bureau of Standards, 1971). Smoke densities were measured for these materials but are not reported under this contract.

The evolution of certain toxic gases (HCl, HF, HCN, NO_x, SO_2) was measured using gas detector tubes located in the center of the chamber above the specimen. At specific times during the test (1, 2, 4, and 10 minutes), aliquot portions of the chamber atmosphere were drawn through the detector tubes, using a semi-automatic pumping system located outside of the chamber. Following the test, the tubes were removed, and the concentrations of the specific toxicants were calculated from the length of the observed color change (stain) produced.

The evolution of two gases was monitored by pumping chamber gas through two specific analytical instruments, a Beckman Model 865 Nondispersive Infrared Analyzer for CO, and a Wilks Instrument Co. Miran I Infrared Analyzer for CO_2. Concentrations of these gases at 1, 2, 4, and 10 minutes were read from the continuous recorder traces.

Specific gas detector tubes manufactured for Dragerwerks A.G. of Lubeck, Germany (Drager tubes) were used for all gases except HCl, which was determined using a detector tube manufactured by Mine Safety Appliances. Tests were conducted only for toxicants whose formation was anticipated, based upon the chemical composition of the test material.

Gas detector tubes were developed for determining specific toxicants in clean atmospheres, i.e., as in industrial hygiene applications. Accuracies of about $\pm$ 20 percent are typically claimed by the manufacturer. Although they have been widely applied for analysis of combustion gases in the NBS Smoke Chamber and elsewhere, this application is subject to the possibility of unknown interferences. In our opinion, the results obtained by this method are probably accurate within $\pm$ 50 percent.

Gas evolution measurements were made at flux levels of 5.0, 3.5, 2.5, and 1.5 watts/cm^2 in both the flaming mode (sample impinged by a pilot flame) and in the smoldering mode (sample irradiated without an ignition source present). Cost and time limitations prohibited duplicate determinations of each toxicant at 1, 2, 4, and 10 minutes at each flux level. Testing was begun at 5.0 watts/cm^2 and proceeded to lower flux levels. As soon as the amount of a specific toxicant dropped to a negligible value, testing for that toxicant was discontinued, and when the evolution of all toxicants had dropped to negligible values, testing for that material was discontinued. For this reason, very few data were collected at 1.5 watts/cm^2.

TABLE I

Material Number	Description	Material Use (Test)	Specimen Construction
1	Vinyl-coated aluminum	Sidewall (15M-P)	-0.032 aluminum -0.010 vinyl
2	Vinyl-0.25 aluminum laminate (BMS 8-89, Type 1, Class 1)	Sidewall (727-P)	-0.032 aluminum -0.010 vinyl -0.001 clear Tedlar
3	Omitted	---	---
4	Nomex-honeycomb core, fire-retardant epoxy fiberglass-laminate-faced sandwich panel with printed Tedlar surface	Sidewall (15M-B) Ceiling (15M-A, 15M-B, 727-B)	-0.001 clear Tedlar -ink -0.002 opaque Tedlar -Type 181 fiberglass-epoxy prepreg -Type 120 fiberglass-epoxy prepreg -0.25, 1/8" cell, 3 lb/cu ft Nomex honeycomb -2 plies, Type 120 fiberglass-epoxy prepreg
5	Same as Material No. 4	Hatrack (15M-B, 727-B)	---
6	Polyurethane foam covered with vinyl-coated fiberglass cloth	Hatrack (15M-P)	-0.50 polyurethane foam -vinyl-coated fiberglass
7	Paper-honeycomb core, fire-resistant resin aluminum skin, vinyl-coated fiberglass	Hatrack (727-P)	-0.25, 1/4" cell, 3 lb/cu ft paper honeycomb (resin impregnated) -fire-resistant resin glass laminate -0.50 polyurethane foam -vinyl-coated fiberglass
8	Paper-honeycomb core, fire-retardant polyester fiberglass-laminate-faced sandwich panel covered with vinyl-coated fiberglass	Ceiling (15M-P)	-vinyl-coated fiberglass -0.25, 3/8" cell, paper honeycomb -fire-resistant polyester glass laminate

TABLE I (Continued)

Material Number	Description	Material Use (Test)	Specimen Construction
9	Paper-honeycomb core, vinyl covering, fire-resistant resin glass laminate	Ceiling (727-P)	-vinyl-coated fiberglass -0.25, 3/8" cell paper honeycomb -fire-resistant resin glass fabric
10	Same as Material No. 8	Ceiling (727-P)	---
11	Nomex-honeycomb core, fire-retardant epoxy fiberglass-laminate-faced sandwich panel covered with a fiberglass mat for padding and a final covering of vinyl-coated fiberglass	Hatrack (15M-A)	-Type 120 fiberglass-epoxy prepreg -0.25, 1/4" cell Nomex honeycomb -Type 181 fiberglass-epoxy prepreg -3/8" fiberglass matting -vinyl-coated fiberglass
12	Same as Material No. 11	Sidewall (15M-C) Ceiling (15M-C)	---
13	Nomex-honeycomb core, fire-retardant fiberglass-laminate-faced sandwich panel with Tedlar surface	Hatrack (15M-C)	-0.002 opaque Tedlar -Type 181 fiberglass-epoxy prepreg -0.25, 1/4" cell Nomex honeycomb -Type 120 fiberglass-epoxy prepreg
14	Aluminum, polyurethane foam, ABS coating	Hatrack Bullnose (727-P)	-0.025 aluminum -0.5 polyurethane foam -ABS flexible coating
15	0.06" MIL-P-5425 as cast acrylic	Dust Pane (727-P)	-0.06 acrylic
16	ABS cycolac	Window Reveal (727-P) PSU (727-P)	-0.06 ABS cycolac
17	Acrilan carpet, double ball cloth tape muslin, polyurethane foam	Carpet (727-P)	-Acrilan carpet -muslin weave fabric -1/8" polyurethane foam

TABLE I (Continued)

Material Number	Description	Material Use (Test)	Specimen Construction
18	Polysulfone	PSU (727-P)	-0.08 polysulfone P-1747
19	0.010" Lexan 9600	PSU (727-B)	-0.062 opaque polycarbonate
20	Lexan 9600	Dust Pane (727-B) Window Reveal (727-B)	-0.050 clear polycarbonate
21	SE-3 Acrylic	Dust Pane (727-B)	-0.060 SE-3 acrylic
22	Muslin-covered polyurethane foam, upholstered in nylon fabric	Seat Back and Cushion (15M-P, 15M-A, 727-P)	-nylon fabric -muslin weave fabric -1/2" polyurethane foam
23	Muslin-covered polyurethane foam, upholstered in wool fabric	Seat Back and Cushion (727-P)	-wool fabric -muslin, unbleached -1/2" polyurethane foam
24	Delete	Seat Back and Cushion (727-P)	---
25	Flame-retardant polyurethane covered with a Nomex fabric slipcover and upholstered with Nomex fabric	Seat Back and Cushion (15M-B)	-Nomex fabric -Nomex slipcover -1/2" polyurethane foam, flame retardant
26	Flame-retardant polyurethane (#PTR 023-12, 1.8 lb/cu ft) covered with unbleached muslin (4 oz/sq yd, flame proofed), and upholstered with Nomex (8 oz/sq yd)	Seat Back and Cushion (727-B)	-Nomex fabric -muslin, unbleached -3/8" fiberglass padding

TABLE I (Continued)

Material Number	Description	Material Use (Test)	Specimen Construction
27	Fiberglass cushion in a Nomex slipcover, upholstered with Nomex fabric	Seat Back and Cushion (15M-C)	-Nomex fabric -Nomex slipcover -3/8" fiberglass padding
28	Omitted	Carpet (727-B)	---
29	Polyurethane foam	Foam in Seat Cushions and Backs (15M-P, 15M-A, 727-P)	-1/2" polyurethane foam
30	Flame-retardant polyurethane foam	Foam in Seat Cushions and Backs (15M-B, 727-B)	-1/2" polyurethane foam, flame retardant
31	Fiberglass padding	Padding in Seat Cushions and Backs (15M-C)	-3/8" fiberglass padding

APPENDIX C
DACFIR2 USER'S GUIDE

This appendix is a guide for use of Version 2 of the Dayton Aircraft Cabin Fire simulation program (DACFIR2). DACFIR2 differs substantially from Version 1 of the DACFIR program, a user's guide for which was given in Volume III of Reference [1]. While this appendix draws from material presented in the earlier volume, familiarity with Version 1 of DACFIR is not assumbed for the use of the present material. The intent of this user's guide is to provide instruction for the efficient use of DACFIR2, but not to present the construction of the computer code in detail. The guide provides an annotated flow chart of the main controlling program, instructions for preparing the input data, sample input and output, program statistical data, and information for obtaining copies of the program. Due to the large size of DACFIR, over three thousand source statements, a listing of the code is not included.

C.1 BASIC DEFINITIONS AND CONVENTIONS

In the DACFIR program, cabin interior geometry is represented by a connected group of horizontal and vertical surfaces. The program recognizes a maximum of twenty (20) cabin lining surfaces (floor, sidewalls, ceiling, etc.) and nine (9) seat groups. The cabin lining surfaces and seat surfaces are divided into square elements of fixed dimension, 0.5 by 0.5 ft, for purposes of tracking the fire growth. Each surface and seat group is identified by a single number and each element on a surface by a pair of numbers, the element i,j indices. Assignment of the surface and seat numbers and element indices is made by the program based upon the values of the input data

---

[1] Reeves, J.B., and C.D. MacArthur, "Dayton Aircraft Cabin Fire Model," Volumes I, II, and III, FAA-RD-76-120, June 1976. Volume III, "Computer Program User's Guide" was written by P.M. Kahut.

describing the surfaces and seat groups and upon the order of the input data. DACFIR2 is designed to minimize the amount of geometric input information required. To do so, a number of conventions and assumptions are adopted of which the user must be aware in preparing the geometric input. The conventions and assumptions are as follows.

(1) All cabin lining surfaces are assumed to be parallel to the cabin y-axis (See Figure C-1 and Figure 2-1, Section 2) and each surface must be eitherparallel to perpendicular to the x-y plane (floor plane). The seat group configuration is as described in Section 2, all dimensions fixed except width, and all seats must face forward.

(2) All cabin lining surfaces are assumed to extend unbroken from the start of the "detailed" section length (Figure 2-1) to its end; this distance is fixed as 7.5 ft, that is 15 element lengths.

(3) Numbering of the cabin lining surfaces always starts with the floor as surface number one and proceeds counterclockwise (facing aft) across the floor, up the sidewall, across the ceiling and down the sidewall to return to the floor. This scheme is shown in Figure C-1.

(4) Each seat group is constructed of seven surfaces shown in Figure C-2. Numbering of the elements of a seat group is fixed by the program and starts with the cushion bottom, proceeding up the backrest, over the backrest top, down the front to the seat cushion top, over the cushion top and returning to the front edge of the cushion bottom.

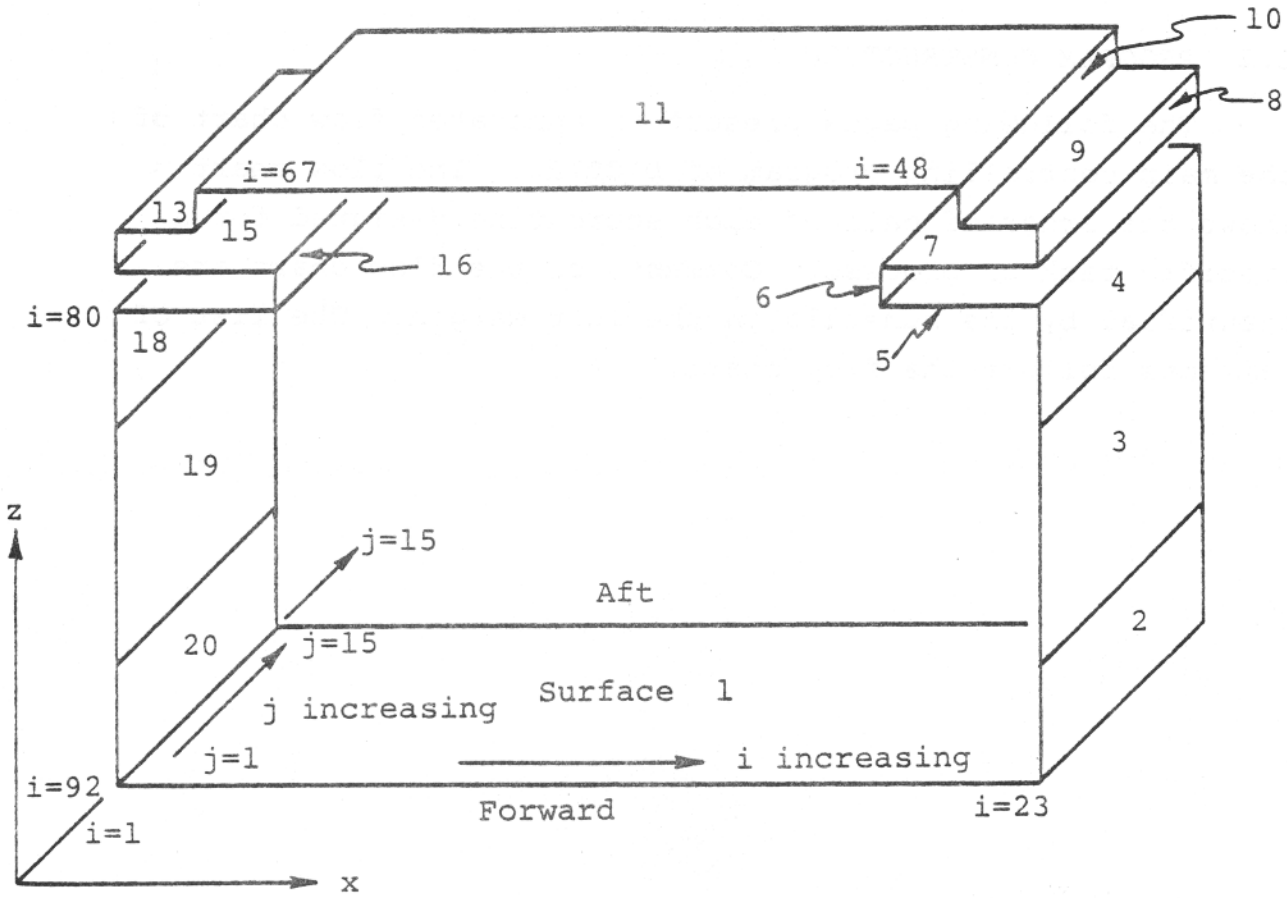

Figure C-1. Cabin Lining Surfaces. Configuration shown is that used for Cases 26P and 26N.

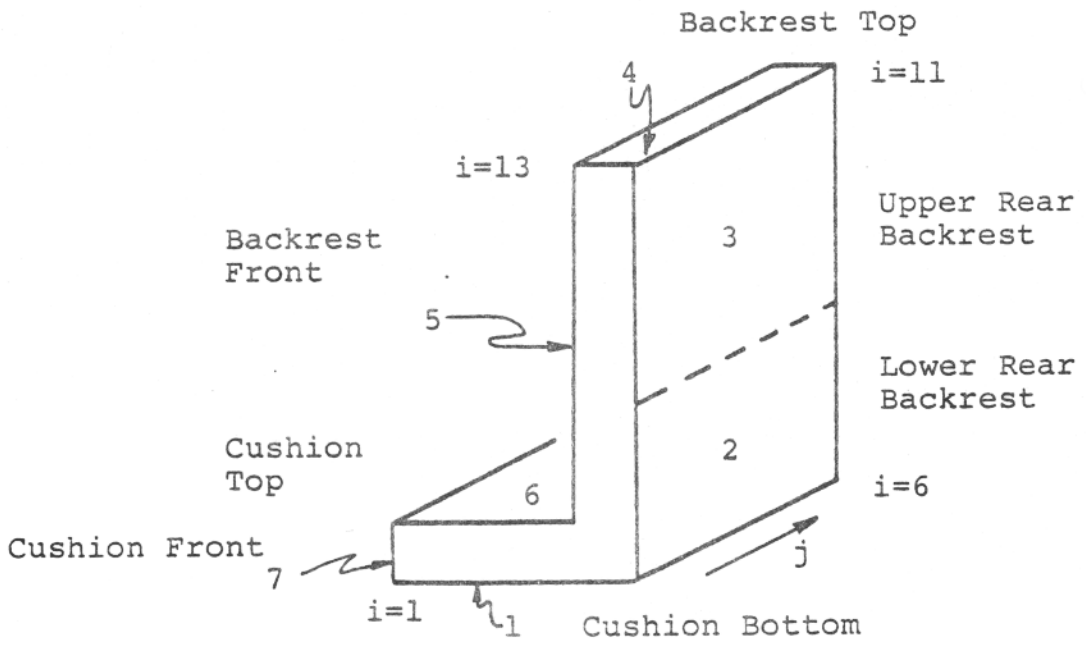

Figure C-2. Seat Surfaces

C.2 PROGRAM CONSTRUCTION

The following pages present an annotated flow chart of the main controlling program of DACFIR2. The flow chart shows the order of call of each subroutine designed for a specific task or process. Comments on the flow chart are identified by the numerals in the left margin. The list of comments follows the flow chart.

'MAIN PROGRAM' FLOW CHART

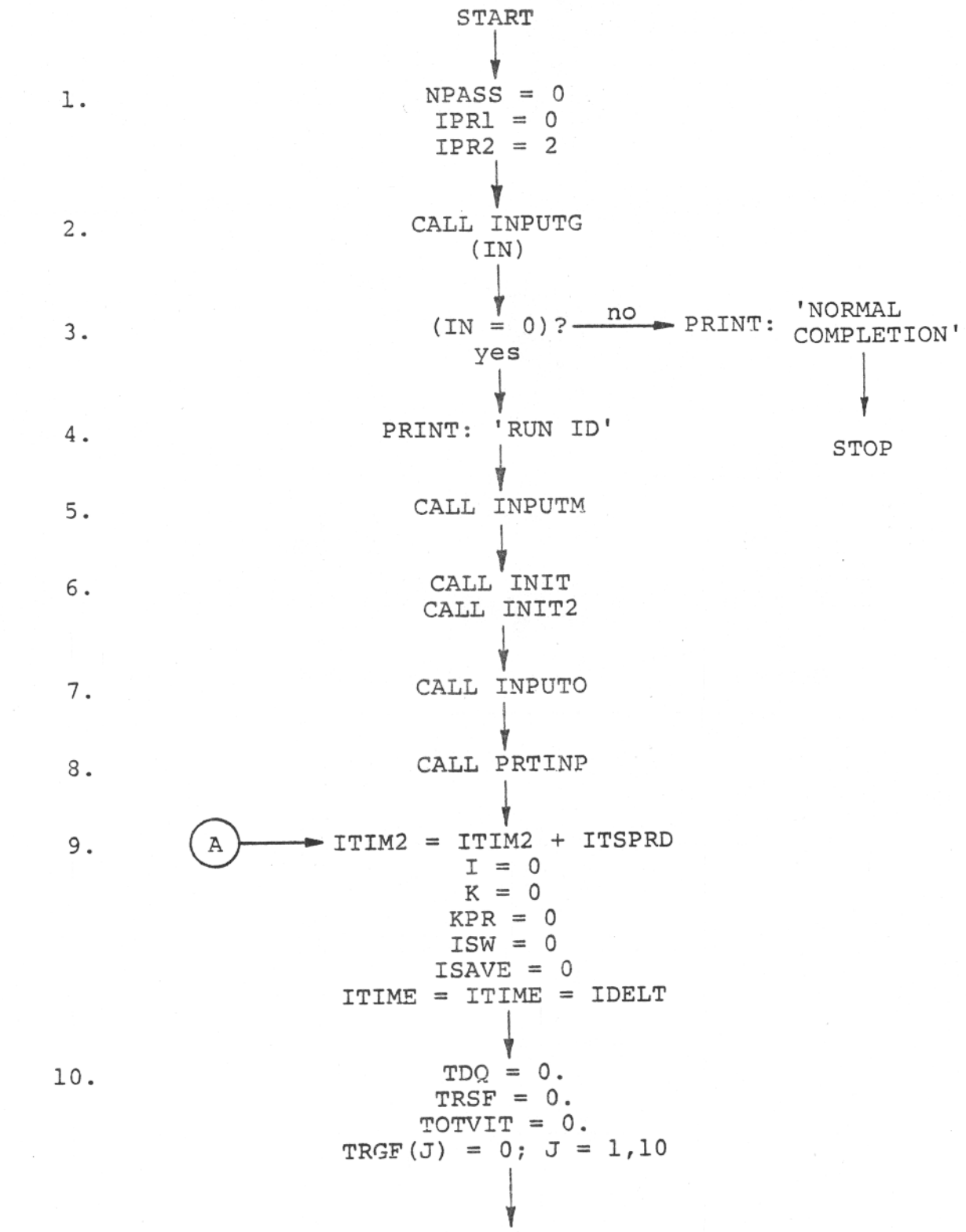

'MAIN PROGRAM' FLOW CHART (Continued)

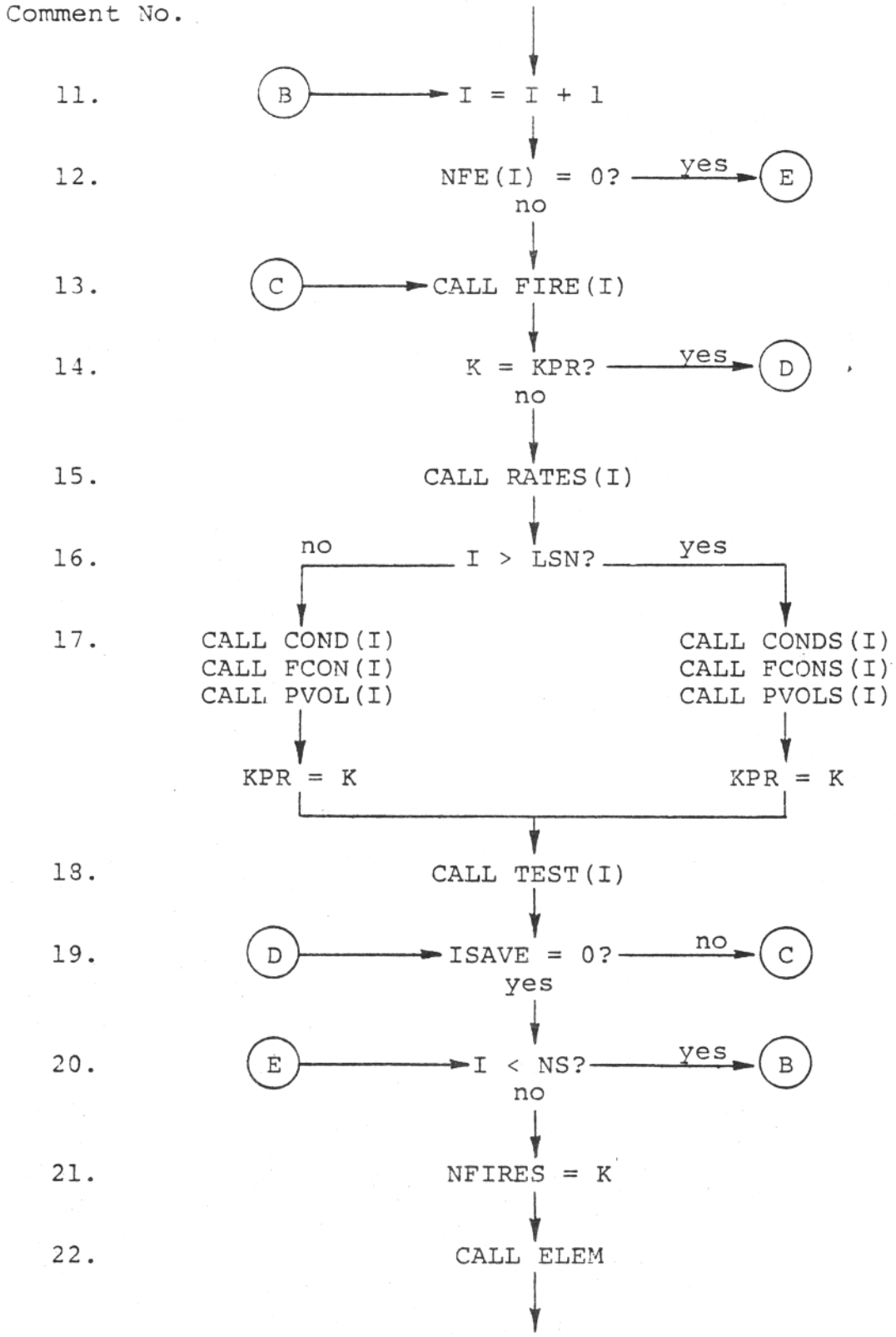

'MAIN PROGRAM' FLOW CHART (Continued)

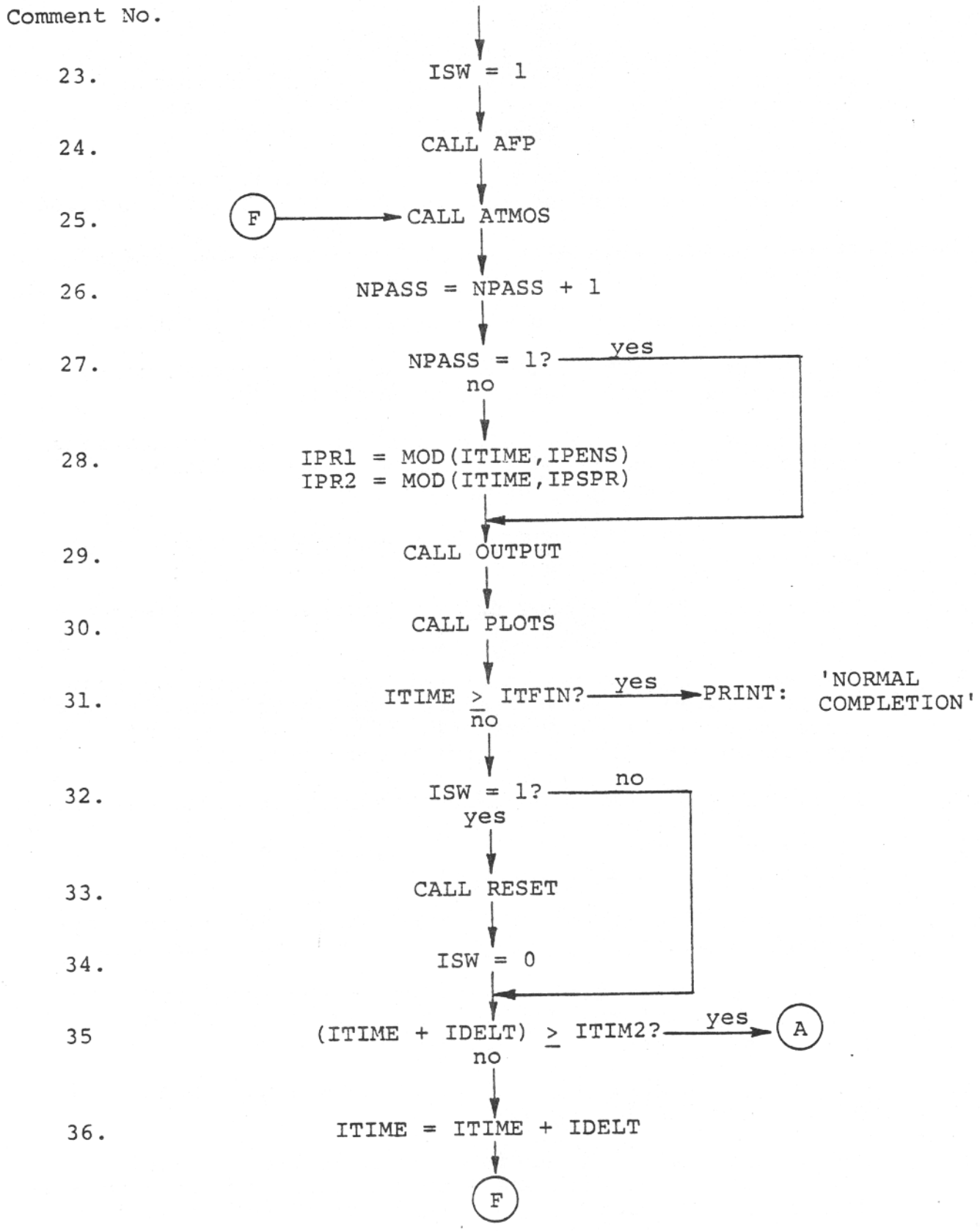

COMMENTS FOR PROGRAM FLOW CHART

No.

1. 'NPASS' is a counter, initialized at this point, which will contain the number of times the cabin atmosphere computations have been performed. IPR1, IPR2 are print controls.

2. Subroutine 'INPUTG' initializes and defines those variables pertaining to the geometry of the cabin section.

3. Test for run termination (no additional input cards to be read).

4. Eighty characters of run identification are printed.

5. Subroutine 'INPUTM' reads all input data pertaining to the material properties of each surface.

6. Subroutine 'INIT' and 'INIT2' perform basic computations from the input data and initialize those variables required to start the integration.

7. Subroutine 'INPUTO' reads all data relating to the ignition source.

8. Subroutine 'PRTINP' provides an input-echo of selected input data.

9. This point is the start of the primary integration loop in the program. 'ITIM2' is the time associated with the flame propagation computations, 'ITIME' is the time associated with the cabin atmosphere computations.

10. Initialize sums which contain emission rates for all fires.

11. 'I' is the surface index (1 through 20 are cabin lining surfaces, 21 through 29 are seat groups).

12. Test: Any flaming elements on surface 'I'? If not, by-pass flame propagation computations for this surface.

13. Subroutine 'FIRE' isolates a fire on the specified surface and performs the computations of the flame properties.

14. If K = KPR at this point, a new fire was not found in subroutine 'FIRE'.

15. Subroutine 'RATES' determines the heat flux at various points associated with one specific fire and interpolates for material properties as a function of this heat flux.

COMMENTS FOR PROGRAM FLOW CHART (continued)

No.

16. If I LSN, the fire under consideration is located on a seat; otherwise the fire is located on a cabin lining surface.

17. Subroutines 'COND', 'CONDS' determine flame propagation via conduction (creeping flame spread).
Subroutine 'FCON', 'FCONS' determine flame propagation via flame contact.
Subroutines 'PVOL!, 'PVOLS' test for possible elemental change of state due to the pyrolysis (smoldering) of elements in the vicinity of a fire.

18. Subroutine 'TEST' determines if any flaming elements change to the charred state and sums the emission rates for each fire.

19. If 'ISAVE' $\neq$ 0; then return control to subroutine 'FIRE' (continue to search surface 'I' for fires).

20. Test: Have all cabin lining surfaces and seat groups been examined during this time step? If not, increment for next surface.

21. The variable 'NFIRES' contains the total number of distinct fires in progress during this time interval.

22. Subroutine 'ELEM updates the time counters and indicators associated with each element.

23. 'ISW' is a switch. When ISW = 1, indicates that the flame propagation computations have been performed this time step.

24. Subroutine 'AFP' determines the total number of flaming and smoldering elements and sums emission rates.

25. Subroutine 'ATMOS' contains all of the equations describing the cabin atmosphere.

26. Add 'one' to the pass counter.

27. Test: If this is the first pass through the program, automatically print flame propagation and cabin atmosphere data.

28. Determine if flame propagation and/or cabin atmosphere data is to be printed this time step.

COMMENTS FOR PROGRAM FLOW CHART (continued)

No.

29. Subroutine 'OUTPUT' consists of the required print and format statements and controls to obtain the output data as required.

30. Subroutine 'PLOTS' writes selected output variables to a file for later plotting.

31. Test: If simulation time has expired, print appropriate message and terminate the run.

32.-34. If the flame propagation computations have been performed this pass, reset computer words containing the element states information.

35. If flame propagation computations are to be performed the next time step, re-enter appropriate loop.

36. If flame propagation computations are not required next time step, increment cabin atmosphere 'Δt' and re-enter cabin atmosphere computations.

C.3 INPUT DATA PREPARATION

This section describes the input requirements of DACFIR2. The preparation of each input card is described, and, where necessary, a brief explanation of the input data requirements and options is included. Following the input preparation instructions is a listing of a sample input data deck. Numbers in the left column of the data description identify specific cards in the sample input deck. The specific set of input data shown in the listing was used to create Case 26P.

In the data description shown below, three format types are referenced. They are as follows.

Type	Description
A	Alphanumeric, any combination of letters, numbers, and special characters (including blanks) may be entered in the appropriate column.
I	Integer, the entry must be right justified in the field (range of columns). Example: when the number '25' is entered in a five-column field, it must be preceded by three blanks.
F	Floating point, the entry may appear anywhere in the specified field, but the insertion of a decimal point is mandatory.

INPUT DATA DESCRIPTION

Card Number	Card Type	Variable Name	Dimension	Column	Fmt Type	Description
1	1	IDENT	(20)	1-80	A	Run I.D.
2	2	LSN	----	1-5	I	Number lining surfaces
		NSG	----	6-10	I	Number seat groups
		ICLL	----	11-15	I	Surface number of leftmost ceiling surface
		ICLR	----	16-20	I	Surface number of rightmost ceiling surface
		NTXG	----	21-25	I	Number of gases (excluding O_2) to be used
		ID	----	26-30	I	Flag to specify the use of "square" or "round" cabin cross section for gas-dynamics calculations, ID=0 indicates "round" case to be used, ID=1 the "square."
3	3	RFWS	----	11-20	F	Flame spread rate sidewall to seat or seat to sidewall (ft/sec)
		DWS	----	21-30	F	Separation distance outboard seats to sidewall (ft)
		CH	----	31-40	F	Cabin Floor to ceiling height (ft)
		CL	----	41-50	F	Cabin section length (see Figure 2-1)
		CW	----	51-60	F	Cabin width at floor (ft)
		SL	----	61-70	F	Detailed section length (see Figure 2-1) (ft)

Card Number	Card Type	Variable Name	Dimension	Column	Fmt Type	Description
4-23	4	SWD	20	1-10	F	Surface "width" - surface dimension in feet, perpendicular to the y (down cabin direction) - this is the actual width for horizontal surfaces and the height for vertical surfaces. (ft)
		Z	20	11-20	F	z displacement (height) of the lowest part of surface from floor (ft)
		VN	20,3	21-30 31-40 41-50	F F F	x component of surface normal (ft) y component of surface normal (ft) z component of surface normal (ft)
		IMATL	20	51-55	I	Surface material ident. number *Material identification number is determined by the order of input of the materials data. Thus IMATL(i)=j indicates that surface i is of material type j and this material's data is the jth in the input order (see below)
24-29	5	SGWD	9	1-10	F	Seat group width (ft)
		XCOR	9	11-20	F	x-coordinate of lefthand forward corner of seat group (ft)
		YCOR	9	21-30	F	y-coordinate of lefthand forward corner of seat group (ft)
30	6	IMATS	7	1-2 3-4 : 13-14	I I : I	Seat surfaces material ident. number - follows format of lining surfaces material identification
31	7	NV	----	1-5	I	Number of openings (vents) in cabin section to exterior or other cabin volumes. Includes doors and emergency exits.
32-33	8	VENTT	10	1-10	F	Distance to top of opening from floor (ft)
		VENTH	10	11-20	F	Height (z dimension) of opening (ft)
		VENTW	10	21-30	F	Width (y or x dimension) of opening (ft)
		FLOW	10	31-40	F	Imposed air flow rate through opening; may be positive, negative, or zero (ft^3/min)

Card Number	Card Type	Variable Name	Dimension	Column	Fmt Type	Description
34-40	9	QTAB	7	1-10	F	Heat of combustion (BTU/lbm) of material
		GTAB	7	11-20	F	Stoichiometric fuel to oxygen ratio of material (no units)
		RTAB	7	21-30	F	Fuel vapor (pyrolyzate) density at burning material surface (lbm/ft^3)
		UTAB	7	31-40	F	Fuel vapor (pyrolyzate) flow velocity at burning material surface (ft/sec)
		RADTAB	7	41-50	F	Fraction of material's heat of combustion released to envirms by flame radiation (no units)
	* One card of type 9 must be prepared for each material.					
41	10	TP	7	1-10 11-20 : 61-70	F F : F	Time of transition of an element from the original state to the smoldering state (sec). Enter values in the order of material identification
42	11	TPC	7	1-10 11-20 : 61-70	F F : F	Time of transition of an element from the smoldering to the charred state (sec). Enter values in the order of materials identification
43	12	RSS	7	1-10 11-20 : 61-70	F F : F	Smoke production rate for each material in the smoldering state ($particles/ft^2$-sec) Enter values in the order of materials i.d.
44-50	13	RSG	10,7	1-10 11-20 61-70	F F F	Toxic gas production rate for each material in the smoldering state (10^{-6} lbm/ft^2-sec) One card of this type for each toxic gas. Rate data for all materials for the ith gas on a single card in the order of materials identification.
51-57	14	TABX	18,7,6	1-5	F	Radiant flux (BTU/ft^2-sec)
		TABY	18,7,6	6-13	F	Material horizontal flame spread rate at above flux level (ft/sec)
		TABX	18,7,6	14-18	F	Radiant flux (BTU/ft^2-sec)
		TABY	18,7,6	19-26	F	Flame spread rate at above flux (ft/sec)
	This format followed for six pairs per card					

Card Number	Card Type	Variable Name	Dimension	Column	Fmt Type	Description
58-64	15	- format identical to card type 14 - Vertical upward flame spread rate (ft/sec)				
65-71	16	- format identical to card type 14 - Vertical downward flame spread rate (ft/sec)				
72-78	17	- format identical to card type 14 - Time to ignite (virgin to flaming) (sec)				
79-85	18	- format identical to card type 14 - Heat release rate-flaming state (BTU/ft^2-sec)				
86-92	19	- format identical to card type 14 - Smoke release rate-flaming (Particles/ft^2-sec)				
93-99	20	- format identical to card type 14 - Time-pyrolysis to extinction (sec) (No data for this item, zero entered)				
100-106	21	- format identical to card type 14 - Time to burn out (flaming to charred) (sec)				
107-113	22	- format identical to card type 14 - Release rate (flaming) for 1st toxic gas (10^{-6} lbm/ft^2-sec)				
114-120	23	- format identical to card type 14 - Release rate (flaming) for 2nd toxic gas (10^{-6} lbm/ft^2-sec)				
121-127	24	- format identical to card type 14 - Release rate (flaming) for 3rd toxic gas (10^{-6} lbm/ft^2-sec)				
128-34	25	- format identical to card type 14 - Release rate (flaming) for 4th toxic gas (10^{-6} lbm/ft^2-sec)				
133-141	25*	- format identical to card type 14 - Release rate (flaming) for 5th toxic gas (10^{-6} lbm/ft^2-sec)				
142-148	27	- format identical to card type 14- Release rate (flaming) for 6th toxic gas (10^{-6} lbm/ft^2-sec)				
149-155	28	- format identical to card type 14- Release rate (flaming) for 7th toxic gas (10^{-6} lbm/ft^2-sec)				

*NOTE: The sample deck contains data on 7 toxic gases: the procedure above can be continued for up to 10 gases.

Card Number	Card Type	Variable Name	Dimension	Column	Fmt Type	Description
156-162	32*	NGAS	10	1-6	A	Alphanumeric name of toxic gas, max. 6 characters.
		XMW	11-22		E	Gas molecular weight (lbm/lbmole)
		GLV1	23-24		E	First check level (PPM)
		GLV2	35-46		E	Second check level (PPM)
		GLV3	47-58		E	Third check level (PPM)
*NOTE:	Up to 10 cards of type 32 can be entered. The order in which they are entered must correspond to the order in which the release data (flaming and smoldering) has been entered previously.					
163	33	QP	7	1-10 11-20 : 61-70	F F : F	Threshold flux levels for transition to smoldering state (BTU/ft^2-sec) for each material
164	34	CPM	----	1-10	F	Specific heat of materials at ambient conditions, average value, $BTU/(lbm \cdot {}^oR)$
		PHOM	----	21-30	F	Bulk density of materials, average value(lbm/ft^3)
		XK	----	21-30	F	Thermal conductivity of materials at ambient conditions, average value, $BTU/(ft \cdot sec \cdot {}^oR)$
		XPEN	----	31-40	F	Heat penetration depth of materials, average value, ft
		TO	----	41-50	F	Ambient temperature, ^oR
165	35	DELTAT	----	1-10	F	Integration step size (small step) for gas dynamics model (sec) Minimum step size is 0.001 sec.
		TFINAL	----	11-20	F	Total time for simulation (sec) (starting time assumed to be 0. sec always)
		IRATIØ	----	11-15	I	Ratio of steps through gas dynamics calculation to steps through flame spread calculation - must always be greater than or equal to one
		IPEMS	----	15-20	I	Output printing interval for cabin atmosphere summary expressed as a multiple of DELTAT
		IPSPR	----	21-25	I	Output printing interval for flame spread-fire growth summary expressed as a multiple of DELTAT

Card Number	Card Type	Variable Name	Dimension	Column	Fmt Type	Description
166	36	Q8KGND	----	1-10	F	Externally imposed "background" radiant flux level (BTU/ft^2-sec)
167	37	QCI	----	1-10	F	Heat of combustion of ignition source fuel (BTU/lbm)
		GAMI	----	11-20	F	Stoichiometric fuel to oxygen ratio for ignition source fuel (no units)
		RHØI	----	21-30	F	Ignition fuel vapor density at burning fuel surface (lbm/ft^3)
		XMUI	----	31-40	F	Ignition fuel vapor velocity at burning fuel surface (ft/sec)
		RADI	----	41-50	F	Fraction of ignition fuel's heat of combustion released to environs by flame radiation (no units)
		XMFI	----	51-60	F	*Total amount of ignition source fuel (lbm)
	*Only one ignition fire is allowed; the ignition fire is assumed to be fully developed at time = 0.					
168	38	DQI	----	1-10	F	Heat release rate for ignition source fuel (BTU/ft^2-sec)
169	39	RSI	----	1-10	F	Smoke release rate for ignition source fuel (particles/ft^2-sec)
		RTGI	10	11-20 21-30 31-40 : 71-80	F F F : F	Toxic gas release rates (10^{-6} lbm/ft^2-sec) for ignition source fuel. If there are more than eight toxic gases the last one or two are entered in the first two fields of a second card
Not shown	39	RTGI	10	1-10 11-20	F F	
170	40	IGSN	----	1-5	I	Surface number upon which the ignition source fuel is located
171	41	NIJSQ	----	1-5	I	Number of square elements (0.5 ft x 0.5 ft) which make up the base of the ignition source fire
		PIGN	----	6-15	F	The length of the perimeter of the base of the ignition source fire. (ft)

Card Number	Card Type	Variable Name	Dimension	Column	Fmt Type	Description
172-177	42	I	----	1-5	I	i index of ignition source fire base element
		J	----	6-10	I	j index of ignition source fire base element
	Enter one pair of (i,j) indices per card. The total number of cards will be equal to the value of NIGSQ. For number of elements see Figure .					
178	43	NIJC	----	1-5	I	Total number of elements, on any or all surfaces, which are to be set to the charred (inert) state at the start of the simulation. If the value is entered as zero no cards of type 44 are included in the deck
Not shown	44	I	----	1-5	I	i index of charred (inert) element
		J	----	6-10	I	j index of charred (inert) element
	Enter one pair of (i,j) indices per card. The total number of cards will be equal to the value of NIJC. For numbering of elements see Figure .					

DACFIR2 - Sample Input Data Deck

Card No.	Column 1	11	21	31	41	51	61	71
1	26 FT CABIN MOCK-UP FIRE TEST - IN-SERVICE (1968) MATERIALS (AIA-CDP 3-8-68)							
2	20 6 13 9 7 0							
3	0.2	0.1	7.5	25.83	11.5	7.5		
4	11.5	0.	0.	0.	1.0	1		
5	1.5	0.	-1.0	0.	0.	2		
6	3.0	0.	-1.0	0.	0.	2		
7	1.5	0.	-1.0	0.	0.	2		
8	2.0	6.0	0.	0.	-1.0	3		
9	0.5	0.	-1.0	0.	0.	4		
10	2.0	6.5	0.	0.	1.0	5		
11	0.5	0.	-1.0	0.	0.	6		
12	1.0	7.0	0.	0.	-1.0	6		
13	0.5	0.	-1.0	0.	0.	6		
14	9.5	7.5	0.	0.	-1.0	6		
15	0.5	0.	1.0	0.	0.	6		
16	1.0	7.0	0.	0.	-1.0	6		
17	0.5	0.	1.0	0.	0.	6		
18	2.0	6.5	0.	0.	1.0	5		
19	0.5	0.	1.00	0.	0.	4		
20	2.0	6.0	0.	0.	-1.0	3		
21	1.5	0.	1.00	0.	0.	2		
22	3.0	0.	1.0	0.	0.	2		
23	1.5	0.	1.00	0.	0.	2		
24	3.5	0.	0.					
25	5.0	6.5	0.					
26	3.5	0.	2.5					
27	5.0	6.5	2.5					
28	3.5	0.	5.0					
29	5.0	6.5	5.0					
30	7 7 7 7 7 7 7							
31	2							
32	7.0	7.0	3.0	0.0				
33	4.0	4.0	2.0	0.0				
34	7000.	2.	0.035	0.25	0.25			
35	7000.	2.	0.035	0.25	0.25			
36	7000.	2.	0.035	0.25	0.25			
37	7000.	2.	0.035	0.25	0.25			
38	7000.	2.	0.035	0.25	0.25			
39	7000.	2.	0.035	0.25	0.25			
40	7000.	2.	0.035	0.25	0.25			
41	59.0	49.0	75.2	21.0	3.0	41.0	21.0	
42	455.0	163.0	662.0	334.0	113.0	136.0	162.	
43	2.57	5.8	74.6	17.1	23.1	3.23	10.8	
44	1457.	0.0	0.0	37.2	72.1	256.6	673.0	
45	41.2	5.1	.419	6.23	75.0	61.2	145.6	
46	27.8	88.8	0.0	27.7	58.4	39.9	0.035	
47	1.18	0.0	0.0	.80	.432	.74	1.65	
48	0.0	8.5	0.0	0.0	0.0	0.0	0.0	
49	.55	0.0	0.0	0.0	0.0	0.0	0.63	
50	0.0	0.0	1.92	0.0	0.0	0.0	0.0	
51	0.0 0.005	1.32 0.0082	2.20 0.0079	3.08 0.0198	4.4 0.0144	6.0 0.0144		
52	0.0 0.0	1.32 0.01	2.20 .0106	3.08 .0408	4.4 .0632	6.0 .0632		
53	0.0 0.0	1.32 0.0	2.20 0.0033	3.08 0.0079	4.4 0.0145	6.0 0.0145		
54	0.0 .001	1.32 .0038	2.20 .0076	3.08 .0326	4.4 .0216	6.0 .0216		
55	0.0 0.1	1.32 .1042	2.20 .1389	3.08 .1389	3.96 .4167	6.0 .4167		

Card No.	Column 1	11	21	31	41	51	61	71
56	0.0	0.005	1.32 0.0139	2.20 .0463	3.08 .0556	3.96 .0740	6.0	.0740
57	0.0	0.0179	1.32 0.0179	2.2 0.0246	3.08 0.0463	4.4 0.0716	6.0	0.0716
58	0.0	0.005	1.32 0.0082	2.20 0.0079	3.08 0.0198	4.4 0.0144	6.0	0.0144
59	0.0	0.0	1.32 .0111	2.20 .0833	3.08 .0764	4.4 .0875	6.0	.0875
60	0.0	0.0	1.32 0.0	2.20 0.0098	3.08 0.0201	4.4 0.0471	6.0	0.0471
61	0.0	.01	1.32 .0227	2.20 .0179	3.08 .0336	4.4 .0398	6.0	.0398
62	0.0	0.1	1.32 .1042	2.20 .1389	3.08 .1389	3.96 .4167	6.0	.4167
63	0.0	0.005	1.32 0.0139	2.20 .0463	3.08 .0556	3.96 .0740	6.0	.0740
64	0.0	0.0179	1.32 0.0179	2.2 0.0417	3.08 0.105	4.4 0.333	6.0	0.333
65	0.0	0.005	1.32 0.0082	2.20 0.0079	3.08 0.0198	4.4 0.0144	6.0	0.0144
66	0.0	0.0	1.32 .0038	2.20 .0227	3.08 .0321	4.4 .0820	6.0	.0820
67	0.0	0.0	1.32 0.0	2.20 0.0015	3.08 0.0087	4.4 0.0146	6.0	0.0146
68	0.0	.002	1.32 .0025	2.20 .0064	3.08 .01	4.4 .0419	6.0	.0419
69	0.0	0.1	1.32 .1042	2.20 .1389	3.08 .1389	3.96 .4167	6.0	.4167
70	0.0	0.005	1.32 0.0139	2.20 .0463	3.08 .0556	3.96 .0740	6.0	.0740
71	0.0	0.00633	1.32 0.00633	2.2 0.0330	3.08 0.0590	4.4 0.264	6.0	0.264
72	0.0	20.0	1.32 12.0	2.20 2.0	3.08 1.3	4.4 2.30	6.0	2.30
73	0.0	30.0	1.32 26.7	2.20 20.00	3.08 11.56	4.4 9.89	6.0	9.89
74	0.0	30.0	1.32 20.0	2.20 16.25	3.08 14.75	4.4 35.33	6.0	35.33
75	0.0	20.0	1.32 14.3	2.20 5.0	3.08 8.7	4.4 3.9	6.0	3.9
76	0.0	15.0	1.32 15.0	2.20 1.0	3.08 4.0	3.96 1.0	6.0	1.0
77	0.0	8.0	1.32 6.0	2.20 2.0	3.08 4.0	3.96 1.0	6.0	1.0
78	0.0	20.0	1.32 16.3	2.2 5.00	3.08 7.19	4.4 4.58	6.0	4.58
79	0.0	3.0	1.32 4.0	2.20 5.18	3.08 6.28	3.96 0.9387	6.0	0.9387
80	0.0	.20	1.32 .433	2.20 2.37	3.08 3.15	4.4 2.73	6.0	2.73
81	0.0	0.0	1.32 0.0	2.20 0.917	3.08 2.84	4.4 3.51	6.0	3.51
82	0.0	5.0	1.32 7.47	2.20 9.77	3.08 13.6	4.4 7.3	6.0	7.3
83	0.0	2.0	1.32 2.871	2.20 4.051	3.08 2.896	3.96 3.136	6.0	3.136
84	0.0	0.5	1.32 1.694	2.20 2.389	3.08 3.167	3.96 3.234	6.0	3.234
85	0.0	5.0	1.32 5.37	2.2 5.50	3.08 5.46	4.4 4.47	6.0	4.47
86	0.0	10.0	1.32 20.0	2.20 26.84	3.08 38.92	3.96 83.05	6.0	83.05
87	0.0	2.0	1.32 5.92	2.20 15.28	3.08 37.95	4.4 67.0	6.0	67.0
88	0.0	0.0	1.32 0.0	2.20 2.41	3.08 33.9	4.4 55.5	6.0	55.5
89	0.0	98.0	1.32 98.4	2.20 98.2	3.08 426.0	4.4 116.2	6.0	116.2
90	0.0	5.0	1.32 11.66	2.20 0.0	3.08 14.07	3.96 19.46	6.0	19.46
91	0.0	10.0	1.32 8.695	2.20 11.25	3.08 2.186	3.96 16.45	6.0	16.45
92	0.0	4.0	1.32 5.68	2.2 8.02	3.08 10.9	4.4 20.6	6.0	20.6
93	0.0	0.0	1.32 0.0	2.20 0.0	3.08 0.0	4.4 0.0	6.0	0.0
94	0.0	0.0	1.32 0.0	2.20 0.0	3.08 0.0	4.4 0.0	6.0	0.0
95	0.0	0.0	1.32 0.0	2.20 0.0	3.08 0.0	4.4 0.0	6.0	0.0
96	0.0	0.0	1.32 0.0	2.20 0.0	3.08 0.0	4.4 0.0	6.0	0.0
97	0.0	0.0	1.32 0.0	2.20 0.0	3.08 0.0	3.96 0.0	6.0	0.0
98	0.0	0.0	1.32 0.0	2.20 0.0	3.08 0.0	3.96 0.0	6.0	0.0
99	0.0	0.0	1.32 0.0	2.2 0.0	3.08 0.0	4.4 0.0	6.0	0.0
100	0.0	750.0	1.32 615.0	2.20 327.0	3.08 279.0	4.4 186.3	6.0	186.3
101	0.0	130.0	1.32 126.3	2.20 83.0	3.08 56.3	4.4 52.6	6.0	52.6
102	0.0	20000	1.32 2000	2.20 1106	3.08 606.0	4.4 538.1	6.0	538.1
103	0.0	250.0	1.32 221.3	2.20 211.3	3.08 152.0	4.4 134.6	6.0	134.6
104	0.0	150	1.32 180.0	2.20 124.0	3.08 321.0	3.96 270.0	6.0	270.0
105	0.0	150	1.32 174.0	2.20 245.0	3.08 225.0	3.96 324.7	6.0	324.7
106	0.0	562.	1.32 551.	2.2 542.	3.08 607.	4.4 813.	6.0	813.
107	0.0	500.0	1.32 680.8	2.20 2241.0	3.08 2071.0	4.4 4249.0	6.0	4249.0
108	0.0	0.0	1.32 0.0	2.20 0.0	3.08 348.6	4.4 0.0	6.0	0.0
109	0.0	0.0	1.32 0.0	2.20 25.6	3.08 0.0	4.4 178.0	6.0	178.0
110	0.0	1500.	1.32 1500.	2.20 1548.	3.08 1535.	4.4 36.78	6.0	36.78

Card No.	Column 1	11	21	31	41	51	61	71
111	0.0	150	1.32 200	2.20 231.6	3.08 636.6	3.96 545.7	6.0	545.7
112	0.0	0.0	1.32 0.0	2.20 0.0	3.08 0.0	3.96 0.0	6.0	0.0
113	0.0	2500.	1.32 2500.	2.2 3049.	3.08 1979.	4.4 2280.	6.0	2280.
114	0.0	15.0	1.32 19.63	2.20 56.02	3.08 87.54	4.4 170.6	6.0	170.6
115	0.0	50.0	1.32 50.0	2.20 80.25	3.08 135.6	4.4 213.7	6.0	213.7
116	0.0	0.0	1.32 0.0	2.20 5.02	3.08 15.2	4.4 53.9	6.0	53.9
117	0.0	150.	1.32 150.	2.20 197.0	3.08 230.1	4.4 509.3	6.0	509.3
118	0.0	100	1.32 150.	2.20 184.2	3.08 137.0	3.96 88.96	6.0	88.96
119	0.0	20	1.32 36.69	2.20 121.8	3.08 141.2	3.96 113.0	6.0	113.0
120	0.0	169.	1.32 169.	2.2 169.	3.08 182.	4.4 169.	6.0	169.
121	0.0	7.5	1.32 11.77	2.20 33.19	3.08 45.39	4.4 77.68	6.0	77.68
122	0.0	190.0	1.32 194.0	2.20 174.4	3.08 64.26	4.4 481.5	6.0	481.5
123	0.0	0.0	1.32 0.0	2.20 0.0	3.08 0.060	4.4 0.202	6.0	0.202
124	0.0	80.	1.32 80.	2.20 85.6	3.08 119.0	4.4 134.4	6.0	134.4
125	0.0	50	1.32 50.	2.20 80.04	3.08 67.42	3.96 37.21	6.0	37.21
126	0.0	25	1.32 51.98	2.20 59.07	3.08 80.40	3.96 90.0	6.0	90.0
127	0.0	0.	1.32 0.	2.2 0.	3.08 0.	4.4 0.250	6.0	0.250
128	0.0	0.0	1.32 0.2176	2.20 1.228	3.08 1.919	4.4 4.310	6.0	4.310
129	0.0	0.0	1.32 0.0	2.20 0.0	3.08 0.0	4.4 0.0	6.0	0.0
130	0.0	0.0	1.32 0.0	2.20 0.0	3.08 0.0	4.4 0.0	6.0	0.0
131	0.0	0.0	1.32 5.0	2.20 13.9	3.08 6.2	4.4 4.4	6.0	4.4
132	0.0	0.0	1.32 0.0	2.20 0.0	3.08 1.662	3.96 0.9175	6.0	0.9175
133	0.0	0.0	1.32 0.0	2.20 .8739	3.08 .8326	3.96 .8490	6.0	.8490
134	0.0	3.5	1.32 3.50	2.2 3.70	3.08 3.30	4.4 1.36	6.0	1.36
135	0.0	0.0	1.32 0.0	2.20 0.0	3.08 0.0	4.4 0.0	6.0	0.0
136	0.0	30.0	1.32 30.0	2.20 35.83	3.08 52.82	4.4 37.69	6.0	37.69
137	0.0	0.0	1.32 0.0	2.20 0.0	3.08 0.0	4.4 0.0	6.0	0.0
138	0.0	0.0	1.32 0.0	2.20 0.0	3.08 0.0	4.4 0.0	6.0	0.0
139	0.0	0.0	1.32 0.0	2.20 0.0	3.08 0.0	3.96 0.0	6.0	0.0
140	0.0	0.0	1.32 0.0	2.20 0.0	3.08 0.0	3.96 0.0	6.0	0.0
141	0.0	0.0	1.32 0.0	2.20 0.0	3.08 0.0	4.4 0.0	6.0	0.0
142	0.0	0.0	1.32 0.0	2.20 0.0	3.08 0.0	4.4 1.224	6.0	1.224
143	0.0	0.0	1.32 0.0	2.20 0.0	3.08 0.0	4.4 0.0	6.0	0.0
144	0.0	0.0	1.32 0.0	2.20 0.0	3.08 0.0	4.4 0.0	6.0	0.0
145	0.0	0.0	1.32 0.0	2.20 0.0	3.08 0.0	4.4 0.0	6.0	0.0
146	0.0	0.0	1.32 0.0	2.20 0.0	3.08 0.0	3.96 0.0	6.0	0.0
147	0.0	0.0	1.32 0.0	2.20 0.0	3.08 0.0	3.96 0.0	6.0	0.0
148	0.0	0.0	1.32 0.0	2.2 0.0	3.08 0.0	4.4 0.631	6.0	0.631
149	0.0	0.0	1.32 0.0	2.20 0.0	3.08 0.0	4.4 0.0	6.0	0.0
150	0.0	0.0	1.32 0.0	2.20 0.0	3.08 0.0	4.4 0.0	6.0	0.0
151	0.0	0.0	1.32 0.0	2.20 11.9	3.08 16.8	4.4 35.4	6.0	35.4
152	0.0	0.0	1.32 0.0	2.20 0.0	3.08 0.0	4.4 0.0	6.0	0.0
153	0.0	0.0	1.32 0.0	2.20 0.0	3.08 0.0	3.96 0.0	6.0	0.0
154	0.0	0.0	1.32 0.0	2.20 0.0	3.08 0.0	3.96 0.0	6.0	0.0
155	0.0	0.0	1.32 0.0	2.20 0.0	3.08 0.0	4.4 0.0	6.0	0.0
156	CO2	44.0		1.0E+3	1.0E+4	1.0E+5		
157	CO	28.0		5.0E+1	5.0E+1	8.0E+3		
158	HCL	36.5		5.0E+0	3.5E+1	1.0E+3		
159	HCN	27.0		1.0E+1	1.0E+1	2.8E+2		
160	HF	20.0		3.0E+0	3.2E+1	5.0E+1		
161	NO2	46.0		5.0E+0	5.0E+1	2.5E+2		
162	SO2	48.0		5.0E+0	2.0E+1	1.0E+2		
163	2.2	2.2	2.2	2.2	2.2	2.2	2.2	2.2
164	0.25	35.0	0.000084	0.00833	530.0			
165	0.005	250.	1000	5 5				

Card No.	Column 1	11	21	31	41	51	61	71
166	0.							
167	18000.	3.5	0.271	0.0198	0.40	10.8		
168	214.6							
169	86.7	18720.	34.1	0.0	0.0	0.0	0.0	0.0
170	1							
171	6	5.0						
172	22	6						
173	23	6						
174	22	7						
175	23	7						
176	22	8						
177	23	8						
178	0							

C.4 PROGRAM OUTPUT

The following pages contain a sample of the printed output of DACFIR2. This output was produced by the sample input deck shown above. On pages C-24, C-25, and C-26 the automatic input summary is given. All input data except the tables of materials' properties is printed. A plan of the seat location is shown, and the burning time of the ignition fire, computed from the input data, is given. Pages C-27, C-28, and C-29 show the output at 60 seconds of Case 26P.

DACFIR2 also writes the values of certain variables to a disk file or tape (as determined by the user) for off-line plotting or other purposes. The variables are written to unit 8 using a formatted FORTRAN write statement with an E12.5 format for each variable. The variables are as follows.

Variable and Unit	Variable Name
Record 1	
Time (seconds)	TIME
Upper zone gas temperature (°F)	TUF
Lower zone gas temperature (°F)	TLF
Smoke concentration (optical density/ft)	SOD
Smoke concentration (% transmission/ft)	PTRANS
Record 2	
Time (seconds)	TIME
Oxygen concentration (% vol.)	OPRCNT
Depth of the lower gas zone (ft)	HEIGHT
Upper zone materials surface temperature (°F)	TSUF
Lower zone materials surface temperature (°F)	TSLF

DACFIR2 - Sample Output

PROGRAM DACFIR VERSION 2.0—1 MAY 78

COMPUTER SIMULATION OF FIRE WITHIN A COMMERCIAL AIRCRAFT CABIN

DATA CASE: 26 FT CABIN MOCK-UP FIRE TEST - IN-SERVICE (1968) MATERIALS (AIA-CDP 3-8-68)

DATE 05/06/78 TIME 13.45.14.

TIME DATA(SEC)—— INTGR STEP= .01 RUN TERMINATION= 250.0 ATMOS PRT INT= 5 FLM SPRD PRT INT= 5

GEOMETRY-

	CABIN DIMENSIONS(FT)	SECTION DIMENSIONS(FT)
WIDTH	11.50	5.75
LENGTH	25.83	7.50
MAX HGT	7.50	7.50

NO OF SURFACES,EXCL SEATS=20 NO OF SEAT GROUPS=6

VENT DATA- NO VENTS= 2

VENT NO	DIMENSIONS(FT) HEIGHT	WIDTH	DISTANCE(FT) FLOOR TO TOP OF VENT	FORCED FLOW RATE(CFM)
1	7.00	3.00	7.00	0.00
2	4.00	2.00	4.00	0.00

LOOKING FROM THE FRONT OF THE CABIN TOWARD THE REAR,THE FLOOR IS SURFACE NO 1, THE LWR RGT SIDEWALL IS SURFACE NO 2,THE RGT SIDE CEILING SURFACE IS 9, THE LEFT SIDE CEILING SURFACE IS 13,AND THE LWR LEFT SIDEWALL IS SURFACE NO 20

THE ELEMENTS(IN THE I DIRECTION)ARE NUMBERED IN THE SAME MANNER AS THE SURFACES THE FRONT MOST ELEMENT IS J=1,THE REAR MOST ELEMENT IS J=15

SURFACE DATA(EXCL SEATS)——

SURF NO	WIDTH,FT	HGT,FT	UNIT NORM				MATL TYPE	IMIN	IMAX	XMN	XMX
1	11.5	0.0	0.0	0.0	1.0		1	1	23	0.0	0.0
2	1.5	0.0	-1.0	0.0	0.0		2	24	26	0.0	1.5
3	3.0	0.0	-1.0	0.0	0.0		2	27	32	1.5	4.5
4	1.5	0.0	-1.0	0.0	0.0		2	33	35	4.5	6.0
5	2.0	6.0	0.0	0.0	-1.0		3	36	39	6.0	6.0
6	.5	0.0	-1.0	0.0	0.0		4	40	40	6.0	6.5
7	2.0	6.5	0.0	0.0	1.0		5	41	44	6.5	6.5
8	.5	0.0	-1.0	0.0	0.0		6	45	45	6.5	7.0
9	1.0	7.0	0.0	0.0	-1.0		6	46	47	7.0	7.0
10	.5	0.0	-1.0	0.0	0.0		6	48	48	7.0	7.5
11	9.5	7.5	0.0	0.0	-1.0		6	49	67	7.5	7.5
12	.5	0.0	1.0	0.0	0.0		6	68	68	7.0	7.5
13	1.0	7.0	0.0	0.0	-1.0		6	69	70	7.0	7.0
14	.5	0.0	1.0	0.0	0.0		6	71	71	6.5	7.0
15	2.0	6.5	0.0	0.0	1.0		5	72	75	6.5	6.5
16	.5	0.0	1.0	0.0	0.0		4	76	76	6.0	6.5
17	2.0	6.0	0.0	0.0	-1.0		3	77	80	6.0	6.0
18	1.5	0.0	1.0	0.0	0.0		2	81	83	4.5	6.0
19	3.0	0.0	1.0	0.0	0.0		2	84	89	1.5	4.5
20	1.5	0.0	1.0	0.0	0.0		2	90	92	0.0	1.5

SEAT GROUP DATA—

ST GRP NO	WIDTH,FT	LOCATION XCOR,FT	YCOR,FT
1	3.5	0.0	0.0
2	5.0	6.5	0.0
3	3.5	0.0	2.5
4	5.0	6.5	2.5
5	3.5	0.0	5.0
6	5.0	6.5	5.0

EACH SEAT GROUP HAS 7 SURFACES:

SURF NO	SURFACE	MATL TYPE
1	CUSHION BOTTOM	7
2	LWR REAR BACKREST	7
3	UPR REAR BACKREST	7
4	TOP OF BACKREST	7
S	FRONT OF BACKREST	7
6	CUSHION TOP	7
7	CUSHION FRONT	7

OVERHEAD VIEW OF SEATS SUPERIMPOSED ON FLOOR(NON-ZERO INTEGER IS SEAT GROUP NUMBER)

```
15 00000000000000000000000
14 55555550000006666666666
13 55555550000006666666666
12 55555550000006666666666
11 55555550000006666666666
10 00000000000000000000000
 9 33333330000004444444444
 8 33333330000004444444444
 7 33333330000004444444444
 6 33333330000004444444444
 5 00000000000000000000000
 4 11111110000002222222222
 3 11111110000002222222222
 2 11111110000002222222222
 1 11111110000002222222222
   FRONT
```

MATLS DATA—

MATL NO	HEATG VALUE (BTU/LB)	STOCH RATIO	PYROLZATE DENS (LBM/CU FT,	PYROLZATE VEL (FT/SEC)
1	7000.0	2.00	.0350	.25
2	7000.0	2.00	.0350	.25
3	7000.0	2.00	.0350	.25
4	7000.0	2.00	.0350	.25
5	7000.0	2.00	.0350	.25
6	7000.0	2.00	.0350	.25
7	7000.0	2.00	.0350	.25

SPEC HEAT(BTU/LBM-R)= .250
DENSITY (LBM/CU FT)=35.00
THERM COND(BTU/FT-SEC-R)= .000084

THERMAL PENETRATION DEPTH(FT)= .00833
AMBIENT TEMP(DEGR R) =530.0

IGNITION SOURCE DATA

IGNITION SOURCE IS ON SURFACE NO 1 NO OF ELEM= 6 AREA(SQ FT)= 1.5 PERIMETER(FT)= 5.0 TIME TO BURN(SEC)= 1341.8

AMT OF FUEL(LBS)= 10.8 BACKGRD RAD INTENSITY(BTU/SQ FT-SEC)= 0.0 SMOKE GEN RATE(PART/SQ FT-SEC)= 86.7

TOXIC GAS GEN RATES-

GAS	RATE(LBS/SQ FT-SEC)
CO2	.187200E-01
CO	.341000E-04
HCL	0.
HCN	0.
HF	0.
NO2	0.
SO2	0.

ELEMEMTS AFLAME——

I	J
22	6
23	6
22	7
23	7
22	8
23	8

END OF INPUT SUMMARY

TIME= 60.000 SEC AFTER IGNITION

CABIN ATMOSPHERE SUMMARY

STRATIFIED GAS MODEL	ZONE DEPTH (FT)	GAS DENSITY (LBM/CU FT)	GAS TEMP (DEG F)	MATL SURF TEMP (DEG F)	HEAT RATE TO SURF (BTU/SQ FT-SEC)
UPPER ZONE	5.617	.0442	438.6	90.9	.425
LOWER ZONE	1.883	.0748	70.9	79.8	.206

	TOTAL FLOW RATE THRU VENTS (LBM/SEC)	UPWD GAS FLOW,ALL FIRES (LBM/SEC)
OUT	.373	.804
IN	0.000	

SMOKE CONCENTRATION IN UPPER ZONE

OPTICAL DENSITY/FT= .565
PERCNT TRANSMISSION/FT= 27.2

OXYGEN CONCENTRATION IN UPPER ZONE

OXYGEN PERCNT BY VOLUME= 14.57

TOXIC GAS CONCENTRATION IN UPPER ZONE

GAS	CONCENTRATION (PPM)	LEVELS EXCEEDED (0=NO 1=YES) LVL1	LVL2	LVL3
CO2	.2469751E+05	1	1	0
CO	.7742417E+03	1	1	0
HCL	.4374796E+03	1	1	0
HCN	.1061680E+02	1	1	0
HF	.7624775E+02	1	1	1
NO2	.5521900E+00	0	0	0
SO2	0.	0	0	0
	0.	0	0	0
	0.	0	0	0
	0.	0	0	0

DISTINCT FIRES AT START OF FLAME SPREAD CALCULATIONS

FIRE NO	ZONE	DIST-FIRE BASE FROM FLOOR(FT)	FLAME HEIGHT(FT)	FIRE BASE AREA(SQ FT)	BASE RADIUS,FLAME VOL(FT)
1	LWR	0.00	3.25	1.50	.60
2	LWR	0.00	2.92	1.75	.35
3	LWR	1.17	4.24	3.50	.78
4	LWR	1.18	4.27	2.75	.79
5	LWR	1.18	2.57	1.25	.42
6	LWR	1.18	1.71	.25	.25

ELEMENT STATE SUMMARY - CONDITIONS ON ALL SURFACES AT END OF FLAME SPREAD CALCULATIONS

	1	2	3	4	5	6	7	8	9	10	11	12	13	14	15	16	17	18	19	20	21	22	23	24	25	26	27
SMOLDERING	0	0	0	0	0	0	0	0	0	0	0	0	0	0	0	0	0	0	0	0	0	0	0	0	0	0	0
FLAMING	13	15	8	0	0	0	0	0	0	0	0	0	0	0	0	0	0	0	0	0	0	0	0	21	0	0	0
CHARRED	0	0	0	0	0	0	0	0	0	0	0	0	0	0	0	0	0	0	0	0	0	0	0	0	0	0	0

FLAMING AND SMOLDERING AREAS BY MATERIAL TYPE (SQ FT)

MATERIAL NO	1	2	3	4	5	6	7
AREA AFLAME	3.25	5.75	0.00	0.00	0.00	0.00	5.25
AREA SMLDRG	0.00	0.00	0.00	0.00	0.00	0.00	0.00

TIME= 60.000 SEC AFTER IGNITION

DISTRIBUTION OF ELEMENTAL STATES AT END OF FLAME SPREAD CALCULATIONS

INTEGERS CORRESPOND TO STATES OF INDIVIDUAL ELEM-

1=AMBIENT STATE
2=SMOLDERING STATE
3=AFLAME
4=CHARRED
5=HEATING,NOT IN CONTACT WITH FLAME
6=HEATING,IN CONTACT WITH FLAME
7=SMOLDERING,COOLING

AFT

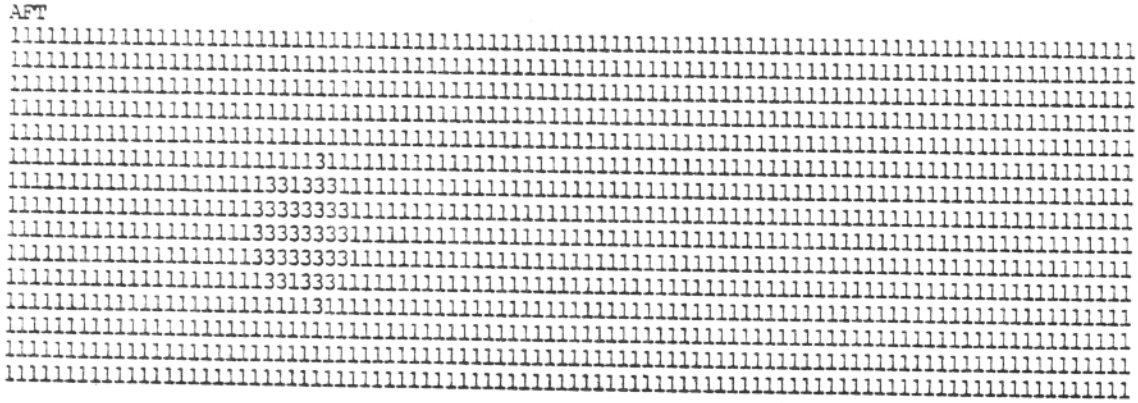

TIME= 60.000 SEC AFTER IGNITION

FOR SEAT GROUPS——J= 1- 4 CUSHION,BOTTOM
J= 5- 7 BACKREST,LWR REAR
J= 8-11 BACKREST,UPR REAR
J=12 BACKREST,TOP
J=13-18 BACKREST,FRONT
J=19-21 CUSHION,TOP
J=22 CUSHION,FRONT

SEAT GROUP NO 4

22 1111111133
21 1111111133
20 1111111133
19 1111111133
18 1111111113
17 1111111111
16 1111111111
15 1111111111
14 1111111111
13 1111111111
12 1111111111
11 1111111111
10 1111111111
9 1111111111
8 1111111111
7 1111111111
6 1111111111
5 1111111113
4 1111111133
3 1111111333
2 1111111333
1 1111111333

Variable and Unit	Variable Name
Record 3	
Time (seconds)	TIME
Concentration of the first toxic gas (ppm)	CONC(1)
Concentration of the second toxic gas (ppm)	CONC(2)
.	
.	
.	
Concentration of the last toxic gas (ppm)	CONC(NTXG)

C.5 PROGRAM STATISTICS

DACFIR2 is written in Control Data Corporation (CDC) FORTRAN EXTENDED but except for a very few statements conforms to ANSI standard FORTRAN IV. The following descriptive statistics pertain to use of the program on a CDC 6600 computer system using the NOS/BE operating system.

Core Storage - 130,000 words (octal)
Number of Source Statements - 3129
Compile Time - 21 CPU seconds
Execution Time* - 248 CPU seconds for 175 sec simulated time with an integration step of 0.01 sec.

*Execution time is highly dependent on the integration step size used.

C.6 PROGRAM AVAILABILITY

Copies of the program code and sample input data may be obtained by contacting

Mr. Charles D. MacArthur
University of Dayton Research Institute
300 College Park Avenue
Dayton, Ohio 45469
Telephone (513) 229-3921

or

Mr. Charles C. Troha ARD 520
Department of Transportation
Federal Aviation Administration
Trans Point Building
2100 Second Street, S.W., Room 1400
Washington, D.C. 20591
Telephone (202) 426-8416.

APPENDIX D

DERIVATION OF SEVERAL RELATIONSHIPS PRESENTED IN SECTION 2

This appendix contains the derivation of several relationships presented in Section 2.

D.1 EFFECTIVE VIEW FACTORS FOR UPPER ZONE GAS RADIATION

Equations (2-2a) and (2-2b) contain the terms $\bar{F}_u$ and $\bar{F}_l$, the effective view factors for radiation from the upper zone gas, at temperature T_u, to the solid surfaces in contact with the gas and to the surfaces in contact with the cooler lower zone gas. To compute these terms, the radiant exchanges among the major cabin lining surfaces and the upper zone gas were evaluated separately. Exchanges between the ceiling and floor, gas and floor, upper walls and floor, ceiling and lower walls, gas and lower walls, and upper walls and lower walls were considered. The magnitude of each exchange was determined by computing the view factor in each exchange for the range of upper zone thicknesses from zero to the full cabin height. It was found that the gas to surface exchanges were always much larger than the surface to surface exchanges, and so only the contributions from the gas-surface exchanges were used in computing $\bar{F}_u$ and $\bar{F}_l$. To speed computing, linear functions were fit to the more complicated view factor expressions for each significant exchange. The resulting expressions for the effective view factors are

(a) for the rectangular cabin cross-section

$$\bar{F}_l = 0.7587 + 0.02754L$$

$$\bar{F}_u = 1.0$$

and (b) for the circular cabin cross section

$$\bar{F}_l = \begin{cases} 0.4782 + 0.0784L \text{ for } L < 2r - C_H \\ 0.1965 + 0.1457L \text{ for } L > 2r - C_H \end{cases}$$

$$\bar{F}_u = 1.0$$

where L is the upper zone layer thickness, r is the cabin cross-section radius, and C_H is the floor to ceiling height.

D.2 FLAME ABSORPTION COEFFICIENT

Equation (2-3) relates the flame absorption coefficient, k_f, to the smoke generation rate of the burning material, $\dot{p}"$, and the flame height, h_f, for the purpose of computing the flame emittance and thus the radiation feedback to the fuel. This relationship should be regarded as very approximate due to the overly simplified assumptions involved. The motivation for developing Eq. (2-3) is that since smoke data is available the relative radiative output of fires on the different materials can be judged.

The derivation of Eq. (2-3) assumes that the flame is a right circular cylinder of height h_f and base radius y_o. The volume of the flame is then

$$V_f = \pi y_o^2 h_f \qquad \text{(D-1)}$$

To compute the concentration of smoke in this volume, the average residence time of a smoke particle in the flame must be known. If it is assumed that all smoke particles are created at the flame base at the rate $\dot{p}"$ per unit area (which in reality is not true) the number of particles crossing any plane parallel to the base is

$$\dot{P} = A\dot{p}" = \pi y_o^2 \dot{p}" = \pi y_o^2 v \rho_s \qquad \text{(D-2)}$$

where v is the gas flow velocity and ρ_s is the particle density at the position of the plane. Thomas, et. al[1] give an estimate for the gas flow velocity at a height z in a buoyant diffusion flame

$$v = 0.36 \left(2z \frac{\Delta T}{T} g\right)^{1/2} \qquad \text{(D-3)}$$

where $\Delta T/T$ is the ratio of the temperature rise in the flame to the ambient temperature and g is gravity. The flame is assumed

---

[1] Thomas, P.H., R. Baldwin, and A.J.M. Heselden, "Buoyant Diffusion Flames: Some Measurements of Air Entrainment, Heat Transfer, and Flame Mergin," Tenth Symposium (International) on Combustion, The Combustion Institute, 1965.

to be at a constant absolute temperature, $T_f = T + \Delta T$, and the gas at the flame base is assumed to accelerate from zero velocity so that the number of particles in the flame volume N is

$$N = \int_{V_f} \rho_s dV = \int_0^{h_f} \frac{\dot{p}''}{v} dz \cdot A \quad . \tag{D-4}$$

Substituting (D-3) into (D-4) and assuming that $\Delta T/T = 2000\ °R/500\ °R = 4$, the integral can be evaluated giving

$$N = 2\dot{p}''(hf/g)^{1/2}A \quad . \tag{D-5}$$

Now making the further simplifying assumption that the N particles are uniformly distributed in the flame the mean particle concentration is

$$C = \frac{N}{V_f} = \frac{2\dot{p}''}{(h_f g)^{1/2}} \quad . \tag{D-6}$$

The absorption coefficient is employed in the Bouguer-Lambert law (uniform grey gas) as

$$i = i_o \exp(-k_f s) \tag{D-7}$$

where i is the intensity at a distance s along a straight ray path away from the point where the intensity is i_o. The definition of a "particle" of smoke is based on the Bouguer-Lambert relationship but in a different form

$$i = i_o\ 10^{-0.04575CS} \quad . \tag{D-8}$$

By equating (D-7) and (D-8) C is related to k_f to obtain Equation (2-3)

$$k_f = (0.105)C = 0.21\ \dot{p}''/(h_f g)^{1/2} \quad .$$